CHAPTER ONE

INTRODUCTION

1.1 Background of the Study

In general terms, excavators are used for the rapid removal of soil and other materials in mines, quarries, and construction sites. These are usually self-powered machines deployed for digging or earth-moving operations in civil engineering, road works and mining. In the course of operation, the machines interact with the medium to be loaded or excavated. They have to overcome the resistive force experienced by the bucket when penetrating through a medium. Generally, the penetration is in form of cutting, digging and scooping. The automation of these machines offers promise for increasing productivity and improving safety. However to date, most of the research in this area has focused on selected parts of the problem.

Excavation productivity (amount of work done), efficiency (cost of work done in terms of labour and machinery) and operator safety, particularly in underground mining or during the removal of hazardous waste, are constantly of concern in the industry. Full or partial automation may offer the possibility of improving each metric but has been only slowly accepted by industry. After decades of increases in machine size and power, practical limits are now being approached and automation is being sought for further improvements. Furthermore, computing and sensing technologies have reached a stage where they can affordably and reliably be applied to automatic excavation.

Beyond industrial development, automated excavators are needed in workplaces that are hazardous to humans. For example, the US National Aeronautic and Space Administration (NASA) is interested in setting up Lunar and Martian habitats, and it is proposed that automated excavators would do most of the earthmoving work before humans arrive, Singh (1995). Another example is in the remediation of chemical and nuclear waste sites, where safety is of crucial importance to human operators, Singh (1997).

Much of the machinery involved in excavation work has a basic kinematic configuration very similar to that of many industrial robots. Automation of the excavation process through the adoption of robotics technologies would appear to present a possibility for improving machine

utilization and output. Currently, human operators may require two to five years of experience before they can be considered experts. Full, or even partial, automation of earth removal may also be seen as providing further benefits by way of a reduced dependence on operator skill and a lower operator work load, both of which are likely to contribute to a more consistent, higher quality performance. At the same time, increased competition and globalization in the mineral industry has resulted in higher demand for advanced equipment technology.

The automated loading problem entails the design of a system capable of regulating complicated bucket-rock interactions that take place during excavation. A notable amount of previous work have examined this issue, although such work have mostly focused on the excavation of granular material such as soil rather than on rock. Nonetheless such efforts are beginning to promote a move towards automated mobile equipment, including robotic excavation. Although the concept of autonomous excavation has gained some attention in the last decade, few investigations into the development of such technologies have been reported for large and non-homogenous excavation media, such as fragmented rock.

In fact as of today, there is lack of knowledge with regard to the fragmented rock excavation process, and more specifically, with regard to the interpretation of dynamic forces that impact the loader's bucket as it passes through the rockpile. It is perhaps for this reason that effective, systematic techniques for excavation control are yet to be produced for this task.

The surface mining of metals, quarrying of rocks, and construction of highways require the rapid removal and handling of massive quantities of soil, ore, and rock. Typically, explosives or mechanical techniques are used to pulverize the material; thereafter digging machines such as excavators load the material into trucks for haulage to landfills, storage areas, stockpiles or processing plants. As shown in Fig. 1, an excavator sits atop a bench and loads material into trucks that queue up to its side. The operator is responsible for designating where the truck should park, digging material from the face and depositing it in the truck bed, and stopping as may be necessary upon introduction of people and obstacles in the loading zone.

Fig.1: Excavator loading a truck with soil in a typical mass excavation work scenario

1.2 Excavating Machines

These are usually self-powered machines deployed for digging or earth-moving operations in construction sites, road work and mining. In the course of operation, the machines interact with the medium to be loaded or excavated. They have to overcome the resistive force experienced by their bucket when penetrating through a medium. Generally, the penetration is in the form of cutting, digging and scooping.

Some examples are as stated below:

1.2.1 Backhoe

A backhoe, also called a rear actor or back actor, is a piece of excavating equipment or digger consisting of a digging bucket on the end of a two-part articulated arm. They are typically mounted on the back of a tractor or front loader. The section of the arm closest to the vehicle is known as the boom, and the section which carries the bucket is known as the dipper or dipperstick. The boom is attached to the vehicle through a pivot known as the kingpost, which allows the arm to swing left and right, usually through a total of around 200 degrees. Modern backhoes are powered by hydraulics. A typical backhoe is shown in fig. 2 below.

Fig. 2: A Backhoe

Source: http://en.wikipedia.org/wiki/backhoe

1.2.2 Dragline Excavator

A dragline excavator is a piece of heavy equipment used in civil engineering and surface mining.

In civil engineering the smaller types are used for road, port construction, and as pile driving rigs. The larger types are used in strip-mining operations to move overburden above coal, and for tar-sand mining. Draglines are among the largest mobile equipment ever built on land, and weigh in the vicinity of 2000 metric tonnes, though specimens weighing up to 13,000 metric tonnes have also been constructed.

A dragline bucket system consists of a large bucket which is suspended from a boom (a large truss-like structure) with wire ropes. The bucket is maneuvered by means of a number of ropes and chains. The hoist rope is powered by large diesel or electric motors. It supports the bucket and hoist-coupler assembly from the boom. The dragrope is used to draw the bucket assembly horizontally. The bucket is controlled for various operations by skillful maneuver of the hoist and the dragropes. A schematic of a large dragline bucket system is shown in figure 3 below.

Fig: 3. Dragline Excavator

Source: http://en.wikipedia.org/wiki/Dragline_excavator

1.2.3 Wheel Tractor-Scraper

In civil engineering, a wheel tractor-scraper is a piece of heavy equipment used for earthmoving.

The rear part has a vertically moveable hopper (also known as the bowl) with a sharp horizontal front edge. The hopper can be hydraulically lowered and raised. When the hopper is lowered, the front edge cuts into the soil or clay like a plane or cheese slicer and fills the hopper. When the hopper is full, it is raised and closed with a vertical blade (known as the apron). The scraper can transport its load to the fill area where the blade is raised, the back panel of the hopper, or the ejector, is hydraulically pushed forward and the load tumbles out. Then the empty scraper returns to the cut site and repeats the cycle. On the elevating scraper the hopper is filled by a type of conveyor belt with cutting edges.

Scrapers can be very efficient on short hauls where the cut and fill areas are close together and have sufficient length to fill the hopper. The heavier scraper types have two engines ('tandem powered'), one driving the front wheels, one driving the rear wheels, with engines up to 400 kW). Two scrapers can work together in a push-pull fashion but this requires a long cut area. The wheel tractor-scraper is shown in figures 4 and 5 below.

Fig. 4: Wheel Tractor-Scraper

Fig.5: Wheel Tractor-Scraper a typical work scenario

Source: http://en.wikipedia.org/wiki/Wheel_tractor-scraper

1.2.4 Power Shovel

A power shovel is also called stripping, front or electric mining shovel. It is a bucket-equipped machine and it is usually electrically powered. It is used for digging and loading earth or fragmented rock and for mineral extraction. Shovels normally consist of a revolving deck with a power plant, driving and controlling mechanisms, usually a counterweight, and a front attachment, such as a boom or crane which supports a handle with a digger at the end. The machinery is mounted on a base platform with tracks or wheels. The bucket is also known as the dipper.

A shovel's work cycle, or digging cycle, consists of four phases:

- digging
- swinging
- dumping
- returning

The digging phase consists of crowding the dipper into the bank, hoisting the dipper to fill it, then retracting the full dipper from the bank. The swinging phase occurs once the dipper is clear of the bank both vertically and horizontally. The operator controls the dipper through a planned swing path and dump height until it is suitably positioned over the haul unit (e.g. truck). Dumping involves opening the dipper door to dump the load, while maintaining the correct dump height. Returning is when the dipper swings back to the bank, and involves lowering the dipper into the tuck position to close the dipper door. Figure 6 shows a typical power shovel.

Fig 6: Power shovel

Source: http://en.wikipedia.org/wiki/Power_shovel

1.2.5 Bulldozer

Bulldozer, also called Dozer, is a powerful machine for pushing earth or rocks, used in road building, farming, construction, and wrecking. It consists of a heavy, broad steel blade or plate mounted on the front of a tractor. Sometimes it uses a four-wheel-drive tractor, but usually a

track or crawler type, mounted on continuous metal treads, is employed. The blade may be lifted and forced down by hydraulic rams. For digging, the blade is held below surface level; for transporting, it is held at the surface level; and for spreading, it is held above the surface level, as the tractor moves forward.

Fig. 7: Bulldozer

1.2.6. Hydraulic Based Track Excavator

This is also an earthmoving machine. It is commonly used for digging rocks, soil, minerals, etc. A typical hydraulic excavator is shown in figure 8 below.

Fig 8: Hydraulic Based Track Excavator

1.2.7 Underground Mine Loader

This machine is mostly used in underground mining operations. The picture is shown in figure 9.

Fig.9: Undergound Mine Loader

1.3 Need for Automation

Advantages of automation are compelling as an operator's performance peaks early in the work shift and degrades as the shift wears on. Typically, loading a truck requires several passes, each of which takes 15 to 20 seconds. Reducing the time of each loading pass by even a second translates into an enormous gain across the entire job. Scheduled idle times, such as lunch and other breaks, also diminish average production across a shift. All of these factors are areas where automation can improve productivity. Thus automation of the loading task has the potential to provide enhanced productivity, through improved machine utilization and superior machine performance. Unlike a human operator, an automated machine could remain steadily productive, irrespective of environmental conditions for prolonged work hours provided work zone conditions remain the same. Furthermore, an automated loader might generate more accurate loading, making up for shortcomings in operator skill. Finally, operator abuse and machine wear would most likely be diminished through automation, possibly resulting in better machine reliability and reduced maintenance costs.

Automation can improve safety by removing the operator from the machine and by providing complete sensor coverage to watch out for potential hazards entering the work area. Excavator operators are most likely to be injured when mounting and dismounting the machine. Operators tend to focus on the task at hand and may fail to notice other site personnel or equipment

entering the loading zone. The environments in which Loading, Haulage and Dumping (LHD) machines are required to operate tend to be somewhat hazardous in that the loading of ore occurs at underground drawpoints. These drawpoints often pose the danger of experiencing falling or shifting broken rock during loading. In order to increase safety during such operations, remote control and tele-operation technologies have already been developed for LHD operators (Kumar and Vagenas, 1993). The obvious next step is the development of a reliable system for autonomous loading of fragmented rock.

1.4 Statement of Problem

The problem of earthmoving has been an issue of great concern in mining and construction industry with several aspects of the problem being handled by various researchers. Also, within this context, evaluating the forces acting on excavating machines from the bucket has long been a major problem in the field of simulations. Methodology and basic formulations of forces between the tool and the material to be moved as well as the internal forces in the pile to be dug from are areas of utmost concern. The force formulation is based on simple physical parameters such as internal cohesion, density, angle of friction of the material and finally the adhesion between the tool and the granulated material. The model is correlated with measurements and is based on a minimal set of physical parameters that can be easily measured for prediction of excavation forces in materials.

The motivation for this study is hinged in part on the growing demand for a well designed hydraulic excavation system in various cases of application. It is expected that the results from this study can be a basis for meeting the ever increasing demand for robotic excavation where human operators will not be useful especially in hazardous environment.

In concise terms, the statement of the problem is to:

(i) determine the forces acting on excavating machines from the bucket.

(ii) establish methodology and basic formulations of forces between the tool and the material based on physical parameters such as internal cohesion, density, angle of friction of the

material, adhesion between the tool and the material and the internal forces in the pile to be dug.

1.5 Objectives of Study

The objectives of the current research are the following:

(i) To develop a generalised form of dynamic equations governing the motion of the various links of the excavator, the transmitted force and the cutting force of the blade of the excavator bucket.

(ii) To solve the foregoing equations with the aim of simulating the forces acting on excavator bucket when excavating granulated material such as dry sand, and in particular illustrate various specialised cases so as to demonstrate the effect of link length on other variables such as cutting force, transmitted force, etc.

(iii) To derive analytical expression for predicting scooped volume when cutting through a medium such as dry sand by considering various excavation scenerios.

(iv) To develop an analytical model for the bucket trajectory during hydraulic excavation through a medium.

Essentially, this research work intends to answer these set of questions.

- What is the relationship between the various links of the excavator in terms of angular displacement, angular velocity, angular acceleration?
- How can the transmitted force from the links of the excavator be determined?
- How can expression for the cutting force of the excavator be derived?
- What is the optimum range of values of the maximum cutting force?
- How can the various scenarios be extended to real life applications?
- How can optimum scooped volume be achieved?

1.6 Limitation/Scope of the Study

This research is limited to the operations and geometrical dimensions of a hydraulic excavator using Newtonian approach, rigid body dynamics and circular functions. However, the scope of this research work includes the following:

(i) The earthmoving machine considered in this research is an hydraulic excavator.

(ii) All the parts of the hydraulic excavator are assumed to be in good operating conditions.

(iii) The excavation operation is in free swing and through a medium such as dry sand.

Hydraulic excavators are basically an assemblage of linkages. These linkages operate in relative motion to one another. Through the hydraulic mechanism, force is transmitted through the linkages to the excavator bucket and then to the surface of the pile. This is what gives rise to the loading, haulage and dumping exercise. The sketch below illustrates this conceptual framework.

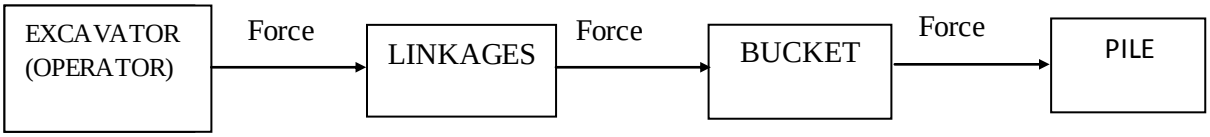

1.7 Overview of the Thesis

In Chapter one, the thesis is introduced. Chapter two presents an extensive review of literature. In Chapter three, a generalized set of dynamic equations governing the motion of the various links of the excavator, the transmitted and cutting forces of the blade of the excavator bucket are derived. In Chapter four is a presentation of the derivation of the model for analytical prediction of scooped volume during hydraulic excavation. Chapter five is the description of the analytical modeling of bucket trajectory during hydraulic excavation. Chapter six is a presentation of simulation results for the effect of cutting force in free swing, as well as in a cutting medium and also the results of analytical modeling of bucket trajectory in hydraulic excavation. Chapter seven is the conclusion which contains the summary of our findings, the contribution to knowledge and identified areas of future work.

1.8 Significance of the Study

There is an ever increasing need for excavators to load materials into trucks for haulage to landfills, storage areas, or processing plants. The robustness and versatility of application areas for rapid removal and handling of massive quantities of soil, ore, and rock in mines and construction sites as well as usage in rescue mission when natural disaster occurs provide a good basis of this research. The advantages of this research can be found in the areas of optimization of excavating technique, enhancement of design analysis and local/global mining application.

The surface mining of metals, quarrying of rock, and construction of highways require the rapid removal and handling of massive quantities of soil, ore, and rock. Typically, explosive or mechanical techniques are used to pulverize the material, and digging machines such as excavators load the material into trucks for haulage to landfills, storage areas, or processing plants.

The operator's performance peaks early in the work shift and falls as the shift wears on. Scheduled idle times, such as lunch and other breaks, also diminish average production across a shift. All of these factors are areas where automation can improve productivity. Safety is another opportunity. Excavator operators are most likely to be injured when mounting and dismounting the machine. Automation can improve safety by removing the operator from the machine and by providing complete sensor coverage to watch for potential hazards entering the work area. This is useful in the following areas viz:

- For operations such as bomb disposal or hazardous material management, which would be potentially dangerous for humans.
- Typically, loading a truck requires several passes, each of which takes 15 to 20 seconds. Reducing the time of each loading pass by even a second translates into an enormous gain across the entire job.
- Scheduled idle times, such as lunch and other breaks, also diminish average production across a shift, hence improved productivity.
- Improved safety.

1.9 Definition of Basic Terms

Mine: An excavation made in the earth to extract minerals.

Mining: The activity, occupation and industry concerned with the extraction of minerals.

Mining Engineering: The art and science applied to the processes of mining and the operations of mines.

Mineral: A naturally occuring substance, usually inorganic, having a definite chemical composition and distinctive characteristics.

Rock: An assemblage of minerals in hardened form or mass.

Ore: Mineral that has sufficient utility and value to be extracted at a profit.

Gangue: Mineral that lacks utility and value when mined.

Mineral Deposit: Geologic occurence of minerals in relatively concentrated form.

Ore deposit: Economic occurence of minerals that can be extracted at a profit.

Excavator: Machine that is used for the rapid removal of soil and other materials in mines, quarries, and construction sites.

Scooped Volume: Volume of pile excavated by the bucket of the hydraulic excavator.

Geometrical parameters: This refers to the lengths of the the linkages and the various angles between them.

1.10 Brief Historic Development of Mining

Mining began with Paleolothic man some 450,000 years ago when flint implements were found with the bones of early man from the old stone age (Lewis & Clark, 1964). He extracted these from the earth and learned to shape them by crude fabrication techniques. At first he was satisfied to recover the stone raw materials from surface excavations but by the beginning of the new stone age, he had progressed to underground mining in systematic openings of 0.6-0.9m height and 9m depth (Storces, 1954). However, the oldest known underground mine is from the

old stone age and is believed to be 40,000 years old, a hematite mine at Bomvu Ridge, Swaziland (Gregory, 1981). Early crude miners employed crude methods of ground control, ventilation, hoisting, lighting and rock breakage. Underground mines attained depths of 250m by Egyptian times. The first notable feat that challenged miners in the excavation of stone or ore in place was how to break it loose from the constraining rock mass. As social systems and culture evolved, mining became more organised. Because of the arduous, hazardous nature of the work, slaves and convicts were often committed to the mines. The greatest impact on the need for and use of minerals, however, was registered by the industrial revolution, coming at the close of the eighteenth century. A chronological development of mining technology and raw materials distribution in Nigeria are shown below in tables 1 and 2 respectively.

Table1: Chronological Development of Mining Technology

S/N	DATE	EVENT
1	450,000 BC	First mining (at surface) by Paleolithic man for stone implements
2	40,000	Surface mining progresses underground in Swaziland, Africa
3	30,000	Fired clay pots used in Czechoslovakia
4	18,000	Possible use of gold and copper in native form
5	5,000	Fire setting, used by Egyptians to break rock
6	4,000	Early use of fabricated metals; start of bronze age
7	3,400	First recorded mining of turquoise by Egyptians in Sinai
8	3,000	Probable first smelting of copper with coal by Chinese; First use of iron implements by Egyptians
9	2,000	Earliest known gold artifacts in the world, in Peru
10	1,000	Steel used by Greeks
11	AD100	Thriving Roman mining industry
12	122	Coal used by Romans in Great Britain
13	1185	Edict by bishop of Trent gives right to miners
14	1524	First recorded mining in New World by Spaniards in Cuba
15	1550	First use of lift pump at Joachimstal , Czechoslovakia
16	1556	First mining technical work, De Re Metallica, published in Germany by Georgius Agricola
17	1585	Discovery of iron ore in North America, in North Carolina
18	1600s	Mining commences in Eastern United States (iron, coal, lead, gold)
19	1627	Explosives first used in Europian mines in Hungary
20	1646	First blast furnace installed in North America, in Massachusetts
21	1716	First school of mines established at Joachimstal, Czechoslovakia
22	1780	Beginning of industrial revolution; pumps first modern machines used in mines
23	1800s	Mining progresses in US; gold rush opens up the West

S/N	DATE	EVENT
24	1815	Sir Humphery Davy invented miner's safety lamp in England
25	1855	Bessemer steel process first used, England
26	1867	Dynamite invented by Nobel, applied in mining
27	1903	Era of mechanisation and mass production begin in US, mining with development of first low-grade copper porphyry, in Utah; while the first modern mine was an open pit, subsequent operations were underground as well.

Source: Hartman (1987)

Table 2: Raw Materials Distribution in Nigeria

S/N	STATE	RAW MATERIALS
1	**ABIA**	Glass sand, limestone, salt, shale, ball clay, galena, granite, marble, lateritic sand, bentonitic clay, phosphate, kaolin, pyrite, feldspar, bentonite, petroleum, lignite, gypsum, sphalerite, clay.
2	**ADAMAWA**	Granite, clay, gypsum, limestone, uranium, kaolin, coal, trona, baryte, salt, sand, ilminite, marble, magnesite, lateritic clay
3	**AKWA IBOM**	Clay, glass sand, salt, Silica sand, granite, coal, petroleum, natural gas, kaolin, limestone, lignite
4	**ANAMBRA**	Clay, iron stone, natural gas, petroleum, sand stone, kaolin, pyrite, lignite
5	**BAUCHI**	Kaolin, trona, gypsum, cassiterite, mica, clay, tantalite, galena, iron ore, gemstone, sphalerites, silica sand, granite, baryte, columbite, zinc, lead, muscovite, quartz, columbite, tin, glass sand, salt, monazite, feldspar, graphite, wolfram, coal, agate, tantalum, calcophyrite (traces), rutile, tungsten, copper, talc, ilmenite, zircon
6	**BAYELSA**	Salt, petroleum, natural gas, silica sand
7	**BENUE**	Bentonite, crude salt, petroleum, limestone, glass sand, gemstone, barytes, feldspar, marble, mica, silica sand, quartz, galena, brine (salt solution), lead, zinc ore, silica sand, clay, coal, gypsum, kaolin, anhydrite, calcium, sulphate, brick clay, crushed and dimension stone, fluorspar, wolframite, bauxite, shale, magnetite, ilmenite, brenite.
8	**BORNO**	Silica sand, natural salt, sapphire, topaz, mica, quartz, gypsum, uranium, iron ore, alluvial, magnesite, feldspar, granite, aquamarine, nepheline, limestone, kaolin, bentonite, laterite clay, refractory clay,trona, gold, tin, kaolinitic clay, potash, fullers earth, diatomite.
9	**CROSS RIVER**	Salt, limestone, coal, manganese, mica, ilmenite, gold, quartz, glass sand, tourmaline, petroleum, natural gas, kaolin, tin ore, mica, sharp sand, clay, spring water, salt deposits,

S/N	STATE	RAW MATERIALS
		talc, granite, galena, lead zinc, tin ore, goethite, muscovite, pure quartz, uranium, barytes
10	**DELTA**	Kaolin, lateritic clay, gravel, silica sand, lignite, natural gas, petroleum, ball clay, crude oil, bauxite, granite, river sand, clay, spring water.
11	**EBONYI**	Lead/ zinc, salt, limestone, ball clay, refractory clay, gypsum, granite
12	**EDO**	Charnockite, copper, gold, marble, granite, gypsum, petroleum, diorite, lignite, limestone, ceramic clay
13	**EKITI**	Clay, Charnockite, quartzite, lignite, limestone, granite, gemstone, bauxite, cassiterite,columbite, tantalite, feldspar, kaolin
14	**ENUGU**	Lateritic clay, crude oil, kaolinitic clay, ball clay, iron ore, glass sand, petroleum, gypsum, coal, silica sand, ceramic clay
15	**FCT**	Kaolin, Limestone, Granite, Marble, Feldspar, Mica, Dolomite, Clay, Sand, Talc
16	**GOMBE**	Graphite, kaolin, limestone, silica sand, uranium, coal, halites, clay, gypsum, diatomite, granite
17	**IMO**	Crude oil, shale, natural gas, kaolin, laterite, sand, limestone, salt, marble, gypsum, clay
18	**JIGAWA**	Glass sand, granite, laterite clay, silica, kaolin, iron ore, quartz, potash, talc, limestone
19	**KADUNA**	Muscovite, granite, gold, manganese, clay, graphite, sand, zir con, kyanite, tin ore, ilmenite, gemstone, columbite
20	**KANO**	Clays, laterite, cassiterite, columbite, ilmenite, galena, phyrochlorite, kaolin, gemstone, silica sand, tin ore, monazite, wolframite, thorium, granite, rhyolite, kaolin, beryl, amethyst, gold,
21	**KATSINA**	Gold, Manganese, Lateritic clay, Feldspar, Black tourmaline, Amethyst, Quartz, Kaolin, Mica, Gypsum, Silimanite, Clay, Granite sand, Uranium, Asbestos, Tourmaline, Serpentinite (Chrysolite asbestos), Chromite, Ilmenite & Diamond, Graphite, Iron–ore, Potash, Silica sand
22	**KEBBI**	Salt, Iron ore , Gold, Feldspar, Limestone, Quartz, Bauxitic clay, Manganese, Kaolin, Mica
23	**KOGI**	Clay, Iron ore, Gemstone, Marble, Limestone, Feldspar, Dolomite, Phosphate, Mica, Cassiterite, Granite, Ornamental stone, Coal, Kaolin.
24	**KWARA**	Clay, Kaolin, Silica sand, Quartz, Dolomite, Marble, Feldspar, Gold, Tantalite, Cassiterite, Granite, Limestone.
25	**LAGOS**	Silica sand, Bitumen, Sharp sand, Gravel, Petroleum, Laterite
26	**NASSARAWA**	Cassiterite, Gemstone, Amethyst, Berly, Chrysolite, Emerald, Garnet, Sapphire, Topaz, Barytes, Galena, Salt, Monazite,

S/N	STATE	RAW MATERIALS
		Zircon, Glass sand, Coal.
27	**NIGER**	Ball clay, Kaolin, Limestone, Granite, Glass sand, Iron ore, Red clay, Feldspar, Gold, Graphite, Cyanite, Silica sand, Quartz, Asbestos, Marble, Talc, Gemstone.
28	**OGUN**	Kaolin, Feldspar, Silica sand, Mica, Granite, Clay, Phosphate, Gypsum, Limestone, Quartz, Tar sand
29	**ONDO**	Marble, Gold, Gemstone, Clay, Diorite, Lignite
30	**OSUN**	Clay, granite , talc, dolomite, ilmenite, feldspar, quartz, limestone, mica, clay, gold
31	**OYO**	clay, feldspar, granite, ilmenite, iron ore, kaolin, quartz, talc, marble, dolomite, tourmaline, aquamarine, amethyst
32	**PLATEAU**	Monazite, columbite, feldspar, clay, cassiterite, gemstone, kaolin, dolomite, mica,zircon, marble, ilmenite, barytes, quartz, talc, galena
33	**RIVERS**	Petroleum, natural gas, silica sand, glass sand, clay
34	**SOKOTO**	Silica sand, clay, salt, limestone, phosphate, gypsum, kaolin, laterite, salt lakes, potash, granite
35	**TARABA**	Graphite, feldspar, iron ore, muscovite, glassy quartz, fluorspar, garnet, tourmaline, sapphire, zircon, tantalite, columbite, cassiterite, baryte, galena, gypsum, limestone, laterite, brine (salt solution), calcite, bauxite, magnetite, pyrite, salt (evaporates),lead/zinc ore
36	**YOBE**	Salt, trona, diatomite, clay, gypsum, kaolin, silica sand, limest one, epsomite, iron ore, trona, shale, uranium , granite, bentonitic clay
37	**ZAMFARA**	Gold, Alluvial gold, Granite, Chromite, Charnockite, Clay, Feldspar, Spring water

Source: http://www.rmrdc.gov.ng

CHAPTER TWO

LITERATURE REVIEW

2.0 Preamble

This chapter gives a detailed review of literature of various aspects of excavation. Several researchers have worked in the various fields of robotic excavation using different types of models. Some of these areas are highlighted below.

2.1 Excavator Kinematics

Kinematic models deal only with considerations of space and time. Kinematics problems can be expressed either in form of forward kinematics or inverse kinematics. The inverse kinematics problem is simply stated as, "Given the desired position of the robot's hand, what must be the angles at all of the robot's joints?". This is in contrast to the forward kinematics problem, which is, "Given the angles at all of the robot's joints, what is the position of the hand?" Humans solve the inverse kinematics problem constantly without conscious effort. For example, when eating cereal in the morning, humans reach out for their spoons without considering the relative configuration of their shoulder and elbow required to reach the spoon.

Also, the forward kinematics relating joint angles to the positions of the boom, arm and bucket are most useful for simulating the environment of the machine. Given a path for the excavator bucket to follow, the inverse kinematics relationship provides joint angle reference for the machine. Furthermore, the inverse relationship provides a method of determining if a hypothetical bucket pose is reachable. A pose of the bucket might not be reachable because it requires joint angles beyond the limits of the machine or because it is outside the workspace of the excavator. Both of these conditions are detectable through inverse kinematics solution.

Kinematic models involve purely geometric relationships and have been used to describe robotic motion in both known and unknown environments (Ayomoh, 2008), (Asaolu, 2002), (Olunloyo and Ayomoh, 2009, 2010, 2011), (Olunloyo et al. 2009), (Ibidapo-Obe and Asaolu, 2006), (Ibidapo-Obe et al. 1999, 2002, 2011). In the case of excavator motion, some researchers have

worked in this area. Vaha et al. (1991) derived the kinematic relationships that relate the joint angles of a backhoe excavator to the pose of the bucket tip by defining various coordinate frames. However, the coordinate frames are often not assigned systematically. Moreover, the relationships between the joint shaft angles and the positions of the cylinder rods in the hydraulic actuators are not always given.

Kiovo (1994), developed a complete kinematic model for an excavator (bachhoe and loader) by following Denavit-Hertenberg guidelines to derive the forward and inverse kinematic equations representing the pose of the bucket based on the angular positions of the joints and the lengths of the hydraulic actuators.

2.2 Excavator Dynamics

While kinematic models have a purely geometric basis, dynamical models capture considerations such as force, acceleration, inertia and friction. The purpose of such models is to relate joint torques and external forces to the motion of the excavator links. The forward dynamic model is used for simulation: given the joint torques and external forces and moments, the motion of the entire machine can be predicted. The inverse dynamic model offers greater utility. It provides a reference joint torque trajectory given the desired end-effector motion and external forces.

Langrangian approach considers the constraints and kinematics first. Then the equations of motion are written, one for each degree of freedom. In Newtonian approach, we first write the force and moment balances for all bodies separately and then use kinematical relations and the constraint forces to reduce the number of equations. Also, Langrangian approach uses velocities and scalar quantities while Newtonian approach uses accelerations and vector quantities. The Newtonian approach was used as a method of solution for the dynamic analysis carried out in this thesis.

A Langrangian formulation of wheel loader dynamics where the machine is modelled as a three-link manipulator was proposed by Serata et al. (1995). The model captures the second order effects of centripetal and Coriolis forces due to the linkage mass and end-effector load.

Lawrence (1995) used a similar formulation to model an excavator backhoe modified for a forestry application. According to him, these two models are chiefly relevant for trajectory control when the bucket is moving through free space as opposed to the contacting terrain.

Vaha (1991) proposed a model based on the Newton-Euler approach to dynamical modeling. The model developed is, however, intractable. In fact, its interpretation raises a number of general questions: for example, many of the symbols used are not defined.

2.3 Fragmented Rock Excavation

Hemami and Danneshmend (1992) in a pioneering exercise, derived the kinematics and performed a force analysis for a generalized LHD (Load, Haul, Dump) loader mechanism. The work presented an analytical study of the loader mechanism geometry and the required hydraulic cylinder forces through treatment of the mechanism as a robot manipulator.

Hemami (1992) acknowledged that the trajectory control of standard industrial robots (e.g. welding or cutting robots) is different from the control required for loading of an LHD bucket. He suggested that the trajectory a loader bucket should follow through the rock pile should not have priority in the control scheme, since the objective is to effectively fill the bucket, not to follow a strictly specifed path. Some conceptual discussion was also provided on the topic of motion control. The forces acting on the bucket were described as potentially stochastic in nature, and the need for trajectory alteration in the event of detected prematurely high loads on the bucket was stated.

Also, Hemami (1992,1993,1994) divided the possible bucket-rock interaction forces into five major components. Ways of analytically determining, or at least approximating, some of these dynamic forces were subsequently presented. The following reasons were also given for the complexity of the excavation problem: Firstly, the shape, size, geometry and composition of the cutting device may vary from machine to machine. Secondly was adding teeth to the cutting edge changes the scenario, and lastly, material properties were determined by many factors, including hardness, cohesion, uniformity, water content, temperature, size, and compactness.

Hemami (1993a,b) presented a method for determining an appropriate bucket trajectory. However, a method for tailoring the derived loading trajectory was not explained in any detail, and its potential effectiveness at completely filling the bucket was not determined.

Hemami (1994a,b,c) later repeated the works described above with some additions that are worth noting. He formulated a mathematical model for the variation of one of the forces using the knowledge of the geometry developed during the loading operation. He also concluded that analysis of the force should be done experimentally.

Hemami (1995) provided a fundamental analysis required for the design of an automated excavation machine where he considered a mass-spring-damper model for the excavation machine, as well as the excavation media. However, it was suggested that this type of model cannot be used in practice, since there is insufficient understanding of the mass, spring, and damper coefficients.

2.4 Excavation Planning

Some researchers have also worked on the problem of autonomous rock excavation from a perspective similar to Hemami's. Sarata et al. (1998) proposed a generalized machine dynamics, although not actually computed.

Singh and Simmons (1992) proposed a methodology to automatically generate plans for a robot excavator like a bucket loader or a backhoe. The task was formulated as one of constrained optimization in an action space that is spanned by the parameters of a prototypical digging plan. The work showed how geometric and force constraints are imposed on the action space to build the set of feasible plans, and discussed methods to optimize a cost function within the set. The proposed approach is not only a means to a solution for robotic excavation, but also a means of analysis and learning about how to represent the task.

Under a pioneering Russian project, Mikhirev (1983,1986) formulated a set of ideas relating to force, motion, and trajectory control for various loader mechanism styles. Mikhirev's analysis

was based on a technique using work functions to find an efficient bucket trajectory that would minimize the work for scooping rock masses, with complete filling of the bucket. Additional constraints were determined by the bucket capacity, the natural slope angle, and the pile height. He advocated that measurement of the resistive forces to excavation could be used as a signal for automatic activation of the mechanism used of bucket rotation in the vertical plane (i.e., motions of the dump cylinder).

2.5 Teleoperation

Here, the excavator is controlled by levers mounted on a remote control panel in the machine cabin. In some cases, the operator controls a "master", a scaled-down replica of the excavator, while the excavator itself behaves as a "slave". When using the "master-slave" system, the control of the excavator is said to be more intuitive. Instead of controlling the joints individually, the operator controls the excavator bucket directly.

Quite a number of researchers have addressed aspects of automated earthmoving, of which the lowest and most common level of automation is teleoperation (Singh,1997). Teleoperated excavators are used in applications that pose a danger to humans, such as the uncovering of buried ordnance (Nease & Alexander,1993) and waste (Burks et al. 1992 & Wohlford et al. 1990) or excavation around buried utilities. A higher level of autonomy is achieved by systems that share control of the excavation cycle with a human operator. Typically, these systems concentrate on the process of digging, Bradely et al. (1993), Bullock and Oppenheim (1989), Xuang and Bernold (1994), Lever et al. (1994), Rocke (1994), Sakai and Cho (1988), Salcudeen (1997), Sameshima and Tozawa (1992), Seward et al. (1992). An operator chooses the starting location for the excavator's bucket and a control system takes over the process of filling the bucket using force and/or joint position feedback to accomplish the task. At the next level of autonomy are systems that automatically select where to dig. Such systems measure the topology of the terrain using ranging sensors and compute dig trajectories that maximize excavated volume, Feng et al. (1992), Singh (1995a,b), and Takahashi et al. (1995). At the highest level of autonomy are systems that sequence digging operations over a long period (Bullock and Oppenheim, 1989, Romero-Lois, 1989, Singh and Cannon, 1998).

Kojima et al. (1990) described a tele-operated backhoe used for digging deep footings. The operator watches a video monitor while operating a master control mechanism.

Nakano (1989) demonstrated a prototype controller for a backhoe excavator that allows an operator to control the bucket in Cartesian coordinates and to perform slope control. In this case, the operator is able to directly specify the motion of the bucket, rather than that of the joints. Bearing in mind that force information plays an important role in the control of an excavator, some attention has been focused on force-reflecting master-slave systems.

Vaha et al. (1991) proposed a method that provides force feedback to a tele-operator using a kinematically equivalent master to control the excavator position and provide joint-level force feedback. In contrast, researchers at the University of British Columbia (UBC) proposed a system that provides force feed-back in rate mode using a six degree of freedom magnetically-leviated hand controller, Parker et al. (1993), Lawrence (1995). The UBC system uses a dynamical model of the excavator to control the joints such that a smooth trajectory is produced at the bucket.

Other authors have approached the problem of autonomous rock excavation from another perspective. Machine vision has been put forward as a means for autonomous loading of mining machines. Ji and Sanford (1993) developed a laboratory-scale excavation system that utilized a video camera for environment sensing. Digitized images were then interpreted to develop control and navigation signals.

Using machine vision, Petty et al. (1997) developed a scale model which was constructed to mimic the motions of an LHD vehicle as closely as possible. A loading strategy was formulated such that the bucket followed one of a range of trajectories developed for various rock pile conditions.

At Tohoku University in Japan, a group of researchers used a CCD camera vision system to obtain images of the rock pile, from which the excavation task was planned based on an

estimated contour of the rock pile (Takahashi et al. 1998). Based on experiments performed using a scale model excavator, the authors suggested that such a camera based system would be advantageous in its capability for recognizing changes in rock pile shape at each iteration towards the excavation goal. Despite the results, it was conceded that illumination would become a problem that would likely be compounded in an underground mining situation.

2.6 Control Design

Electrohydraulic actuators have been widely used in industrial systems for a long time. A wide variety of control design techniques have been used, ranging from linear control to robust adaptive control.

Considering linear control, hydraulic servo control problems are generally treated as position control problems (Viersma, 1990), as velocity control problems, generally for rotary drive applications (Merritt, 1976), or as force control problems (Chen and Lu, 1985). In some applications, motion control problem is treated as a force control problem at the actuator level, (Heintze, 1997).

Linear Control techniques such as classical feedback control (Viersma, 1990), frequency domain techniques (FitzSimons and Palazzolo, 1997) are widely applied. Proportional, Integral and Derivative (PID) controllers have been proposed as solution in most cases. Both initial tuning and maintenance of good tuning of a PID controller, as indicated by (Ozsoy et al. 1994) is generally time-consuming.

Modern applications of robust control techniques found in literature also show better performance than classical model-based control design techniques. As the uncertainties of parameters such as the bulk modulus and the inefficient stroke for cylinders can be around fifty percent, very conservative controllers will result from these methods. In addition, both the control design procedure and the resulting controller are so complicated that the practical use of such control design may be questioned.

Other researchers have utilized acceleration feedback control for tracking purposes to obtain high performance hydraulic servomechanisms (Tafazoli, 1998). In a research by FitzSimons and Palazzolo (1997), the root locus method was used to find the controller gain for a single-rod

hydraulic excavator. According to Welch (1962), the quadratic resonance phenomenon that is generally observed in transfer functions relating the load velocity to the servovalve current was addressed. Acceleration feedback was shown to be an effective way of damping the hydraulic system in order to achieve a higher bandwidth. Welch assumed that the load was purely inertial and used pressure measurements to calculate accelerations. By using a linear analysis of system dynamics, the effectiveness of adding a pressure feedback term as a minor feedback loop to a conventional Proportional, Derivative (PD) controller was verified. Welch also suggested high-pass filtering the pressure feedback signal in the frequency range of load resonance where he named the approach "derivative pressure feedback" and presented experimental results using a hydraulic motor. Matsuura (1994) employed a similar technique for damping the resonance of a hydraulic cylinder in an industrial application. Tafazoli et al. (1998) used the same approach with a heuristic method to choose the controller gain where an observer was used to estimate frictional effects. However, the main contribution of tafazoli's work lies in the development of a new nonlinear observer, which is based on the Friedland-Park Coulomb friction observer (Friedland and Park, 1992).

Linear hydraulic system control methods are based on local linearization of the non-linear dynamics about a nominated operating point, such as the servo valve spool null position, and a nominal loading configuration. The nonlinearities and parameter variations from the nominal operating condition will then act as plant uncertainties.

There are, however, definite setbacks to this approach. First, nonlinearities such as asymmetric actuators and transmission nonlinearities will cause gain uncertainties over the whole frequency range. Secondly, variations in the volume of the trapped fluid of load inertia represent uncertainties in the natural frequency. Since all such uncertainties influence the system gain in the range from DC to the cross-over frequency, they have a direct impact on the bounds of achievable performance. To guarantee robustness, it is necessary to typically design the controller for the worst case condition: that is, for the system with the highest gain, lowest natural frequency and minimum resonant mode damping. This design strategy sacrifices performance over the lower frequencies range by providing robustness at higher frequencies and produces closed-loop systems with overly sluggish responses. Since for the best performance it is

essential that the low frequency uncertainties be minimized, an approach differing from local linearization is necessary.

Related research in adaptive learning and control shows that the controller can be given learning capabilities in the case of repetitive tasks. Examples given by Yao et al. (1997) are self-turning regulators, adaptive learning controllers and the non-model-based technique of neural networks. In the case of self-tuning regulators, tuning parameters for a well-designed hydraulic servo system is a straight forward task that does not need a specific parameterized model. An arbitrary placement of the poles, according to design transcient requirements, is not possible with this method.

In order to compensate for time-varying effect, Kulkarni et al. (1984) and Chen and Lu (1985) investigated model reference adaptive control (MRAC). These investigations deal with the positioning control of linearised hydraulic systems without external load disturbances.

2.7 Towards Automation

Automated excavation tasks can be divided into a number of levels and sorted by increasing level of abstraction. The lowest level is that of tele-operated machines. The operator is physically removed from the machine but it is still required to control the joints much in the same manner as the original machine was controlled.

An autonomous rock excavation system for front-end-loader type machines that uses bucket force/torque feedback, fuzzy logic, and neural networks for control was proposed by researchers at the University of Arizona (Lever and Wang,1995, Lever et al. 1996 and Shi et al. 1996). Lever and Wang (1995) justifed their approach by stating that a mathematical model for the bucket-rock interaction would be too complex and computationally expensive. Instead, a set of basic bucket action sequences, typically used by human operators, was compiled for use by the controller where a method using finite-state machines (FSMs) was described.

Stenz et al. (1998) demonstrated an autonomous loading system for excavators which is capable of loading trucks with soft material at the speed of expert human operators. The system uses two

scanning laser rangefinders to recognize the truck, measure the soil on the dig face and in the truck, and to detect obstacles in the workspace. The system modifies both its digging and dumping plans based on settlement of soil as detected by its sensors. Expert operator knowledge is encoded into templates called scripts which are adjusted using simple kinematic and dynamics rules to generate very fast machine motions. The excavator's software decides where to dig in the soil, where to dump in the truck, and how to quickly move between these points while detecting and avoiding obstacles. The system was fully implemented and was demonstrated to load trucks as fast as human operators.

Marshall (2001) revisited the autonomous excavation problem for fragmented rock with particular focus on the problem of autonomous excavation using load-haul-dump (LHD) underground mining machines where he presented the results of pioneering full-scale experimental studies. These studies were carried out with the intent of identifying the evolution of machine parameters during free-space motions of the employed LHD mechanism, and during a selection of excavation trials conducted by skilled operators in fragmented rock typical of an underground hard-rock mining scenario.

Having reviewed the conventional techniques for development of robot dynamical equations of motion, the results are presented of modelling the LHD loader mechanism motions in free-space and while in contact with a rock pile using the nonlinear system identifcation technique known as parallel cascade identifcation (PCI). Although the resulting identifed models were not as accurate as might have been hoped for, it was concluded, through subsequent observations, that an excavation control system might be realizable by interpretation of measured forces in the LHD machine dump cylinder as an indication of bucket-rock interaction intensity. Based on these fndings, he provided a framework for an admittance-type control system, where the bucket is commanded to respond to sensed cylinder forces with prescribed dynamics, providing a basis for the autonomous excavation of fragmented rock.

2.8 Related Researches in Excavation

In the work concerning the shear properties of fragmented rock, Forsman and Pan (1989) suggested an improvement over Coulomb's equation, commonly used for modelling fine grained

materials, in the form of a mathematical expression, derived empirically, for the shear strength of large grained loose material. Material porosity was implied to be related to the size distribution of a fragmented rock pile, as well as the degree of interlocking between particles. In addition, they related the material porosity to fluctuations of the measured normal force in their experimental results.

Fabrichnyi and Kolokolov (1975) proposed a means for calculation of the scooping resistance to blasted rock based on knowledge of the rock pile's changing shear angle. They found out that the experimentally recorded variations in the scooping resistance can only be due to changes in the inclination of the shear surface, leading to increases or decreases in the volumes of rock being shifted.

In related work, Mikhirev (1983) reported some potentially applicable results. Although techniques for control and bucket trajectory generation were the focus of this research, insight into the forces associated with resistance to movement of the bucket through rock was provided. Mikhirev cited the experimental research of Rodionov, which apparently established that a compact nucleus is created in the pile in front of the working edge of the bucket. The characteristics of this compact nucleus were found to relate most notably to average particle size, bucket shape, and bucket pose.

Singh (1995a), a researcher at Carnegie Mellon University proposed a technique for robotic excavators to predict resistive forces during excavation and to improve its predictions based on experience using computer learning methods. He presented a development of the mechanics of excavation, resulting in the formation of what is known as the fundamental equation of earthmoving (FEE) for a flat blade moving through soil. He used assumptions required to validate the FEE were to demonstrate its impracticality in the context of excavation. A simple analytical model of a flat blade moving through soil and how this analysis can be extended to account for the phenomena specific to excavation was presented. In addition, he examined how representation of the learning problem and methodology affect prediction performance using several criteria.

Further research work at Carnegie Mellon University resulted in a patented system for robotic excavation and autonomous truck loading (Bares et al. 2000 & Rowe, 2000). The system described utilized two scanning laser rangefinders to recognize and localize the truck, measure the soil face, and detect obstacles. Onboard software was used to make decisions regarding digging and dumping operations. Actual digging was described as executed by a force based closed loop control scheme, after previous research in excavation planning by one of the authors. Dumping and truck detection routines were also included as part of the work.

Ericsson and Slättengren (2000) proposed a method of simulating the forces acting on a wheel loader or excavator shovel when excavating granulated material such as gravel or seed. The force formulation, which can be adapted to different types of material, is based on simple physical parameters viz: internal cohesion, density, angle of friction of the material and the adhesion between the tool and the granulated material. The model was implemented in an ADAMS model of a wheel loader in the form a general force subroutine and is used by Volvo Wheel Loaders to predict the forces acting on the machines during digging cycles in different materials. The method has been verified with measurements of cylinder pressures from excavation of coarse gravel and the correlation is excellent.

In his work, Singh (1995b) presented methods for a robot to predict the resistive forces and to improve its predictions based on experience. He stated a simple analytical model of a flat blade moving through soil and showed how this analysis can be extended to account for the phenomena specific to excavation. In addition, he examined how representation of the learning problem and methodology affects prediction performance using several criteria. Upon experimental evaluation, he found that representation based on physical models is superior to a naive representation based purely on geometry.

There has been some research on the operation of earthmoving machinery by Alekseeva et al. (1992) and Zelenin et al. (1992) that explicitly addresses the issue of estimating forces necessary to overcome the shear strength of soil. Unfortunately, this work is mostly stated in empirical

terms for specific types of machines and it is not clear how to extrapolate the methodology for arbitrary mechanisms.

Hemami and Daneshmend (1992) studied force analysis for automation of the loading operation in an LHD loader. In the work, the force requirement in the (hydraulic) actuators and the vehicle push were found in terms of the external force/torque at the cutting edge that the machine must overcome, and the instantaneous configuration of the loader bucket. The study was based on analysis of the motion as a robot manipulator. Determination of the required forces was achieved by considering the loading mechanism as a slow manipulator (static loads), through the Jacobian matrix. The Jacobian of the manipulator was analytically found in terms of the physical dimensions and the measurable angles and also considered the joint variables for manipulation, which can be used for velocity relations when necessary.

Kiovo et al (1996) presented a dynamic model for an excavator performing a digging formation using Newton-Euler's formation. Equations of motion were derived by first presenting the velocities and accelerations of the gravity centres of the links as forward difference equations relative to the link number. He then described the equations for the forces and the torques acting on the links by backward difference equations relative to the link number. By combining the equations, the dynamical model for the joint variables was obtained, which is in a form similar to the equation of motion of robotic excavators. The model derived systematically corrects several inadequacies that appear in previously published Vaha and Skibniewski (1993) model of excavators. He presented simulations that illustrate the use of the proposed dynamical model and the performance of the proposed scheme. The dynamical model obtained can be used as the basis for automating the operations of excavators. The approach presented can be well applied to the operation of backhoes.

Blouin et al. (2001) reviewed previous investigations on forces encountered during earthmoving processes by cyclic (but nonrotary) excavation machines with the aim of integrating the formulation for cutting and penetrating forces with those for excavation. The work presented common practices for characterizing an unfrozen medium and the associated tool actions, followed by a general overview of various models describing earthmoving tasks of penetration, cutting, and excavation. Observation and analysis of cutting and excavation models revealed that

there is not a common ground for their validation, but it also identified a core of key parameters, reduced in number and essential to any further excavation model. The work suggested a normalized experimental verification and comparism of the models before they can be further used.

Marshall et al. (2008) presented the results and subsequent analysis of full-scale excavation experiments aimed at developing a practical understanding of how actuator forces evolve during excavation and how they relate to the interactions that occur between an excavator's end-effector and its environment. The focus is on the excavation problem for fragmented rock, as is common in mining and construction applications. He postulated an example admittance-type autonomous excavation controller based on an analysis of the experimental data. The main contributions of the work are the disclosure of experiments and subsequent analyses, resulting in a practical understanding of the excavation process. For example, distinct phases of excavation were identified. Specifically, it was determined that information contained within the dump cylinder force and motion data is sufficient to reveal the bucket-rock interaction status and, hence, serve as a feedback signal.

Also, researchers from the University of Arizona, (Lever and Wang, 1995 & Shi et al. 1996) proposed an autonomous excavation system for front-end-loader style machines that uses bucket force/torque feedback, fuzzy logic, and neural networks for control. In their approach, a set of basic bucket action sequences, typically used by human operators, was compiled for use by the controller. A reactive approach, using fuzzy behaviors, was designed to act on force/torque data in order to assess the excavation status and determine an appropriate control input. Experimental results, using a PUMA 560 arm, were reported.

Hemami (1994), in his work about the trajectory of motion during scooping, considered automatic loading based on modeling a loader as a robot manipulator and carried out analysis of the forces concerned in the process of scooping from the information about the kinematics of motion. Based on the results of a preliminary study on the nature of the forces involved, and bearing in mind the preference for simplicity in the control action, he determined an easy to follow trajectory for the cutting edge of the bucket of a loader, which is regarded as the end-effector in a robot manipulator. He discussed the way to find a minimum energy consuming

trajectory for each individual bucket and for a particular material to be loaded. This work studies the motion pattern. The cutting edge of a loader bucket is considered as the end effector in a robotic arm. Based on an analysis of the resistive forces that act on the bucket, he concluded that with a proper choice of bucket trajectory, certain force components can be reduced to zero, leading to availability of more power. Such a motion can further be customized for minimum energy consumption. He also derived a systematic way of determining this trajectory for the cutting edge of a bucket. Availability of more power can be used for speeding up the loading operation.

Some studies have been carried out in the area of automation of wheel loaders (Tsubouchi et al. 2002). Their scheme involved the solution to three composite problems. Firstly was the problem of obtaining suitable rock pile models for designing (Takahashi et al. 1999), (Carter and Alleyne, 2003), (Tan et al. 2005). Secondly was generating bucket trajectory for scooping soil efficiently (Hemami, 1994), (Singh & Cannon, 1998), (Sarata et al. 2001), (Zhang et al. 2001), (Sarata et al. 2003) and lastly, development of controllers which is applicable to the environment with changing external factors (Osumi et al. 2004).

Saeedi et al. (2005) presented a vision-based control system for a tracked excavator. The system involves several controllers that collaborate to move the excavator from an initial position to a goal state. The work addressed both path tracking accuracy and slippage control problems.

Serata et al. (2004) proposed a method for appropriate arrangement of bucket trajectory for scooping motion where the relation between resistance force and advancing direction of the bucket is analyzed theoretically. In scooping procedure, scooped volume is estimated using 3D model obtained with stereo-vision system. The results of the developed method and system show good performance for different conditions of pile.

Dimajo et al. (2001) developed an excavator simulator to facilitate the training of human operators and to evaluate control strategies for heavy-duty hydraulic machines. The simulator comprises an impedance model of the excavator arm, a model for the bucket-ground interaction forces, a graphically rendered visual environment, and a haptic interface.

Fox et al. (2002) presented the dynamics of actuator mechanisms using a multibody modelling approach to concisely express the structure of the system equations. The Lagrange equations were used to obtain the Newton–Euler equations to which constraint equations are augmented to form a system of differential algebraic equations. The results show the nature of the actuator dynamics involved in maintaining specified bucket trajectories.

Yu et al. (2010) investigated modeling and remote control issues of industry excavators and proposed architecture for remote- controlling such.

Bodur et al. (1994) developed the cognitive force control for the automation of the land excavation to include the dynamics of the excavator arm. He proposed the control of the forces of the arm by regulating the digging depth and the trajectory speed.

Kusmierczyk et al. (2008) presented excavation process optimization for backhoe excavator. Test rig and developed soil preparation methodology were used to solve the problem of excavation process optimization. Results show that optimal trajectory was achieved with automatic control of the bucket movement and measurement system.

Ridley and Corke, (2001), examined the feasibility of automation of dragline bucket excavators to strip overburden from open pit mines. The work focused on the automatic control of the bucket carry angle and bucket trajectory. He devised and implemented a strategy for automatic control of carry angle using bucket angle and rate feedback.

Related work concerning the control of autonomous excavators (Bradely et al. 2004) uses task-centred goal oriented planning structures which define goals for a specific trench excavation task based on real operator behaviour (Sakaida et al. 2006).

Serata et al. (2005) developed a method for planning of scooping point and approach path in the loading operation of wheel loader. The planning of scooping position and direction was obtained through processing pile model.

Ha et al. (2000) used a robust sliding controller technique that implements impedance control for a backhoe excavator to solve the problem of tracking performance with attenuation vibration at the bucket-soil contact points where the piston position and ram force can be obtained. The

technique can provide robust performance when employed in excavation with soil contact consideration.

Research on machine kinematics and dynamics is a key to understanding and improving their operator performance. In their work, Frimpong et al. (2002, 2003) advanced excavator dynamics to simulate the excavator boom-dipper teeth interactions with in-situ formation and muckpile.

Lee and Chang (2001) proposed a TDCSA (Time –Delay Control and Switching Action) using an integral sliding surface for the control of heavy duty robotic excavator. Their experimental results show that the proposed control achieved better tracking performance than an expert operator.

In trajectory Control, a major complication in the control of an excavator is that the interaction force during contact with the terrain can be significant. Simple trajectory control almost never suffices unless the mechanism can completely overpower the soil resistance during digging. Most methods that control the bucket during earth-moving operations therefore involve coupled force and position feedback.

A simple control scheme is to use symbolic rules to choose between various control actions. For example, researchers at the University of Lanchaster, England, developed an automated excavator (LUCIE) that uses a rule-based method to dig trenches (Bradly and Seward, 2004). Digging is broken down into three phases: penetrate, drag and empty. The excavator is not only designed to follow a predetermined path but also has rules that allow it to react to conditions encountered during the excavation.

Researchers at the University of Arizona implemented a fuzzy-logic baseddigging system, Lever et al (1994), Xiaobo et al. (1998). A wrist force-torque sensor and a small shovel mounted on a Puma robotic manipulator was used to demonstrate digging through sand. Instead of looking at the velocities of the links, their system uses the forces and torques observed during digging.

Rowe and Stenz (1997) described a method of parameterising the motion of an excavator during a “bench loading” cycle. They proposed a “template” that encodes the skill of expert operators performing the task of moving the bucket from a dig surface to a truck.

Bhaveshkumar et al. (2011) analysed the excavation forces necessary to cut the soil by the excavator bucket in order to improve the design of the bucket teeth, the leap plate of the bucket, and the side cutting plates. The method used for calculating the excavation force is based on 2D analytical soil-tool interaction models.

Aluko and Seig (2000) presented the transition between two failure modes which occur and are governed by certain soil and implement factors, namely blade rake angle, soil strength and soil-blade interface condition. These factors provides a basis for the reliable prediction of the failure type, and hence the quality of soil tilth expected in two-dimensional soil cutting operations.

Bhaveshkumar and Prajapati (2011), carried out a review on soil-tool interaction is divided in three different parts namely soil-tool model forresistive forces and trajectory planning, soil-tool model for soil properties and soil-tool model for soil failure.

Fiorenzo Malaguti (2009) presented a work on the periodic outline of soil cutting force and its dependence on cutting depth. It considers this phenomenon by 2D and 3D classical soil cutting models with single and double wedge and it demonstrates that the distance between consecutive clod rupture surfaces depends on cutting depth and cutting angle.

Karmakar and Kushwaha (2006) proposed soil dynamic behavior using the CFD simulation for tool design and its optimization with different shapes in order to reduce tool draft and energy demand over a wide speed range and for modeling deferent types of soils based on their visco-plastic parameters.

In this chapter we have reviewed the literature in different aspects of excavation. Also, the various research areas have been highlighted to include excavator kinematics, excavator dynamics, fragmented rock excavation, excavation planning, teleoperation, control design, automation and related researches in excavation.

CHAPTER THREE

3.0 DYNAMIC ANALYSIS OF CUTTING FORCE IN HYDRAULIC EXCAVATION

3.1 PREAMBLE

The problem of earthmoving has been an issue of great concern in mining and construction industry with several aspects of the problem being handled by various researchers. Also, within this context, evaluating the forces acting on excavating machines from the bucket has long been a major problem in the field of simulations.

This study draws recourse from an earlier work (Singh, 1995b) where it was assumed that a blade was cutting through a flat surface. The attention here is however focused on how the force acting on the blade of the excavator bucket is transmitted from the hydraulic mechanism and the main objective will be to formulate a generalised form of dynamic equations governing the motion of the various links of the excavator such that we can evaluate the transmitted and the cutting forces of the blade of the excavator bucket. It should also be possible to carry out simulation studies for the forces acting on the excavator bucket and by examining various specialised cases in order to demonstrate the effect of angle of inclination on the cutting force. This problem basically addresses the operation of the hydraulic excavator in free swing.

In this chapter, we present the excavation model and a generalised analytical model with dynamic equations governing the motion of the various links of the excavator, the transmitted and cutting forces of the excavator bucket. Here, an approach which involves the use of rigid body dynamics with analytical geometry and circular functions is being proposed for determining the cutting force of the excavator bucket in order to address the research question. The specific problem addressed in this chapter is to study the effect the geometrical parameters such as link length on the cutting force by considering various scenarios of angle of inclination. The work include derivation of a set of dynamic equations describing the relative motion of the various links of the excavator, the transmitted force and the cutting force of the blade of the excavator bucket.

3.2 Excavation Model

The excavation model for the scooping operation is as shown in figs. 10a and 10b below.

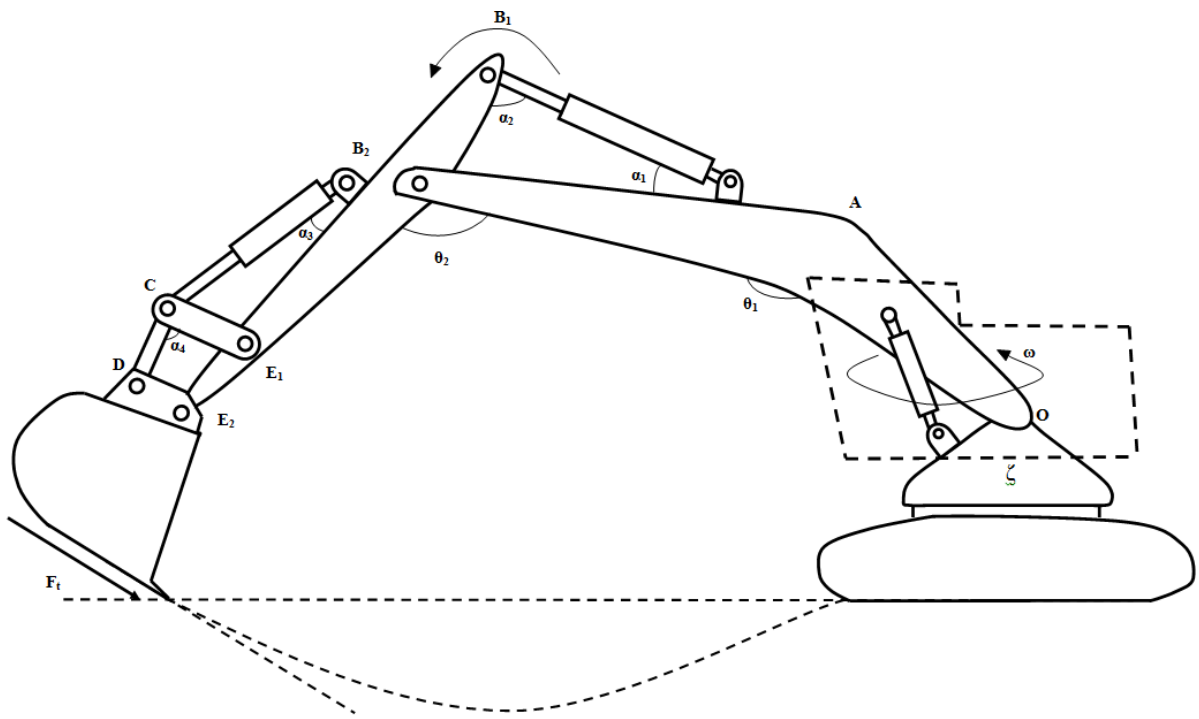

Figure10a: Excavation Model

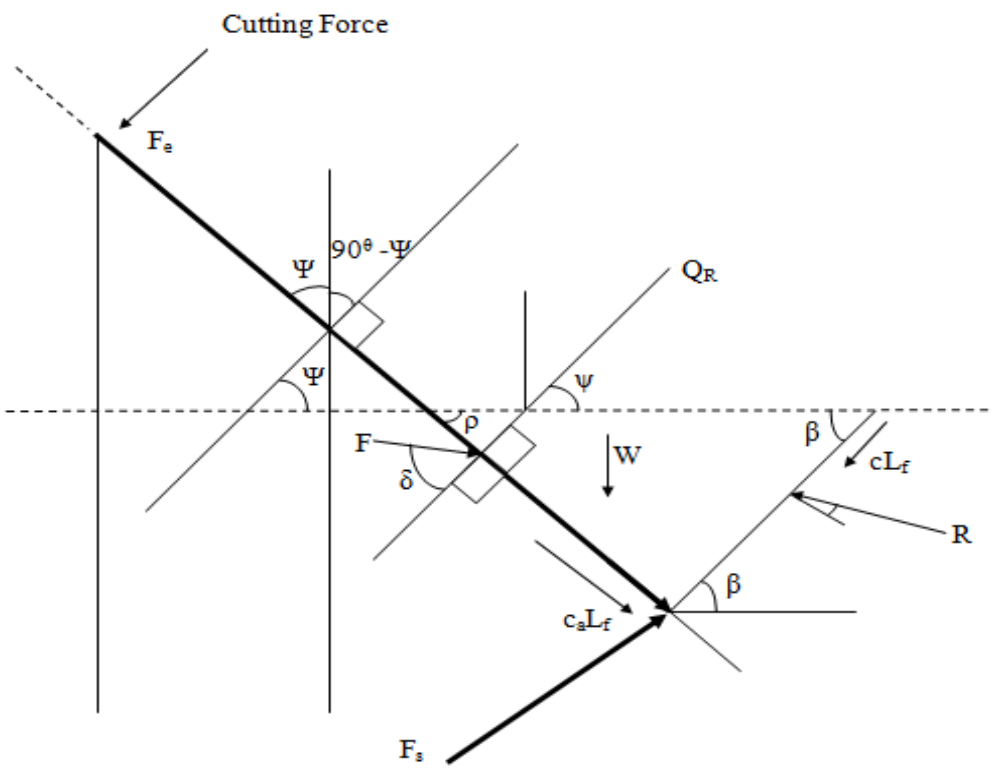

Figure 10b: Force Diagram for Excavation Model

3.2.1 Excavation Model Assumptions

In this study, some of the assumptions made are the following:

1. The hydraulic excavator is in good operating condition.
2. Pile/medium is dry sand.
3. Pile is loose and inelastic
4. Pile is heaped, not a flat surface
5. Hardness of pile is negligible
6. Thermal expansion on the excavator bucket during scooping is negligible

3.3 Dynamic Equations

The starting point is to derive expressions that define the relationship between the displacement, angular velocity and angular acceleration of the various links of the excavator.

Definition of terms

Let $\vec{\omega}_{A/O}$ = angular velocity of point A relative to O

Let $\vec{\alpha}_{A/O}$ = angular acceleration of point A relative to O

Let $\vec{r}_{O/A}$ = displacement of point O relative to A

The angular velocity of each of the links is as expressed in the equations below

$$\vec{\omega}_{A/O} = \vec{\omega}_{B_1/O} - \vec{\omega}_{B_1/A} \quad (1)$$

$$\vec{\omega}_{B_2/O} = \vec{\omega}_{B_2/B_1} + \vec{\omega}_{B_1/A} + \vec{\omega}_{A/O} \quad (2)$$

$$\vec{\omega}_{E_1/O} = \vec{\omega}_{E_1/B_2} + \vec{\omega}_{B_2/B_1} + \vec{\omega}_{B_1/A} + \vec{\omega}_{A/O} \quad (3)$$

$$\vec{\omega}_{E_2/O} = \vec{\omega}_{E_2/E_1} + \vec{\omega}_{E_1/B_2} + \vec{\omega}_{B_2/B_1} + \vec{\omega}_{B_1/A} + \vec{\omega}_{A/O} \quad (4)$$

$$\vec{\omega}_{C/O} = \vec{\omega}_{C/B_1} + \vec{\omega}_{B_1/A} + \vec{\omega}_{A/O} \quad (5)$$

$$\vec{\omega}_{D/O} = \vec{\omega}_{D/C} + \vec{\omega}_{C/B_1} + \vec{\omega}_{B_1/A} + \vec{\omega}_{A/O} \quad (6)$$

By invoking eqn (1),

$$\vec{\omega}_{A/O} = \vec{\omega}_{B_1/O} - \vec{\omega}_{B_1/A}$$

Hence the angular acceleration of point A relative to O is given by

$$\frac{d}{dt}\left(\vec{\omega}_{A/O}\right) = \dot{\vec{\omega}}_{A/O} = \dot{\vec{\omega}}_{B_1/O} - \dot{\vec{\omega}}_{B_1/A} = \vec{\alpha}_{A/O} \tag{7}$$

Similarly, by invoking eqn (2),

$$\vec{\omega}_{B_1/A} = \vec{\omega}_{B_2/O} - \vec{\omega}_{B_2/B_1} - \vec{\omega}_{A/O}$$

$$\frac{d}{dt}\left(\vec{\omega}_{B_1/A}\right) = \dot{\vec{\omega}}_{B_1/A} = \dot{\vec{\omega}}_{B_2/O} - \dot{\vec{\omega}}_{B_2/B_1} - \dot{\vec{\omega}}_{A/O} = \vec{\alpha}_{B_1/A} \tag{8}$$

From eqn (3),

$$\vec{\omega}_{B_2/B_1} = \vec{\omega}_{E_1/O} - \vec{\omega}_{E_1/B_2} - \vec{\omega}_{B_1/A} - \vec{\omega}_{A/O}$$

Hence,

$$\frac{d}{dt}\left(\vec{\omega}_{B_2/B_1}\right) = \dot{\vec{\omega}}_{E_1/O} - \dot{\vec{\omega}}_{E_1/B_2} - \dot{\vec{\omega}}_{B_1/A} - \dot{\vec{\omega}}_{A/O} = \vec{\alpha}_{B_2/B_1} \tag{9}$$

Similarly,

$$\vec{\omega}_{E_1/B_2} = \vec{\omega}_{E_1/O} - \vec{\omega}_{B_2/B_1} - \vec{\omega}_{B_1/A} - \vec{\omega}_{A/O}$$

Hence,

$$\frac{d}{dt}\left(\vec{\omega}_{E_1/B_2}\right) = \dot{\vec{\omega}}_{E_1/O} - \dot{\vec{\omega}}_{B_2/B_1} - \dot{\vec{\omega}}_{B_1/A} - \dot{\vec{\omega}}_{A/O} = \vec{\alpha}_{E_1/B_2} \tag{10}$$

By invoking eqn (4),

$$\vec{\omega}_{E_2/E_1} = \vec{\omega}_{E_2/O} - \vec{\omega}_{E_1/B_2} - \vec{\omega}_{B_2/B_1} - \vec{\omega}_{B_1/A} - \vec{\omega}_{A/O}$$

$$\frac{d}{dt}\left(\vec{\omega}_{E_2/E_1}\right) = \dot{\vec{\omega}}_{E_2/O} - \dot{\vec{\omega}}_{E_1/B_2} - \dot{\vec{\omega}}_{B_2/B_1} - \dot{\vec{\omega}}_{B_1/A} - \dot{\vec{\omega}}_{A/O} = \vec{\alpha}_{E_2/E_1} \tag{11}$$

Invoking eqn (5), we obtain

$$\vec{\omega}_{C/B_1} = \vec{\omega}_{C/O} - \vec{\omega}_{B_1/A} - \vec{\omega}_{A/O}$$

$$\frac{d}{dt}\left(\vec{\omega}_{C/B_1}\right)=\dot{\vec{\omega}}_{C/O}-\dot{\vec{\omega}}_{B_1/A}-\dot{\vec{\omega}}_{A/O}=\vec{\alpha}_{C/B_1} \tag{12}$$

From eqn (6), we obtain

$$\vec{\omega}_{D/C}=\vec{\omega}_{D/O}-\vec{\omega}_{C/B_1}-\vec{\omega}_{B_1/A}-\vec{\omega}_{A/O}$$

$$\frac{d}{dt}\left(\vec{\omega}_{D/C}\right)=\dot{\vec{\omega}}_{D/C}=\dot{\vec{\omega}}_{D/O}-\dot{\vec{\omega}}_{C/B_1}-\dot{\vec{\omega}}_{B_1/A}-\dot{\vec{\omega}}_{A/O}=\vec{\alpha}_{D/C} \tag{13}$$

Similarly,

$$\vec{\omega}_{E_2/D}=\vec{\omega}_{E_2/O}-\vec{\omega}_{D/C}-\vec{\omega}_{C/B_1}-\vec{\omega}_{B_1/A}-\vec{\omega}_{A/O}$$

$$\frac{d}{dt}\left(\vec{\omega}_{E_2/D}\right)=\dot{\vec{\omega}}_{E_2/O}-\dot{\vec{\omega}}_{D/C}-\dot{\vec{\omega}}_{C/B_1}-\dot{\vec{\omega}}_{B_1/A}-\dot{\vec{\omega}}_{A/O}=\vec{\alpha}_{D/C} \tag{14}$$

The next step is to obtain the relevant acceleration equations viz:

Let $\vec{a}_{A/\zeta}$ = acceleration of point A relative to the frame ζ

$$\vec{a}_{A/\zeta}=\vec{a}_{O/\zeta}+\vec{\alpha}_{A/O}\times\vec{r}_{O/A}-\omega_{A/O}^2\vec{r}_{O/A}+\vec{\omega}_{A/O}\times\left(\vec{\omega}_{A/O}\times\vec{r}_{O/A}\right) \tag{15}$$

Next we find the acceleration of point B_1 relative to A as follows

$$\vec{a}_{B_1A}=\vec{a}_{A/\zeta}+\vec{\alpha}_{B_1A}\times\vec{r}_{AB_1}-\omega_{B_1/A}^2\vec{r}_{AB_1}+\vec{\omega}_{B_1A}\times\left(\vec{\omega}_{B_1/A}\times\vec{r}_{AB_1}\right) \tag{16}$$

Similarly, we can find an expression for the acceleration of point B_2 relative to B_1 as

$$\vec{a}_{B_2/B_1}=\vec{a}_{B_1A}+\vec{\alpha}_{B_2B_1}\times\vec{r}_{B_1B_2}-\omega_{B_2/B_1}^2\vec{r}_{B_1B_2}+\vec{\omega}_{B_2/B_1}\times\left(\vec{\omega}_{B_2/B_1}\times\vec{r}_{B_1B_2}\right) \tag{17}$$

Next, we find an expression for the acceleration of point E_1 relative to B_2 as

$$\vec{a}_{E_1/B_2}=\vec{a}_{B_2/B_1}+\vec{\alpha}_{E_1/B_2}\times\vec{r}_{B_2B_1}-\omega_{E_1/B_2}^2\vec{r}_{B_2E_1}+\vec{\omega}_{E_1/B_2}\times\left(\vec{\omega}_{E_1/B_2}\times\vec{r}_{B_2E_1}\right) \tag{18}$$

Similarly, we can find an expression of point E_2 relative to E_1 as

$$\vec{a}_{E_2/E_1}=\vec{a}_{E_1/B_2}+\vec{\alpha}_{E_2/E_1}\times\vec{r}_{E_1/B_2}-\omega_{E_2/E_1}^2\vec{r}_{E_1/E_2}+\vec{\omega}_{E_2/E_1}\times\left(\vec{\omega}_{E_2/E_1}\times\vec{r}_{E_1/E_2}\right) \tag{19}$$

Now eqn (16) in view of eqn (15) becomes

$$\vec{a}_{B_1A} = \begin{Bmatrix} \vec{a}_{O/\zeta} + \vec{\alpha}_{A/O} \times \vec{r}_{O/A} - \omega_{A/O}^2 \vec{r}_{O/A} + \vec{\omega}_{A/O} \times \left(\vec{\omega}_{A/O} \times \vec{r}_{O/A}\right) \\ + \vec{\alpha}_{B_1A} \times \vec{r}_{AB_1} - \omega_{B_1/A}^2 \vec{r}_{AB_1} + \vec{\omega}_{B_1A} \times \left(\vec{\omega}_{B_1/A} \times \vec{r}_{AB_1}\right) \end{Bmatrix} \tag{20}$$

Substituting eqn (7) & eqn (8) into eqn (20) gives

$$\vec{a}_{B_1A} = \begin{Bmatrix} \vec{a}_{O/\zeta} + \left(\dot{\vec{\omega}}_{B_1/O} - \dot{\vec{\omega}}_{B_1/A}\right) \times \vec{r}_{O/A} - \omega_{A/O}^2 \vec{r}_{O/A} + \vec{\omega}_{A/O} \times \left(\vec{\omega}_{A/O} \times \vec{r}_{O/A}\right) \\ + \left(\dot{\vec{\omega}}_{B_2/O} - \dot{\vec{\omega}}_{B_2/B_1} - \dot{\vec{\omega}}_{A/O}\right) \times \vec{r}_{AB_1} - \omega_{B_1/A}^2 \vec{r}_{AB_1} + \vec{\omega}_{B_1A} \times \left(\vec{\omega}_{B_1/A} \times \vec{r}_{AB_1}\right) \end{Bmatrix} \tag{21}$$

Considering the relation below,

$$\begin{Bmatrix} \vec{\omega}_{A/O} \times \left(\vec{\omega}_{A/O} \times \vec{r}_{O/A}\right) = \left(\vec{\omega}_{A/O} \times \vec{r}_{O/A}\right) \vec{\omega}_{A/O} - \omega_{A/O}^2 \vec{r}_{O/A} \\ \vec{\omega}_{B_1A} \times \left(\vec{\omega}_{B_1/A} \times \vec{r}_{AB_1}\right) = \left(\vec{\omega}_{B_1/A} \times \vec{r}_{AB_1}\right) \vec{\omega}_{B_1/A} - \omega_{B_1/A}^2 \vec{r}_{AB_1} \end{Bmatrix}$$

We can re-write eqn (21) as

$$\vec{a}_{B_1A} = \begin{Bmatrix} \vec{a}_{O/\zeta} + \left(\dot{\vec{\omega}}_{B_1/O} - \dot{\vec{\omega}}_{B_1/A}\right) \times \vec{r}_{O/A} - 2\omega_{A/O}^2 \vec{r}_{O/A} + \left(\vec{\omega}_{A/O} \cdot \vec{r}_{O/A}\right) \vec{\omega}_{A/O} \\ + \left(\dot{\vec{\omega}}_{B_2/O} - \dot{\vec{\omega}}_{B_2/B_1} - \dot{\vec{\omega}}_{A/O}\right) \times \vec{r}_{AB_1} - 2\omega_{B_1/A}^2 \vec{r}_{AB_1} + \left(\vec{\omega}_{B_1/A} \cdot \vec{r}_{AB_1}\right) \vec{\omega}_{B_1/A} \end{Bmatrix} \tag{22}$$

Similarly, substituting eqn (22) in eqn (17) gives

$$\vec{a}_{B_2/B_1} = \begin{Bmatrix} \vec{a}_{O/\zeta} + \left(\dot{\vec{\omega}}_{B_1/O} - \dot{\vec{\omega}}_{B_1/A}\right) \times \vec{r}_{O/A} - 2\omega_{A/O}^2 \vec{r}_{O/A} + \left(\vec{\omega}_{A/O} \cdot \vec{r}_{O/A}\right) \vec{\omega}_{A/O} \\ + \left(\dot{\vec{\omega}}_{B_2/O} - \dot{\vec{\omega}}_{B_2/B_1} - \dot{\vec{\omega}}_{A/O}\right) \times \vec{r}_{AB_1} - 2\omega_{B_1/A}^2 \vec{r}_{AB_1} + \left(\vec{\omega}_{B_1/A} \cdot \vec{r}_{AB_1}\right) \vec{\omega}_{B_1/A} \\ + \vec{\alpha}_{B_2B_1} \times \vec{r}_{B_1B_2} - \omega_{B_2/B_1}^2 \vec{r}_{B_1B_2} + \vec{\omega}_{B_2/B_1} \times \left(\vec{\omega}_{B_2/B_1} \times \vec{r}_{B_1B_2}\right) \end{Bmatrix} \tag{23}$$

Substituting eqn (9) in eqn (23) gives

$$\vec{a}_{B_2/B_1} = \begin{Bmatrix} \vec{a}_{O/\zeta} + \left(\dot{\vec{\omega}}_{B_1/O} - \dot{\vec{\omega}}_{B_1/A}\right) \times \vec{r}_{O/A} - 2\omega_{A/O}^2 \vec{r}_{O/A} + \left(\vec{\omega}_{A/O} \cdot \vec{r}_{O/A}\right) \vec{\omega}_{A/O} \\ + \left(\dot{\vec{\omega}}_{B_2/O} - \dot{\vec{\omega}}_{B_2/B_1} - \dot{\vec{\omega}}_{A/O}\right) \times \vec{r}_{AB_1} - 2\omega_{B_1/A}^2 \vec{r}_{AB_1} + \left(\vec{\omega}_{B_1/A} \cdot \vec{r}_{AB_1}\right) \vec{\omega}_{B_1/A} \\ + \left(\dot{\vec{\omega}}_{E_1/O} - \dot{\vec{\omega}}_{E_1/B_2} - \dot{\vec{\omega}}_{B_1/A} - \dot{\vec{\omega}}_{A/O}\right) \times \vec{r}_{B_1B_2} - \omega_{B_2/B_1}^2 \vec{r}_{B_1B_2} + \vec{\omega}_{B_2/B_1} \times \left(\vec{\omega}_{B_2/B_1} \times \vec{r}_{B_1B_2}\right) \end{Bmatrix} \tag{24}$$

Considering the relation

$$\vec{\omega}_{B_2/B_1} \times \left(\vec{\omega}_{B_2/B_1} \times \vec{r}_{B_1B_2}\right) = \left(\vec{\omega}_{B_2/B_1} \times \vec{r}_{B_1B_2}\right)\vec{\omega}_{B_2/B_1} - \omega^2_{B_2/B_1}\vec{r}_{B_1B_2}$$

We can re-write eqn (24) as

$$\vec{a}_{B_2/B_1} = \left\{\begin{array}{l} \vec{a}_{O/\zeta} + \left(\dot{\vec{\omega}}_{B_1/O} - \dot{\vec{\omega}}_{B_1/A}\right)\times \vec{r}_{O/A} - 2\omega^2_{A/O}\vec{r}_{O/A} + \left(\vec{\omega}_{A/O}\cdot\vec{r}_{O/A}\right)\vec{\omega}_{A/O} \\ + \left(\dot{\vec{\omega}}_{B_2/O} - \dot{\vec{\omega}}_{B_2/B_1} - \dot{\vec{\omega}}_{A/O}\right)\times \vec{r}_{AB_1} - 2\omega^2_{B_1/A}\times\vec{r}_{AB_1} + \left(\vec{\omega}_{B_1/A}\cdot\vec{r}_{AB_1}\right)\vec{\omega}_{B_1/A} \\ + \left(\dot{\vec{\omega}}_{E_1/O} - \dot{\vec{\omega}}_{E_1/B_2} - \dot{\vec{\omega}}_{B_1/A} - \dot{\vec{\omega}}_{A/O}\right)\times \vec{r}_{B_1B_2} - 2\omega^2_{B_2/B_1}\times\vec{r}_{B_1B_2} + \left(\vec{\omega}_{B_2/B_1}\times\vec{r}_{B_1B_2}\right)\vec{\omega}_{B_2/B_1} \end{array}\right\} \tag{25}$$

Next, we substitute eqn (25) into eqn (18) to obtain

$$\vec{a}_{E_1/B_2} = \left\{\begin{array}{l} \vec{a}_{O/\zeta} + \left(\dot{\vec{\omega}}_{B_1/O} - \dot{\vec{\omega}}_{B_1/A}\right)\times \vec{r}_{O/A} - 2\omega^2_{A/O}\vec{r}_{O/A} + \left(\vec{\omega}_{A/O}\cdot\vec{r}_{O/A}\right)\vec{\omega}_{A/O} \\ + \left(\dot{\vec{\omega}}_{B_2/O} - \dot{\vec{\omega}}_{B_2/B_1} - \dot{\vec{\omega}}_{A/O}\right)\times \vec{r}_{AB_1} - 2\omega^2_{B_1/A}\times\vec{r}_{AB_1} + \left(\vec{\omega}_{B_1/A}\cdot\vec{r}_{AB_1}\right)\vec{\omega}_{B_1/A} \\ + \left(\dot{\vec{\omega}}_{E_1/O} - \dot{\vec{\omega}}_{E_1/B_2} - \dot{\vec{\omega}}_{B_1/A} - \dot{\vec{\omega}}_{A/O}\right)\times \vec{r}_{B_1B_2} - 2\omega^2_{B_2/B_1}\times\vec{r}_{B_1B_2} + \left(\vec{\omega}_{B_2/B_1}\times\vec{r}_{B_1B_2}\right)\vec{\omega}_{B_2/B_1} \\ + \vec{\alpha}_{E_1/B_2}\times\vec{r}_{B_2B_1} - \omega^2_{E_1/B_2}\times\vec{r}_{B_2E_1} + \vec{\omega}_{E_1/B_2}\times\left(\vec{\omega}_{E_1/B_2}\times\vec{r}_{B_2E_1}\right) \end{array}\right\} \tag{26}$$

Substituting eqn (10) in eqn (26), we obtain

$$\vec{a}_{E_1/B_2} = \left\{\begin{array}{l} \vec{a}_{O/\zeta} + \left(\dot{\vec{\omega}}_{B_1/O} - \dot{\vec{\omega}}_{B_1/A}\right)\times \vec{r}_{O/A} - 2\omega^2_{A/O}\vec{r}_{O/A} + \left(\vec{\omega}_{A/O}\cdot\vec{r}_{O/A}\right)\vec{\omega}_{A/O} \\ + \left(\dot{\vec{\omega}}_{B_2/O} - \dot{\vec{\omega}}_{B_2/B_1} - \dot{\vec{\omega}}_{A/O}\right)\times \vec{r}_{AB_1} - 2\omega^2_{B_1/A}\times\vec{r}_{AB_1} + \left(\vec{\omega}_{B_1/A}\cdot\vec{r}_{AB_1}\right)\vec{\omega}_{B_1/A} \\ + \left(\dot{\vec{\omega}}_{E_1/O} - \dot{\vec{\omega}}_{E_1/B_2} - \dot{\vec{\omega}}_{B_1/A} - \dot{\vec{\omega}}_{A/O}\right)\times \vec{r}_{B_1B_2} - 2\omega^2_{B_2/B_1}\times\vec{r}_{B_1B_2} + \left(\vec{\omega}_{B_2/B_1}\cdot\vec{r}_{B_1B_2}\right)\vec{\omega}_{B_2/B_1} \\ + \left(\dot{\vec{\omega}}_{E_1/O} - \dot{\vec{\omega}}_{B_2/B_1} - \dot{\vec{\omega}}_{B_1/A} - \dot{\vec{\omega}}_{A/O}\right)\times \vec{r}_{B_2B_1} - \omega^2_{E_1/B_2}\times\vec{r}_{B_2E_1} + \vec{\omega}_{E_1/B_2}\times\left(\vec{\omega}_{E_1/B_2}\times\vec{r}_{B_2E_1}\right) \end{array}\right\} \tag{27}$$

Considering the relation

$$\vec{\omega}_{E_1/B_2} \times \left(\vec{\omega}_{E_1/B_2} \times \vec{r}_{B_2E_1}\right) = \left(\vec{\omega}_{E_1/B_2} \cdot \vec{r}_{B_2E_1}\right)\vec{\omega}_{E_1/B_2} - \omega^2_{E_1/B_2} \times \vec{r}_{B_2E_1}$$

We can re-write eqn (27) as

$$\vec{a}_{E_1/B_2} = \left\{ \begin{array}{l} \vec{a}_{O/\zeta} + \left(\dot{\vec{\omega}}_{B_1/O} - \dot{\vec{\omega}}_{B_1/A}\right) \times \vec{r}_{O/A} - 2\omega_{A/O}^2 \vec{r}_{O/A} + \left(\vec{\omega}_{A/O} \cdot \vec{r}_{O/A}\right) \vec{\omega}_{A/O} \\ + \left(\dot{\vec{\omega}}_{B_2/O} - \dot{\vec{\omega}}_{B_2/B_1} - \dot{\vec{\omega}}_{A/O}\right) \times \vec{r}_{AB_1} - 2\omega_{B_1/A}^2 \times \vec{r}_{AB_1} + \left(\vec{\omega}_{B_1/A} \cdot \vec{r}_{AB_1}\right) \vec{\omega}_{B_1/A} \\ + \left(\dot{\vec{\omega}}_{E_1/O} - \dot{\vec{\omega}}_{E_1/B_2} - \dot{\vec{\omega}}_{B_1/A} - \dot{\vec{\omega}}_{A/O}\right) \times \vec{r}_{B_1B_2} - 2\omega_{B_2/B_1}^2 \times \vec{r}_{B_1B_2} + \left(\vec{\omega}_{B_2/B_1} \cdot \vec{r}_{B_1B_2}\right) \vec{\omega}_{B_2/B_1} \\ + \left(\dot{\vec{\omega}}_{E_1/O} - \dot{\vec{\omega}}_{B_2/B_1} - \dot{\vec{\omega}}_{B_1/A} - \dot{\vec{\omega}}_{A/O}\right) \times \vec{r}_{B_2B_1} - 2\omega_{E_1/B_2}^2 \times \vec{r}_{B_2E_1} + \left(\vec{\omega}_{E_1/B_2} \cdot \vec{r}_{B_2E_1}\right) \vec{\omega}_{E_1/B_2} \end{array} \right\} \tag{28}$$

Substituting eqn (28) in eqn (19), we obtain

$$\vec{a}_{E_2/E_1} = \left\{ \begin{array}{l} \vec{a}_{O/\zeta} + \left(\dot{\vec{\omega}}_{B_1/O} - \dot{\vec{\omega}}_{B_1/A}\right) \times \vec{r}_{O/A} - 2\omega_{A/O}^2 \vec{r}_{O/A} + \left(\vec{\omega}_{A/O} \cdot \vec{r}_{O/A}\right) \vec{\omega}_{A/O} \\ + \left(\dot{\vec{\omega}}_{B_2/O} - \dot{\vec{\omega}}_{B_2/B_1} - \dot{\vec{\omega}}_{A/O}\right) \times \vec{r}_{AB_1} - 2\omega_{B_1/A}^2 \times \vec{r}_{AB_1} + \left(\vec{\omega}_{B_1/A} \cdot \vec{r}_{AB_1}\right) \vec{\omega}_{B_1/A} \\ + \left(\dot{\vec{\omega}}_{E_1/O} - \dot{\vec{\omega}}_{E_1/B_2} - \dot{\vec{\omega}}_{B_1/A} - \dot{\vec{\omega}}_{A/O}\right) \times \vec{r}_{B_1B_2} - 2\omega_{B_2/B_1}^2 \times \vec{r}_{B_1B_2} + \left(\vec{\omega}_{B_2/B_1} \cdot \vec{r}_{B_1B_2}\right) \vec{\omega}_{B_2/B_1} \\ + \left(\dot{\vec{\omega}}_{E_1/O} - \dot{\vec{\omega}}_{B_2/B_1} - \dot{\vec{\omega}}_{B_1/A} - \dot{\vec{\omega}}_{A/O}\right) \times \vec{r}_{B_2B_1} - 2\omega_{E_1/B_2}^2 \times \vec{r}_{B_2E_1} + \left(\vec{\omega}_{E_1/B_2} \cdot \vec{r}_{B_2E_1}\right) \vec{\omega}_{E_1/B_2} \\ + \vec{\alpha}_{E_2/E_1} \times \vec{r}_{E_1/B_2} - \omega_{E_2/E_1}^2 \vec{r}_{E_1/E_2} + \vec{\omega}_{E_2/E_1} \times \left(\vec{\omega}_{E_2/E_1} \times \vec{r}_{E_1/E_2}\right) \end{array} \right\} \tag{29}$$

Substituting eqn (11) in eqn (29) gives

$$\vec{a}_{E_2/E_1} = \left\{ \begin{array}{l} \vec{a}_{O/\zeta} + \left(\dot{\vec{\omega}}_{B_1/O} - \dot{\vec{\omega}}_{B_1/A}\right) \times \vec{r}_{O/A} - 2\omega_{A/O}^2 \vec{r}_{O/A} + \left(\vec{\omega}_{A/O} \cdot \vec{r}_{O/A}\right) \vec{\omega}_{A/O} \\ + \left(\dot{\vec{\omega}}_{B_2/O} - \dot{\vec{\omega}}_{B_2/B_1} - \dot{\vec{\omega}}_{A/O}\right) \times \vec{r}_{AB_1} - 2\omega_{B_1/A}^2 \times \vec{r}_{AB_1} + \left(\vec{\omega}_{B_1/A} \cdot \vec{r}_{AB_1}\right) \vec{\omega}_{B_1/A} \\ + \left(\dot{\vec{\omega}}_{E_1/O} - \dot{\vec{\omega}}_{E_1/B_2} - \dot{\vec{\omega}}_{B_1/A} - \dot{\vec{\omega}}_{A/O}\right) \times \vec{r}_{B_1B_2} - 2\omega_{B_2/B_1}^2 \times \vec{r}_{B_1B_2} + \left(\vec{\omega}_{B_2/B_1} \cdot \vec{r}_{B_1B_2}\right) \vec{\omega}_{B_2/B_1} \\ + \left(\dot{\vec{\omega}}_{E_1/O} - \dot{\vec{\omega}}_{B_2/B_1} - \dot{\vec{\omega}}_{B_1/A} - \dot{\vec{\omega}}_{A/O}\right) \times \vec{r}_{B_2B_1} - 2\omega_{E_1/B_2}^2 \times \vec{r}_{B_2E_1} + \left(\vec{\omega}_{E_1/B_2} \cdot \vec{r}_{B_2E_1}\right) \vec{\omega}_{E_1/B_2} \\ + \left(\dot{\vec{\omega}}_{E_2/O} - \dot{\vec{\omega}}_{E_1/B_2} - \dot{\vec{\omega}}_{B_2/B_1} - \dot{\vec{\omega}}_{B_1/A} - \dot{\vec{\omega}}_{A/O}\right) \times \vec{r}_{E_1/B_2} - \omega_{E_2/E_1}^2 \vec{r}_{E_1/E_2} + \vec{\omega}_{E_2/E_1} \times \left(\vec{\omega}_{E_2/E_1} \times \vec{r}_{E_1/E_2}\right) \end{array} \right\} \tag{30}$$

Considering the relation

$$\vec{\omega}_{E_2/E_1} \times \left(\vec{\omega}_{E_2/E_1} \times \vec{r}_{E_1/E_2}\right) = \left(\vec{\omega}_{E_2/E_1} \cdot \vec{r}_{E_1/E_2}\right) \vec{\omega}_{E_2/E_1} - \omega_{E_2/E_1}^2 \vec{r}_{E_1/E_2}$$

We can re-write eqn (30) as follows

$$\vec{a}_{E_2/E_1} = \left\{ \begin{array}{l} \vec{a}_{O/\zeta} + \left(\dot{\vec{\omega}}_{B_1/O} - \dot{\vec{\omega}}_{B_1/A}\right) \times \vec{r}_{O/A} - 2\omega_{A/O}^2 \vec{r}_{O/A} + \left(\vec{\omega}_{A/O} \cdot \vec{r}_{O/A}\right) \vec{\omega}_{A/O} \\ + \left(\dot{\vec{\omega}}_{B_2/O} - \dot{\vec{\omega}}_{B_2/B_1} - \dot{\vec{\omega}}_{A/O}\right) \times \vec{r}_{AB_1} - 2\omega_{B_1/A}^2 \times \vec{r}_{AB_1} + \left(\vec{\omega}_{B_1/A} \cdot \vec{r}_{AB_1}\right) \vec{\omega}_{B_1/A} \\ + \left(\dot{\vec{\omega}}_{E_1/O} - \dot{\vec{\omega}}_{E_1/B_2} - \dot{\vec{\omega}}_{B_1/A} - \dot{\vec{\omega}}_{A/O}\right) \times \vec{r}_{B_1B_2} - 2\omega_{B_2/B_1}^2 \times \vec{r}_{B_1B_2} + \left(\vec{\omega}_{B_2/B_1} \cdot \vec{r}_{B_1B_2}\right) \vec{\omega}_{B_2/B_1} \\ + \left(\dot{\vec{\omega}}_{E_1/O} - \dot{\vec{\omega}}_{B_2/B_1} - \dot{\vec{\omega}}_{B_1/A} - \dot{\vec{\omega}}_{A/O}\right) \times \vec{r}_{B_2E_1} - 2\omega_{E_1/B_2}^2 \times \vec{r}_{B_2E_1} + \left(\vec{\omega}_{E_1/B_2} \cdot \vec{r}_{B_2E_1}\right) \vec{\omega}_{E_1/B_2} \\ + \left(\dot{\vec{\omega}}_{E_2/O} - \dot{\vec{\omega}}_{E_1/B_2} - \dot{\vec{\omega}}_{B_2/B_1} - \dot{\vec{\omega}}_{B_1/A} - \dot{\vec{\omega}}_{A/O}\right) \times \vec{r}_{E_1/B_2} - 2\omega_{E_2/E_1}^2 \vec{r}_{E_1/E_2} + \left(\vec{\omega}_{E_2/E_1} \cdot \vec{r}_{E_1/E_2}\right) \vec{\omega}_{E_2/E_1} \end{array} \right\} \quad (31)$$

Since $\vec{\omega}_{A/\zeta}$ = acceleration of point A relative to the frame ζ and eqn (1) states that

$$\vec{\omega}_{B_1/O} = \vec{\omega}_{B_1/A} + \vec{\omega}_{A/O}$$

From eqn (5),

$$\vec{\omega}_{C/O} = \vec{\omega}_{C/B_1} + \vec{\omega}_{B_1/A} + \vec{\omega}_{A/O}$$

And from eqn (6),

$$\vec{\omega}_{D/O} = \vec{\omega}_{D/C} + \vec{\omega}_{C/B_1} + \vec{\omega}_{B_1/A} + \vec{\omega}_{A/O}$$

We can now find the acceleration of point C relative to B_1. Hence,

$$\vec{a}_{C/B_1} = \vec{a}_{B_1A} + \vec{\alpha}_{C/B_1} \times \vec{r}_{B_1C} - \omega_{C/B_1}^2 \times \vec{r}_{B_1C} + \vec{\omega}_{C/B_1} \times \left(\vec{\omega}_{C/B_1} \times \vec{r}_{B_1C}\right) \quad (32)$$

Similarly, we can find an expression for the acceleration of point D relative to C as

$$\vec{a}_{D/C} = \vec{a}_{C/B_1} + \vec{\alpha}_{DC} \times \vec{r}_{CD} - \omega_{D/C}^2 \times \vec{r}_{CD} + \vec{\omega}_{D/C} \times \left(\vec{\omega}_{D/C} \times \vec{r}_{CD}\right) \quad (33)$$

Substituting eqn (22) in eqn (32), we obtain

$$\vec{a}_{C/B_1} = \left\{ \begin{array}{l} \vec{a}_{O/\zeta} + \left(\dot{\vec{\omega}}_{B_1/O} - \dot{\vec{\omega}}_{B_1/A}\right) \times \vec{r}_{O/A} - 2\omega_{A/O}^2 \vec{r}_{O/A} + \left(\vec{\omega}_{A/O} \cdot \vec{r}_{O/A}\right) \vec{\omega}_{A/O} \\ + \left(\dot{\vec{\omega}}_{B_2/O} - \dot{\vec{\omega}}_{B_2/B_1} - \dot{\vec{\omega}}_{A/O}\right) \times \vec{r}_{AB_1} - 2\omega_{B_1/A}^2 \vec{r}_{AB_1} + \left(\vec{\omega}_{B_1/A} \cdot \vec{r}_{AB_1}\right) \vec{\omega}_{B_1/A} \\ + \vec{\alpha}_{C/B_1} \times \vec{r}_{B_1C} - \omega_{C/B_1}^2 \times \vec{r}_{B_1C} + \vec{\omega}_{C/B_1} \times \left(\vec{\omega}_{C/B_1} \times \vec{r}_{B_1C}\right) \end{array} \right\} \quad (34)$$

Substituting eqn (12) in eqn (34), we obtain

$$\vec{a}_{C/B_1} = \begin{Bmatrix} \vec{a}_{O/\zeta} + \left(\dot{\vec{\omega}}_{B_1/O} - \dot{\vec{\omega}}_{B_1/A}\right)\times \vec{r}_{O/A} - 2\omega_{A/O}^2 \vec{r}_{O/A} + \left(\vec{\omega}_{A/O}\cdot \vec{r}_{O/A}\right)\vec{\omega}_{A/O} \\ + \left(\dot{\vec{\omega}}_{B_2/O} - \dot{\vec{\omega}}_{B_2/B_1} - \dot{\vec{\omega}}_{A/O}\right)\times \vec{r}_{AB_1} - 2\omega_{B_1/A}^2 \vec{r}_{AB_1} + \left(\vec{\omega}_{B_1/A}\cdot \vec{r}_{AB_1}\right)\vec{\omega}_{B_1/A} \\ + \left(\dot{\vec{\omega}}_{C/O} - \dot{\vec{\omega}}_{B_1/A} - \dot{\vec{\omega}}_{A/O}\right)\times \vec{r}_{B_1C} - \omega_{C/B_1}^2 \times \vec{r}_{B_1C} + \vec{\omega}_{C/B_1}\times\left(\vec{\omega}_{C/B_1}\times \vec{r}_{B_1C}\right) \end{Bmatrix} \tag{35}$$

Considering the relation

$$\vec{\omega}_{C/B_1}\times\left(\vec{\omega}_{C/B_1}\times \vec{r}_{B_1C}\right) = \left(\vec{\omega}_{C/B_1}\cdot \vec{r}_{B_1C}\right)\vec{\omega}_{C/B_1} - \omega_{C/B_1}^2 \vec{r}_{B_1C}$$

We can re-write eqn (35) as follows

$$\vec{a}_{C/B_1} = \begin{Bmatrix} \vec{a}_{O/\zeta} + \left(\dot{\vec{\omega}}_{B_1/O} - \dot{\vec{\omega}}_{B_1/A}\right)\times \vec{r}_{O/A} - 2\omega_{A/O}^2 \vec{r}_{O/A} + \left(\vec{\omega}_{A/O}\cdot \vec{r}_{O/A}\right)\vec{\omega}_{A/O} \\ + \left(\dot{\vec{\omega}}_{B_2/O} - \dot{\vec{\omega}}_{B_2/B_1} - \dot{\vec{\omega}}_{A/O}\right)\times \vec{r}_{AB_1} - 2\omega_{B_1/A}^2 \vec{r}_{AB_1} + \left(\vec{\omega}_{B_1/A}\cdot \vec{r}_{AB_1}\right)\vec{\omega}_{B_1/A} \\ + \left(\dot{\vec{\omega}}_{C/O} - \dot{\vec{\omega}}_{B_1/A} - \dot{\vec{\omega}}_{A/O}\right)\times \vec{r}_{B_1C} - 2\omega_{C/B_1}^2 \vec{r}_{B_1C} + \left(\vec{\omega}_{C/B_1}\cdot \vec{r}_{B_1C}\right)\vec{\omega}_{C/B_1} \end{Bmatrix} \tag{36}$$

Similarly, substituting eqn (36) in eqn (33) gives

$$\vec{a}_{D/C} = \begin{Bmatrix} \vec{a}_{O/\zeta} + \left(\dot{\vec{\omega}}_{B_1/O} - \dot{\vec{\omega}}_{B_1/A}\right)\times \vec{r}_{O/A} - 2\omega_{A/O}^2 \vec{r}_{O/A} + \left(\vec{\omega}_{A/O}\cdot \vec{r}_{O/A}\right)\vec{\omega}_{A/O} \\ + \left(\dot{\vec{\omega}}_{B_2/O} - \dot{\vec{\omega}}_{B_2/B_1} - \dot{\vec{\omega}}_{A/O}\right)\times \vec{r}_{AB_1} - 2\omega_{B_1/A}^2 \vec{r}_{AB_1} + \left(\vec{\omega}_{B_1/A}\cdot \vec{r}_{AB_1}\right)\vec{\omega}_{B_1/A} \\ + \left(\dot{\vec{\omega}}_{C/O} - \dot{\vec{\omega}}_{B_1/A} - \dot{\vec{\omega}}_{A/O}\right)\times \vec{r}_{B_1C} - 2\omega_{C/B_1}^2 \vec{r}_{B_1C} + \left(\vec{\omega}_{C/B_1}\cdot \vec{r}_{B_1C}\right)\vec{\omega}_{C/B_1} \\ + \vec{\alpha}_{DC}\times \vec{r}_{CD} - \omega_{D/C}^2 \times \vec{r}_{CD} + \vec{\omega}_{D/C}\times\left(\vec{\omega}_{D/C}\times \vec{r}_{CD}\right) \end{Bmatrix} \tag{37}$$

Substituting eqn (13) in eqn (37) gives

$$\vec{a}_{D/C} = \begin{Bmatrix} \vec{a}_{O/\zeta} + \left(\dot{\vec{\omega}}_{B_1/O} - \dot{\vec{\omega}}_{B_1/A}\right)\times \vec{r}_{O/A} - 2\omega_{A/O}^2 \vec{r}_{O/A} + \left(\vec{\omega}_{A/O}\cdot \vec{r}_{O/A}\right)\vec{\omega}_{A/O} \\ + \left(\dot{\vec{\omega}}_{B_2/O} - \dot{\vec{\omega}}_{B_2/B_1} - \dot{\vec{\omega}}_{A/O}\right)\times \vec{r}_{AB_1} - 2\omega_{B_1/A}^2 \vec{r}_{AB_1} + \left(\vec{\omega}_{B_1/A}\cdot \vec{r}_{AB_1}\right)\vec{\omega}_{B_1/A} \\ + \left(\dot{\vec{\omega}}_{C/O} - \dot{\vec{\omega}}_{B_1/A} - \dot{\vec{\omega}}_{A/O}\right)\times \vec{r}_{B_1C} - 2\omega_{C/B_1}^2 \vec{r}_{B_1C} + \left(\vec{\omega}_{C/B_1}\cdot \vec{r}_{B_1C}\right)\vec{\omega}_{C/B_1} \\ + \left(\dot{\vec{\omega}}_{D/O} - \dot{\vec{\omega}}_{C/B_1} - \dot{\vec{\omega}}_{B_1/A} - \dot{\vec{\omega}}_{A/O}\right)\times \vec{r}_{CD} - \omega_{D/C}^2 \vec{r}_{CD} + \vec{\omega}_{D/C}\times\left(\vec{\omega}_{D/C}\times \vec{r}_{CD}\right) \end{Bmatrix} \tag{38}$$

Considering the relation

$$\vec{\omega}_{D/C}\times\left(\vec{\omega}_{D/C}\times \vec{r}_{CD}\right) = \left(\vec{\omega}_{D/C}\cdot \vec{r}_{CD}\right)\vec{\omega}_{D/C} - \omega_{D/C}^2 \vec{r}_{CD}$$

eqn (38) becomes

$$\vec{a}_{D/C}=\left\{\begin{array}{l}\vec{a}_{O/\zeta}+\left(\dot{\vec{\omega}}_{B_1/O}-\dot{\vec{\omega}}_{B_1/A}\right)\times\vec{r}_{O/A}-2\omega_{A/O}^2\vec{r}_{O/A}+\left(\vec{\omega}_{A/O}\cdot\vec{r}_{O/A}\right)\vec{\omega}_{A/O}\\+\left(\dot{\vec{\omega}}_{B_2/O}-\dot{\vec{\omega}}_{B_2/B_1}-\dot{\vec{\omega}}_{A/O}\right)\times\vec{r}_{AB_1}-2\omega_{B_1/A}^2\vec{r}_{AB_1}+\left(\vec{\omega}_{B_1/A}\cdot\vec{r}_{AB_1}\right)\vec{\omega}_{B_1/A}\\+\left(\dot{\vec{\omega}}_{C/O}-\dot{\vec{\omega}}_{B_1/A}-\dot{\vec{\omega}}_{A/O}\right)\times\vec{r}_{B_1C}-2\omega_{C/B_1}^2\vec{r}_{B_1C}+\left(\vec{\omega}_{C/B_1}\cdot\vec{r}_{B_1C}\right)\vec{\omega}_{C/B_1}\\+\left(\dot{\vec{\omega}}_{D/O}-\dot{\vec{\omega}}_{C/B_1}-\dot{\vec{\omega}}_{B_1/A}-\dot{\vec{\omega}}_{A/O}\right)\times\vec{r}_{CD}-2\omega_{D/C}^2\vec{r}_{CD}+\left(\vec{\omega}_{D/C}\cdot\vec{r}_{CD}\right)\vec{\omega}_{D/C}\end{array}\right\}\tag{39}$$

Also,

$$\vec{\omega}_{E_2/O}=\vec{\omega}_{E_2/D}+\vec{\omega}_{D/C}+\vec{\omega}_{C/B_1}+\vec{\omega}_{B_1/A}+\vec{\omega}_{A/O}\tag{40}$$

We can find an expression for the acceleration of point E_2 relative to D as

$$\vec{a}_{E_2/D}=\vec{a}_{D/C}+\vec{\alpha}_{E_2/D}\times\vec{r}_{DE_2}-\omega_{E_2/D}^2\times\vec{r}_{DE_2}+\vec{\omega}_{E_2/D}\times\left(\vec{\omega}_{E_2/D}\times\vec{r}_{DE_2}\right)\tag{41}$$

eqn (39) in eqn(41) gives

$$\vec{a}_{E_2/D}=\left\{\begin{array}{l}\vec{a}_{O/\zeta}+\left(\dot{\vec{\omega}}_{B_1/O}-\dot{\vec{\omega}}_{B_1/A}\right)\times\vec{r}_{O/A}-2\omega_{A/O}^2\vec{r}_{O/A}+\left(\vec{\omega}_{A/O}\cdot\vec{r}_{O/A}\right)\vec{\omega}_{A/O}\\+\left(\dot{\vec{\omega}}_{B_2/O}-\dot{\vec{\omega}}_{B_2/B_1}-\dot{\vec{\omega}}_{A/O}\right)\times\vec{r}_{AB_1}-2\omega_{B_1/A}^2\vec{r}_{AB_1}+\left(\vec{\omega}_{B_1/A}\cdot\vec{r}_{AB_1}\right)\vec{\omega}_{B_1/A}\\+\left(\dot{\vec{\omega}}_{C/O}-\dot{\vec{\omega}}_{B_1/A}-\dot{\vec{\omega}}_{A/O}\right)\times\vec{r}_{B_1C}-2\omega_{C/B_1}^2\vec{r}_{B_1C}+\left(\vec{\omega}_{C/B_1}\cdot\vec{r}_{B_1C}\right)\vec{\omega}_{C/B_1}\\+\left(\dot{\vec{\omega}}_{D/O}-\dot{\vec{\omega}}_{C/B_1}-\dot{\vec{\omega}}_{B_1/A}-\dot{\vec{\omega}}_{A/O}\right)\times\vec{r}_{CD}-2\omega_{D/C}^2\vec{r}_{CD}+\left(\vec{\omega}_{D/C}\cdot\vec{r}_{CD}\right)\vec{\omega}_{D/C}\\+\vec{\alpha}_{E_2/D}\times\vec{r}_{DE_2}-\omega_{E_2/D}^2\times\vec{r}_{DE_2}+\vec{\omega}_{E_2/D}\times\left(\vec{\omega}_{E_2/D}\times\vec{r}_{DE_2}\right)\end{array}\right\}\tag{42}$$

Also,

$$\vec{\omega}_{E_2/D}\times\left(\vec{\omega}_{E_2/D}\times\vec{r}_{DE_2}\right)=\left(\vec{\omega}_{E_2/D}\cdot\vec{r}_{DE_2}\right)\vec{\omega}_{E_2/D}-\omega_{E_2/D}^2\vec{r}_{DE_2}\tag{43}$$

Substituting eqns (14) and (43) in (42) gives

$$\vec{a}_{E_2/D}=\left\{\begin{array}{l}\vec{a}_{O/\zeta}+\left(\dot{\vec{\omega}}_{B_1/O}-\dot{\vec{\omega}}_{B_1/A}\right)\times\vec{r}_{O/A}-2\omega_{A/O}^2\vec{r}_{O/A}+\left(\vec{\omega}_{A/O}\cdot\vec{r}_{O/A}\right)\vec{\omega}_{A/O}\\+\left(\dot{\vec{\omega}}_{B_2/O}-\dot{\vec{\omega}}_{B_2/B_1}-\dot{\vec{\omega}}_{A/O}\right)\times\vec{r}_{AB_1}-2\omega_{B_1/A}^2\vec{r}_{AB_1}+\left(\vec{\omega}_{B_1/A}\cdot\vec{r}_{AB_1}\right)\vec{\omega}_{B_1/A}\\+\left(\dot{\vec{\omega}}_{C/O}-\dot{\vec{\omega}}_{B_1/A}-\dot{\vec{\omega}}_{A/O}\right)\times\vec{r}_{B_1C}-2\omega_{C/B_1}^2\vec{r}_{B_1C}+\left(\vec{\omega}_{C/B_1}\cdot\vec{r}_{B_1C}\right)\vec{\omega}_{C/B_1}\\+\left(\dot{\vec{\omega}}_{D/O}-\dot{\vec{\omega}}_{C/B_1}-\dot{\vec{\omega}}_{B_1/A}-\dot{\vec{\omega}}_{A/O}\right)\times\vec{r}_{CD}-2\omega_{D/C}^2\vec{r}_{CD}+\left(\vec{\omega}_{D/C}\cdot\vec{r}_{CD}\right)\vec{\omega}_{D/C}\\+\left(\dot{\vec{\omega}}_{E_2/O}-\dot{\vec{\omega}}_{D/C}-\dot{\vec{\omega}}_{C/B_1}-\dot{\vec{\omega}}_{B_1/A}-\dot{\vec{\omega}}_{A/O}\right)\times\vec{r}_{DE_2}-2\omega_{E_2/D}^2\vec{r}_{DE_2}+\left(\vec{\omega}_{E_2/D}\cdot\vec{r}_{DE_2}\right)\vec{\omega}_{E_2/D}\end{array}\right\}\tag{44}$$

We obtain the total acceleration of the system, $\vec{a}_L$, as

$$\vec{a}_L=\left\{\begin{array}{l}2\vec{a}_{O/\zeta}+2\left(\dot{\vec{\omega}}_{B_1/O}-\dot{\vec{\omega}}_{B_1/A}\right)\times\vec{r}_{O/A}-4\omega_{A/O}^2\vec{r}_{O/A}+2\left(\vec{\omega}_{A/O}\cdot\vec{r}_{O/A}\right)\vec{\omega}_{A/O}\\+2\left(\dot{\vec{\omega}}_{B_2/O}-\dot{\vec{\omega}}_{B_2/B_1}-\dot{\vec{\omega}}_{A/O}\right)\times\vec{r}_{AB_1}-4\omega_{B_1/A}^2\vec{r}_{AB_1}+2\left(\vec{\omega}_{B_1/A}\cdot\vec{r}_{AB_1}\right)\vec{\omega}_{B_1/A}\\+\left(\dot{\vec{\omega}}_{E_1/O}-\dot{\vec{\omega}}_{E_1/B_2}-\dot{\vec{\omega}}_{B_1/A}-\dot{\vec{\omega}}_{A/O}\right)\times\vec{r}_{B_1B_2}-2\omega_{B_2/B_1}^2\vec{r}_{B_1B_2}+\left(\vec{\omega}_{B_2/B_1}\cdot\vec{r}_{B_1B_2}\right)\vec{\omega}_{B_2/B_1}\\+\left(\dot{\vec{\omega}}_{E_1/O}-\dot{\vec{\omega}}_{B_2/B_1}-\dot{\vec{\omega}}_{B_1/A}-\dot{\vec{\omega}}_{A/O}\right)\times\vec{r}_{B_2E_1}-2\omega_{E_1/B_2}^2\vec{r}_{B_2E_1}+\left(\vec{\omega}_{E_1/B_2}\cdot\vec{r}_{B_2E_1}\right)\vec{\omega}_{E_1/B_2}\\+\left(\dot{\vec{\omega}}_{E_2/O}-\dot{\vec{\omega}}_{E_1/B_2}-\dot{\vec{\omega}}_{B_2/B_1}-\dot{\vec{\omega}}_{B_1/A}-\dot{\vec{\omega}}_{A/O}\right)\times\vec{r}_{E_1/E_2}-2\omega_{E_2/E_1}^2\vec{r}_{E_1/E_2}+\left(\vec{\omega}_{E_2/E_1}\cdot\vec{r}_{E_1/E_2}\right)\vec{\omega}_{E_2/E_1}\\+\left(\dot{\vec{\omega}}_{C/O}-\dot{\vec{\omega}}_{B_1/A}-\dot{\vec{\omega}}_{A/O}\right)\times\vec{r}_{B_1C}-2\omega_{C/B_1}^2\vec{r}_{B_1C}+\left(\vec{\omega}_{C/B_1}\cdot\vec{r}_{B_1C}\right)\vec{\omega}_{C/B_1}\\+\left(\dot{\vec{\omega}}_{D/O}-\dot{\vec{\omega}}_{C/B_1}-\dot{\vec{\omega}}_{B_1/A}-\dot{\vec{\omega}}_{A/O}\right)\times\vec{r}_{CD}-2\omega_{D/C}^2\vec{r}_{CD}+\left(\vec{\omega}_{D/C}\cdot\vec{r}_{CD}\right)\vec{\omega}_{D/C}\\+\left(\dot{\vec{\omega}}_{E_2/O}-\dot{\vec{\omega}}_{D/C}-\dot{\vec{\omega}}_{C/B_1}-\dot{\vec{\omega}}_{B_1/A}-\dot{\vec{\omega}}_{A/O}\right)\times\vec{r}_{DE_2}-2\omega_{E_2/D}^2\vec{r}_{DE_2}+\left(\vec{\omega}_{E_2/D}\cdot\vec{r}_{DE_2}\right)\vec{\omega}_{E_2/D}\end{array}\right\}\tag{45}$$

Next, we find expression for $\vec{r}_{OA},\vec{r}_{AB_1},\vec{r}_{B_1B_2},\vec{r}_{B_2E_1},\vec{r}_{B_1C},\vec{r}_{CD},\vec{r}_{DE_2}$, respectively. Details of this are shown in APPENDIX I

3.4 Acceleration equation for all the links

Next we substitute Eqns (A1),(A2),(A3),(A4),(A5),(A6),(A7) & (A8) in Eqn (45) to obtain

$$\vec{a}_L = \left\{ \begin{array}{l} 2\vec{a}_{O/\zeta} + 2\left(\dot{\vec{\omega}}_{B_1/O} - \dot{\vec{\omega}}_{B_1/A}\right)\times OA\hat{j} - 4\omega_{A/O}^2 OA\hat{j} + 2\left(\vec{\omega}_{A/O}\cdot\vec{r}_{O/A}\right)\vec{\omega}_{A/O} \\ + 2\left(\dot{\vec{\omega}}_{B_2/O} - \dot{\vec{\omega}}_{B_2/B_1} - \dot{\vec{\omega}}_{A/O}\right)\times r_{AB_1}[-(\sin\theta_1\hat{i} + \cos\theta_1\hat{j}] \quad - 4\omega_{B_1/A}^2 r_{AB_1}[-(\sin\theta_1\hat{i} + \cos\theta_1\hat{j}] \\ + 2\left(\vec{\omega}_{B_1/A}\cdot\vec{r}_{AB_1}\right)\vec{\omega}_{B_1/A} \\ + \left(\dot{\vec{\omega}}_{E_1/O} - \dot{\vec{\omega}}_{E_1/B_2} - \dot{\vec{\omega}}_{B_1/A} - \dot{\vec{\omega}}_{A/O}\right)\times r_{B_1B_2}[\sin\theta_B\hat{i} + \cos\theta_B\hat{j}] - 2\omega_{B_2/B_1}^2 r_{B_1B_2}[\sin\theta_B\hat{i} + \cos\theta_B\hat{j}] \\ + \left(\vec{\omega}_{B_2/B_1}\cdot\vec{r}_{B_1B_2}\right)\vec{\omega}_{B_2/B_1} \\ + \left(\dot{\vec{\omega}}_{E_1/O} - \dot{\vec{\omega}}_{B_2/B_1} - \dot{\vec{\omega}}_{B_1/A} - \dot{\vec{\omega}}_{A/O}\right)\times r_{B_2E_1}[\sin(\theta_1+\theta_2)\hat{i} + \cos(\theta_1+\theta_2)\hat{j}] \\ - 2\omega_{E_1/B_2}^2 r_{B_2E_1}[\sin(\theta_1+\theta_2)\hat{i} + \cos(\theta_1+\theta_2)\hat{j}] + \left(\vec{\omega}_{E_1/B_2}\cdot\vec{r}_{B_2E_1}\right)\vec{\omega}_{E_1/B_2} \\ + \left(\dot{\vec{\omega}}_{E_2/O} - \dot{\vec{\omega}}_{E_1/B_2} - \dot{\vec{\omega}}_{B_2/B_1} - \dot{\vec{\omega}}_{B_1/A} - \dot{\vec{\omega}}_{A/O}\right)\times r_{E_1E_2}[-\sin\alpha_6\hat{i} - \cos\alpha_6\hat{j}] \\ - 2\omega_{E_2/E_1}^2 r_{E_1E_2}[-\sin\alpha_6\hat{i} - \cos\alpha_6\hat{j}] + \left(\vec{\omega}_{E_2/E_1}\cdot\vec{r}_{E_1/E_2}\right)\vec{\omega}_{E_2/E_1} \\ + \left(\dot{\vec{\omega}}_{C/O} - \dot{\vec{\omega}}_{B_1/A} - \dot{\vec{\omega}}_{A/O}\right)\times r_{B_1C}[\sin\theta_A\hat{i} + \cos\theta_A\hat{j}] - 2\omega_{C/B_1}^2 r_{B_1C}[\sin\theta_A\hat{i} + \cos\theta_A\hat{j}] + \left(\vec{\omega}_{C/B_1}\cdot\vec{r}_{B_1C}\right)\vec{\omega}_{C/B_1} \\ + \left(\dot{\vec{\omega}}_{D/O} - \dot{\vec{\omega}}_{C/B_1} - \dot{\vec{\omega}}_{B_1/A} - \dot{\vec{\omega}}_{A/O}\right)\times r_{CD}[\sin(\gamma-\alpha_4)\hat{i} - \cos(\gamma-\alpha_4)\hat{j}] \\ - 2\omega_{D/C}^2 r_{CD}[\sin(\gamma-\alpha_4)\hat{i} - \cos(\gamma-\alpha_4)\hat{j}] + \left(\vec{\omega}_{D/C}\cdot\vec{r}_{CD}\right)\vec{\omega}_{D/C} \\ + \left(\dot{\vec{\omega}}_{E_2/O} - \dot{\vec{\omega}}_{D/C} - \dot{\vec{\omega}}_{C/B_1} - \dot{\vec{\omega}}_{B_1/A} - \dot{\vec{\omega}}_{A/O}\right)\times r_{DE_2}[\sin\alpha_5\hat{i} - \cos\alpha_5\hat{j}] \\ - 2\omega_{E_2/D}^2 r_{DE_2}[\sin\alpha_5\hat{i} - \cos\alpha_5\hat{j}] + \left(\vec{\omega}_{E_2/D}\cdot\vec{r}_{DE_2}\right)\vec{\omega}_{E_2/D} \end{array} \right\} \quad (46)$$

3.5 Transmitted force equation

The force transmitted or acting on the bucket can be derived from the expression

$$\vec{F}_T = m_b\vec{a}_L \quad (47)$$

whereas the cutting force which is the force of the bucket in the direction of the bucket swing is given as

$$\vec{F}_c = \left(\vec{F}_T\cdot\hat{e}_c\right)\hat{e}_c \quad (48)$$

where:

$\vec{F}_c = cutting\ force$

$\vec{F}_T = transmitted\ \ force\ due\ to\ the\ links$

m_b = mass of excavator bucket

$\vec{a}_L$ =acceleration due to the links

Substituting eqn (46) in eqn(47), we obtain the transmitted force equation given as

$$\vec{F}_T = m_b \left\{ \begin{array}{l} 2\vec{a}_{O/\zeta} + 2\left(\dot{\vec{\omega}}_{B_1/O} - \dot{\vec{\omega}}_{B_1/A}\right) \times OA\hat{j} - \\ 4\omega_{A/O}^2 OA\hat{j} + 2\left(\vec{\omega}_{A/O} \cdot \vec{r}_{O/A}\right)\vec{\omega}_{A/O} \\ + 2\left(\dot{\vec{\omega}}_{B_2/O} - \dot{\vec{\omega}}_{B_2/B_1} - \dot{\vec{\omega}}_{A/O}\right) \times r_{AB_1}[-(\sin\theta_1\hat{i} + \cos\theta_1\hat{j}] \\ \quad - 4\omega_{B_1/A}^2 r_{AB_1}[-(\sin\theta_1\hat{i} + \cos\theta_1\hat{j}] + 2\left(\vec{\omega}_{B_1/A} \cdot \vec{r}_{AB_1}\right)\vec{\omega}_{B_1/A} \\ + \left(\dot{\vec{\omega}}_{E_1/O} - \dot{\vec{\omega}}_{E_1/B_2} - \dot{\vec{\omega}}_{B_1/A} - \dot{\vec{\omega}}_{A/O}\right) \times r_{B_1B_2}[\sin\theta_B\hat{i} + \cos\theta_B\hat{j}] \\ - 2\omega_{B_2/B_1}^2 r_{B_1B_2}[\sin\theta_B\hat{i} + \cos\theta_B\hat{j}] + \left(\vec{\omega}_{B_2/B_1} \cdot \vec{r}_{B_1B_2}\right)\vec{\omega}_{B_2/B_1} \\ + \left(\dot{\vec{\omega}}_{E_1/O} - \dot{\vec{\omega}}_{B_2/B_1} - \dot{\vec{\omega}}_{B_1/A} - \dot{\vec{\omega}}_{A/O}\right) \\ \times r_{B_2E_1}[\sin(\theta_1+\theta_2)\hat{i} + \cos(\theta_1+\theta_2)\hat{j}] \\ - 2\omega_{E_1/B_2}^2 r_{B_2E_1}[\sin(\theta_1+\theta_2)\hat{i} + \cos(\theta_1+\theta_2)\hat{j}] \\ + \left(\vec{\omega}_{E_1/B_2} \cdot \vec{r}_{B_2E_1}\right)\vec{\omega}_{E_1/B_2} \\ + \left(\dot{\vec{\omega}}_{E_2/O} - \dot{\vec{\omega}}_{E_1/B_2} - \dot{\vec{\omega}}_{B_2/B_1} - \dot{\vec{\omega}}_{B_1/A} - \dot{\vec{\omega}}_{A/O}\right) \\ \times r_{E_1E_2}[-\sin\alpha_6\hat{i} - \cos\alpha_6\hat{j}] \\ - 2\omega_{E_2/E_1}^2 r_{E_1E_2}[-\sin\alpha_6\hat{i} - \cos\alpha_6\hat{j}] + \left(\vec{\omega}_{E_2/E_1} \cdot \vec{r}_{E_1/E_2}\right)\vec{\omega}_{E_2/E_1} \\ + \left(\dot{\vec{\omega}}_{C/O} - \dot{\vec{\omega}}_{B_1/A} - \dot{\vec{\omega}}_{A/O}\right) \times r_{B_1C}[\sin\theta_A\hat{i} + \cos\theta_A\hat{j}] \\ - 2\omega_{C/B_1}^2 r_{B_1C}[\sin\theta_A\hat{i} + \cos\theta_A\hat{j}] + \left(\vec{\omega}_{C/B_1} \cdot \vec{r}_{B_1C}\right)\vec{\omega}_{C/B_1} \\ + \left(\dot{\vec{\omega}}_{D/O} - \dot{\vec{\omega}}_{C/B_1} - \dot{\vec{\omega}}_{B_1/A} - \dot{\vec{\omega}}_{A/O}\right) \\ \times r_{CD}[\sin(\gamma-\alpha_4)\hat{i} - \cos(\gamma-\alpha_4)\hat{j}] \\ - 2\omega_{D/C}^2 r_{CD}[\sin(\gamma-\alpha_4)\hat{i} - \cos(\gamma-\alpha_4)\hat{j}] \\ + \left(\vec{\omega}_{D/C} \cdot \vec{r}_{CD}\right)\vec{\omega}_{D/C} \\ + \left(\dot{\vec{\omega}}_{E_2/O} - \dot{\vec{\omega}}_{D/C} - \dot{\vec{\omega}}_{C/B_1} - \dot{\vec{\omega}}_{B_1/A} - \dot{\vec{\omega}}_{A/O}\right) \\ \times r_{DE_2}[\sin\alpha_5\hat{i} - \cos\alpha_5\hat{j}] \\ - 2\omega_{E_2/D}^2 r_{DE_2}[\sin\alpha_5\hat{i} - \cos\alpha_5\hat{j}] + \left(\vec{\omega}_{E_2/D} \cdot \vec{r}_{DE_2}\right)\vec{\omega}_{E_2/D} \end{array} \right\} \quad (49)$$

3.6 Cutting force equation

The cutting force can be expressed by employing Eqn (48) which now becomes

$$\vec{F}_c = \left(m_b \left\{ \begin{array}{l} 2\vec{a}_{O/\zeta} + 2\left(\dot{\vec{\omega}}_{B_1/O} - \dot{\vec{\omega}}_{B_1/A}\right) \times OA\hat{j} - 4\omega_{A/O}^2 OA\hat{j} \\ + 2\left(\vec{\omega}_{A/O} \cdot \vec{r}_{O/A}\right)\vec{\omega}_{A/O} + 2\left(\dot{\vec{\omega}}_{B_2/O} - \dot{\vec{\omega}}_{B_2/B_1} - \dot{\vec{\omega}}_{A/O}\right) \\ \times r_{AB_1}[-(\sin\theta_1\hat{i} + \cos\theta_1\hat{j}] \quad - 4\omega_{B_1/A}^2 r_{AB_1}[-(\sin\theta_1\hat{i} + \cos\theta_1\hat{j}] \\ + 2\left(\vec{\omega}_{B_1/A} \cdot \vec{r}_{AB_1}\right)\vec{\omega}_{B_1/A} + \left(\dot{\vec{\omega}}_{E_1/O} - \dot{\vec{\omega}}_{E_1/B_2} - \dot{\vec{\omega}}_{B_1/A} - \dot{\vec{\omega}}_{A/O}\right) \\ \times r_{B_1B_2}[\sin\theta_B\hat{i} + \cos\theta_B\hat{j}] - 2\omega_{B_2/B_1}^2 r_{B_1B_2}[\sin\theta_B\hat{i} + \cos\theta_B\hat{j}] \\ + \left(\vec{\omega}_{B_2/B_1} \cdot \vec{r}_{B_1B_2}\right)\vec{\omega}_{B_2/B_1} + \left(\dot{\vec{\omega}}_{E_1/O} - \dot{\vec{\omega}}_{B_2/B_1} - \dot{\vec{\omega}}_{B_1/A} - \dot{\vec{\omega}}_{A/O}\right) \\ \times r_{B_2E_1}[\sin(\theta_1+\theta_2)\hat{i} + \cos(\theta_1+\theta_2)\hat{j}] \\ - 2\omega_{E_1/B_2}^2 r_{B_2E_1}[\sin(\theta_1+\theta_2)\hat{i} + \cos(\theta_1+\theta_2)\hat{j}] \\ + \left(\vec{\omega}_{E_1/B_2} \cdot \vec{r}_{B_2E_1}\right)\vec{\omega}_{E_1/B_2} \\ + \left(\dot{\vec{\omega}}_{E_2/O} - \dot{\vec{\omega}}_{E_1/B_2} - \dot{\vec{\omega}}_{B_2/B_1} - \dot{\vec{\omega}}_{B_1/A} - \dot{\vec{\omega}}_{A/O}\right) \\ \times r_{E_1E_2}[-\sin\alpha_6\hat{i} - \cos\alpha_6\hat{j}] \\ - 2\omega_{E_2/E_1}^2 r_{E_1E_2}[-\sin\alpha_6\hat{i} - \cos\alpha_6\hat{j}] + \left(\vec{\omega}_{E_2/E_1} \cdot \vec{r}_{E_1/E_2}\right)\vec{\omega}_{E_2/E_1} \\ + \left(\dot{\vec{\omega}}_{C/O} - \dot{\vec{\omega}}_{B_1/A} - \dot{\vec{\omega}}_{A/O}\right) \times r_{B_1C}[\sin\theta_A\hat{i} + \cos\theta_A\hat{j}] \\ - 2\omega_{C/B_1}^2 r_{B_1C}[\sin\theta_A\hat{i} + \cos\theta_A\hat{j}] + \left(\vec{\omega}_{C/B_1} \cdot \vec{r}_{B_1C}\right)\vec{\omega}_{C/B_1} \\ + \left(\dot{\vec{\omega}}_{D/O} - \dot{\vec{\omega}}_{C/B_1} - \dot{\vec{\omega}}_{B_1/A} - \dot{\vec{\omega}}_{A/O}\right) \times r_{CD}[\sin(\gamma-\alpha_4)\hat{i} - \cos(\gamma-\alpha_4)\hat{j}] \\ - 2\omega_{D/C}^2 r_{CD}[\sin(\gamma-\alpha_4)\hat{i} - \cos(\gamma-\alpha_4)\hat{j}] + \left(\vec{\omega}_{D/C} \cdot \vec{r}_{CD}\right)\vec{\omega}_{D/C} \\ + \left(\dot{\vec{\omega}}_{E_2/O} - \dot{\vec{\omega}}_{D/C} - \dot{\vec{\omega}}_{C/B_1} - \dot{\vec{\omega}}_{B_1/A} - \dot{\vec{\omega}}_{A/O}\right) \times r_{DE_2}[\sin\alpha_5\hat{i} - \cos\alpha_5\hat{j}] \\ - 2\omega_{E_2/D}^2 r_{DE_2}[\sin\alpha_5\hat{i} - \cos\alpha_5\hat{j}] + \left(\vec{\omega}_{E_2/D} \cdot \vec{r}_{DE_2}\right)\vec{\omega}_{E_2/D} \end{array} \right\} \cdot \hat{e}_c \right) \hat{e}_c \qquad (50)$$

Since $\vec{F}_c = \left(\vec{F}_T \cdot \hat{e}_c\right)\hat{e}_c$

$$\left|\vec{F}_c\right| = \left|\left(\vec{F}_T \cdot \hat{e}_c\right)\hat{e}_c\right|$$

$$\vec{F}_c = \vec{F}_T \cdot \hat{e}_c$$

We can therefore write eqn (48) as

$$\vec{F}_c = m_b \left\{ \begin{array}{l} 2\vec{a}_{O/\zeta} + 2\left(\dot{\vec{\omega}}_{B_1/O} - \dot{\vec{\omega}}_{B_1/A}\right) \times r_{OA}\ \hat{j} - 4\omega_{A/O}^2 r_{OA}\ \hat{j} \\ + 2\left(\vec{\omega}_{A/O} \cdot \vec{r}_{O/A}\right) \vec{\omega}_{A/O} + 2\left(\dot{\vec{\omega}}_{B_2/O} - \dot{\vec{\omega}}_{B_2/B_1} - \dot{\vec{\omega}}_{A/O}\right) \\ \times r_{AB_1}[-(\sin\theta_1 \hat{i} + \cos\theta_1 \hat{j}] \quad - 4\omega_{B_1/A}^2 r_{AB_1}[-(\sin\theta_1 \hat{i} + \cos\theta_1 \hat{j}] \\ + 2\left(\vec{\omega}_{B_1/A} \cdot \vec{r}_{AB_1}\right) \vec{\omega}_{B_1/A} + \left(\dot{\vec{\omega}}_{E_1/O} - \dot{\vec{\omega}}_{E_1/B_2} - \dot{\vec{\omega}}_{B_1/A} - \dot{\vec{\omega}}_{A/O}\right) \\ \times r_{B_1B_2}[\sin\theta_B \hat{i} + \cos\theta_B \hat{j}] - 2\omega_{B_2/B_1}^2 r_{B_1B_2}[\sin\theta_B \hat{i} + \cos\theta_B \hat{j}] \\ + \left(\vec{\omega}_{B_2/B_1} \cdot \vec{r}_{B_1B_2}\right) \vec{\omega}_{B_2/B_1} + \left(\dot{\vec{\omega}}_{E_1/O} - \dot{\vec{\omega}}_{B_2/B_1} - \dot{\vec{\omega}}_{B_1/A} - \dot{\vec{\omega}}_{A/O}\right) \\ \times r_{B_2E_1}[\sin(\theta_1 + \theta_2)\hat{i} + \cos(\theta_1 + \theta_2)\hat{j}] \\ - 2\omega_{E_1/B_2}^2 r_{B_2E_1}[\sin(\theta_1 + \theta_2)\hat{i} + \cos(\theta_1 + \theta_2)\hat{j}] \\ + \left(\vec{\omega}_{E_1/B_2} \cdot \vec{r}_{B_2E_1}\right) \vec{\omega}_{E_1/B_2} + \left(\dot{\vec{\omega}}_{E_2/O} - \dot{\vec{\omega}}_{E_1/B_2} - \dot{\vec{\omega}}_{B_2/B_1} - \dot{\vec{\omega}}_{B_1/A} - \dot{\vec{\omega}}_{A/O}\right) \\ \times r_{E_1E_2}[-\sin\alpha_6 \hat{i} - \cos\alpha_6 \hat{j}] - 2\omega_{E_2/E_1}^2 r_{E_1E_2}[-\sin\alpha_6 \hat{i} - \cos\alpha_6 \hat{j}] \\ + \left(\vec{\omega}_{E_2/E_1} \cdot \vec{r}_{E_1/E_2}\right) \vec{\omega}_{E_2/E_1} + \left(\dot{\vec{\omega}}_{C/O} - \dot{\vec{\omega}}_{B_1/A} - \dot{\vec{\omega}}_{A/O}\right) \times r_{B_1C}[\sin\theta_A \hat{i} + \cos\theta_A \hat{j}] \\ - 2\omega_{C/B_1}^2 r_{B_1C}[\sin\theta_A \hat{i} + \cos\theta_A \hat{j}] + \left(\vec{\omega}_{C/B_1} \cdot \vec{r}_{B_1C}\right) \vec{\omega}_{C/B_1} \\ + \left(\dot{\vec{\omega}}_{D/O} - \dot{\vec{\omega}}_{C/B_1} - \dot{\vec{\omega}}_{B_1/A} - \dot{\vec{\omega}}_{A/O}\right) \times r_{CD}[\sin(\gamma - \alpha_4)\hat{i} - \cos(\gamma - \alpha_4)\hat{j}] \\ - 2\omega_{D/C}^2 r_{CD}[\sin(\gamma - \alpha_4)\hat{i} - \cos(\gamma - \alpha_4)\hat{j}] + \left(\vec{\omega}_{D/C} \cdot \vec{r}_{CD}\right) \vec{\omega}_{D/C} \\ + \left(\dot{\vec{\omega}}_{E_2/O} - \dot{\vec{\omega}}_{D/C} - \dot{\vec{\omega}}_{C/B_1} - \dot{\vec{\omega}}_{B_1/A} - \dot{\vec{\omega}}_{A/O}\right) \times r_{DE_2}[\sin\alpha_5 \hat{i} - \cos\alpha_5 \hat{j}] \\ - 2\omega_{E_2/D}^2 r_{DE_2}[\sin\alpha_5 \hat{i} - \cos\alpha_5 \hat{j}] + \left(\vec{\omega}_{E_2/D} \cdot \vec{r}_{DE_2}\right) \vec{\omega}_{E_2/D} \end{array} \right\} \cdot \hat{e}_c \quad (51)$$

Where $\hat{e}_c = (\cos\eta\ \hat{i} - \sin\eta\ \hat{j})$

Setting $\vec{a}_{O/\zeta} = \vec{a}_{O/\zeta}\hat{j}$,

$\dot{\vec{\omega}}_{B_1/O} = \dot{\vec{\omega}}_{B_1/O}\ \hat{k}$

$\dot{\vec{\omega}}_{B_1/A} = \dot{\vec{\omega}}_{B_1/A}\ \hat{k}$

$\vec{r}_{OA}\ \hat{j} = r_{OA}\ \hat{j}$

Introducing the above notations, eqn (51) becomes

$$
F_c = m_b \left\{ \begin{array}{l}
2\vec{a}_{O/\zeta}\,\hat{j} + 2\left(\dot{\vec{\omega}}_{B_1/O} - \dot{\vec{\omega}}_{B_1/A}\right)\hat{k}\times r_{OA}\;\hat{j} - 4\omega_{A/O}^2 r_{OA} + 2\left(\vec{\omega}_{A/O}\cdot\vec{r}_{O/A}\right)\vec{\omega}_{A/O}\hat{k} \\
+2\left(\dot{\vec{\omega}}_{B_2/O} - \dot{\vec{\omega}}_{B_2/B_1} - \dot{\vec{\omega}}_{A/O}\right)\hat{k}\times r_{AB_1}[-(\sin\theta_1\hat{i} + \cos\theta_1\hat{j}] \;\; -4\omega_{B_1/A}^2 r_{AB_1}[-(\sin\theta_1\hat{i} + \cos\theta_1\hat{j}] \\
+2\left(\vec{\omega}_{B_1/A}\cdot\vec{r}_{AB_1}\right)\vec{\omega}_{B_1/A}\hat{k} \\
+\left(\dot{\vec{\omega}}_{E_1/O} - \dot{\vec{\omega}}_{E_1/B_2} - \dot{\vec{\omega}}_{B_1/A} - \dot{\vec{\omega}}_{A/O}\right)\hat{k}\times r_{B_1B_2}[\sin\theta_B\;\hat{i} + \cos\theta_B] - 2\omega_{B_2/B_1}^2 r_{B_1B_2}[\sin\theta_B\;\hat{i} + \cos\theta_B\hat{j}] \\
+\left(\vec{\omega}_{B_2/B_1}\cdot\vec{r}_{B_1B_2}\right)\vec{\omega}_{B_2/B_1}\hat{k} \\
+\left(\dot{\vec{\omega}}_{E_1/O} - \dot{\vec{\omega}}_{B_2/B_1} - \dot{\vec{\omega}}_{B_1/A} - \dot{\vec{\omega}}_{A/O}\right)\hat{k}\times r_{B_2E_1}[\sin(\theta_1+\theta_2)\;\hat{i} + \cos(\theta_1+\theta_2)\;\hat{j}] \\
-2\omega_{E_1/B_2}^2 r_{B_2E_1}[\sin(\theta_1+\theta_2)\;\hat{i} + \cos(\theta_1+\theta_2)\;\hat{j}] + \left(\vec{\omega}_{E_1/B_2}\cdot\vec{r}_{B_2E_1}\right)\vec{\omega}_{E_1/B_2}\hat{k} \\
+\left(\dot{\vec{\omega}}_{E_2/O} - \dot{\vec{\omega}}_{E_1/B_2} - \dot{\vec{\omega}}_{B_2/B_1} - \dot{\vec{\omega}}_{B_1/A} - \dot{\vec{\omega}}_{A/O}\right)\hat{k}\times r_{E_1E_2}[-\cos\alpha_6\;\hat{i} - \sin\alpha_6\hat{j}] \\
-2\omega_{E_2/E_1}^2 r_{E_1E_2}[-\cos\alpha_6\;\hat{i} - \sin\alpha_6\hat{j}] + \left(\vec{\omega}_{E_2/E_1}\cdot\vec{r}_{E_1/E_2}\right)\vec{\omega}_{E_2/E_1}\hat{k} \\
+\left(\dot{\vec{\omega}}_{C/O} - \dot{\vec{\omega}}_{B_1/A} - \dot{\vec{\omega}}_{A/O}\right)\hat{k}\times r_{B_1C}[\sin\theta_A\;\hat{i} + \cos\theta_A\hat{j}] - 2\omega_{C/B_1}^2 r_{B_1C}[\sin\theta_A\;\hat{i} + \cos\theta_A\hat{j}] \\
+\left(\vec{\omega}_{C/B_1}\cdot\vec{r}_{B_1C}\right)\vec{\omega}_{C/B_1}\hat{k} + \left(\dot{\vec{\omega}}_{D/O} - \dot{\vec{\omega}}_{C/B_1} - \dot{\vec{\omega}}_{B_1/A} - \dot{\vec{\omega}}_{A/O}\right)\hat{k}\times r_{CD}[\sin(\gamma-\alpha_4)\;\hat{i} - \cos(\gamma-\alpha_4)\;\hat{j}] \\
-2\omega_{D/C}^2 r_{CD}[\sin(\gamma-\alpha_4)\;\hat{i} - \cos(\gamma-\alpha_4)\;\hat{j}] + \left(\vec{\omega}_{D/C}\cdot\vec{r}_{CD}\right)\vec{\omega}_{D/C}\hat{k} \\
+\left(\dot{\vec{\omega}}_{E_2/O} - \dot{\vec{\omega}}_{D/C} - \dot{\vec{\omega}}_{C/B_1} - \dot{\vec{\omega}}_{B_1/A} - \dot{\vec{\omega}}_{A/O}\right)\hat{k}\times r_{DE_2}[\sin\alpha_5\;\hat{i} - \cos\alpha_5\hat{j}] \\
-2\omega_{E_2/D}^2 r_{DE_2}[\sin\alpha_5\;\hat{i} - \cos\alpha_5\hat{j}] + \left(\vec{\omega}_{E_2/D}\cdot\vec{r}_{DE_2}\right)\vec{\omega}_{E_2/D}\hat{k}
\end{array} \right\} [\cos\eta\hat{i} - \sin\eta\hat{j}]
\tag{52}
$$

Taking scalar product, eqn (52) becomes

$$
F_c = m_b \left\{ \begin{array}{l}
-2a_{O/\zeta}\sin\eta - 4\omega_{A/O}^2 r_{OA}(-\sin\eta) + 4\omega_{B_1/A}^2 r_{AB_1}[\sin(\theta_1+\eta)] + 2\omega_{B_2/B_1}^2 r_{B_1B_2}[\sin(\eta-\theta_B)] \\
+2\omega_{E_1/B_2}^2 r_{B_2E_1}[\sin(\eta-\theta_C)] + 2\omega_{E_2/E_1}^2 r_{E_1E_2}[\sin(\alpha_6+\eta)] + 2\omega_{C/B_1}^2 r_{B_1C}[\sin(\eta-\theta_A)] \\
-2\omega_{D/C}^2 r_{CD}[\sin(\theta_D-\eta)] - 2\omega_{E_2/D}^2 r_{DE_2}[\sin(\alpha_6+\eta)]
\end{array} \right\}
\tag{53}
$$

Considering the two links (r_{ab1} and r_{b1c}) operating as a strut system, we can re-write eqn (53) as

$$
F_c = m_b \left\{ \begin{array}{l}
-2a_{O/\zeta}\sin\eta - 4\omega_{A/O}^2 r_{OA}(-\sin\eta) + 4\omega_{B_1/A}^2 \left(\dfrac{r_{B_1B_2}\sin[180-(\alpha_1+\alpha_2)]}{\sin\alpha_1}\right)[\sin(\theta_1+\eta)] \\
+2\omega_{B_2/B_1}^2 r_{B_1B_2}[\sin(\eta-\theta_B)] + 2\omega_{E_1/B_2}^2 r_{B_2E_1}[\sin(\eta-\theta_C)] + 2\omega_{E_2/E_1}^2 r_{E_1E_2}[\sin(\alpha_6+\eta)] + \\
2\omega_{C/B_1}^2 \left(\dfrac{r_{CE_1}\sin[180-(\alpha_3+\alpha_5)]}{\sin\alpha_3}\right)[\sin(\eta-\theta_A)] - 2\omega_{D/C}^2 r_{CD}[\sin(\theta_D-\eta)] - 2\omega_{E_2/D}^2 r_{DE_2}[\sin(\alpha_6+\eta)]
\end{array} \right\}
\tag{54}
$$

For simulation purposes, we further simplify eqn (53) by finding $\frac{\partial F_c}{\partial \eta}$

$$\frac{\partial F_c}{\partial \eta} = m_b \begin{Bmatrix} -2a_{O/\zeta}\cos\eta + 4\omega_{A/O}^2 r_{OA}\cos\eta + 4\omega_{B_1/A}^2 r_{AB_1}[\cos(\theta_1+\eta)] + 2\omega_{B_2/B_1}^2 r_{B_1B_2}[\cos(\eta-\theta_B)] \\ +2\omega_{E_1/B_2}^2 r_{B_2E_1}[\cos(\eta-\theta_C)] + 2\omega_{E_2/E_1}^2 r_{E_1E_2}[\cos(\alpha_6+\eta)] + 2\omega_{C/B_1}^2 r_{B_1C}[\cos(\eta-\theta_A)] \\ +2\omega_{D/C}^2 r_{CD}[\cos(\theta_D-\eta)] - 2\omega_{E_2/D}^2 r_{DE_2}[\cos(\alpha_5+\eta)] \end{Bmatrix} \tag{55}$$

In excavation process, $\omega < 1$ in the limiting case as $\theta_i \to 0$

$$\frac{\partial F_c}{\partial \eta} = m_b \cos\eta \begin{Bmatrix} -2a_{O/\zeta} + 4\omega_{A/O}^2 r_{OA} + 4\omega_{B_1/A}^2 r_{AB_1} + 2\omega_{B_2/B_1}^2 r_{B_1B_2} \\ +2\omega_{E_1/B_2}^2 r_{B_2E_1} + 2\omega_{E_2/E_1}^2 r_{E_1E_2} + 2\omega_{C/B_1}^2 r_{B_1C} \\ +2\omega_{D/C}^2 r_{CD} - 2\omega_{E_2/D}^2 r_{DE_2} \end{Bmatrix} = 0 \qquad \left| \begin{array}{l} \cos\eta = 0 \\ \eta = 90^0 \\ \forall\, \theta_i = 0 \end{array} \right. \tag{56}$$

Assuming $\theta_A, \theta_B, \theta_C, \theta_D, \alpha_5, \alpha_6$ are almost negligible, we obtain

$$\frac{\partial^2 F_c}{\partial \eta^2} = m_b \begin{Bmatrix} -2a_{O/\zeta}\sin\eta - 4\omega_{A/O}^2 r_{OA}\sin\eta - 4\omega_{B_1/A}^2 r_{AB_1}\sin\eta \\ -2\omega_{B_2/B_1}^2 r_{B_1B_2}\sin\eta - 2\omega_{E_1/B_2}^2 r_{B_2E_1}\sin\eta - 2\omega_{E_2/E_1}^2 r_{E_1E_2}\sin\eta \\ -2\omega_{C/B_1}^2 r_{B_1C}\sin\eta - 2\omega_{D/C}^2 r_{CD}\sin\eta + 2\omega_{E_2/D}^2 r_{DE_2}\sin\eta \end{Bmatrix} \tag{57}$$

Setting $\eta = 90^0, \omega < 1$

$$\frac{\partial^2 F_c}{\partial \eta^2} < 0$$

Generally, for any η, the maximum cutting force, F_c, can be computed.

Since $\frac{\partial^2 F_c}{\partial \eta^2} < 0$, it shows that the maximum F_c can be obtained when $\eta = 90^0$

This now allows us to further simplify eqn (55) into the form

$$\begin{Bmatrix} -2a_{O/\zeta}\cos\eta + 4\omega_{A/O}^2 r_{OA}\cos\eta + 4\omega_{B_1/A}^2 r_{AB_1}\cos\eta + 2\omega_{B_2/B_1}^2 r_{B_1B_2}\cos\eta \\ +2\omega_{E_1/B_2}^2 r_{B_2E_1}\cos\eta + 2\omega_{E_2/E_1}^2 r_{E_1E_2}\cos\eta + 2\omega_{C/B_1}^2 r_{B_1C}\cos\eta \\ -2\omega_{D/C}^2 r_{CD}\cos\eta - 2\omega_{E_2/D}^2 r_{DE_2}\cos\eta \end{Bmatrix} = 0$$

Hence we find an expression for $\cos\eta$

$$\cos\eta\begin{Bmatrix} 2a_{O/\zeta} - 4\omega^2_{A/O} r_{OA} - 4\omega^2_{B_1/A} r_{AB_1} - 2\omega^2_{B_2/B_1} r_{B_1B_2} - 2\omega^2_{E_1/B_2} r_{B_2E_1} \\ -2\omega^2_{E_2/E_1} r_{E_1E_2} - 2\omega^2_{C/B_1} r_{B_1C} + 2\omega^2_{D/C} r_{CD} + 2\omega^2_{E_2/D} r_{DE_2} \end{Bmatrix} = 0 \tag{58}$$

We now take any of the kernels representing the link of interest in eqn (58)

It can be shown for link length $r_{E_1E_2}$ that angle η can be expressed in terms of link $r_{E_1E_2}$ via the following relation

$$\sin\eta = \sqrt{1-(16\omega^4_{E_2/E_1} r^2_{E_1E_2})}$$

$$\sin\eta \approx 1 - \frac{1}{2}(16\omega^4_{E_2/E_1} r^2_{E_1E_2}) \tag{59}$$

In view of equation (59), the maximum cutting force can be determined as

$$F_c = m_b\left\{\left(2\omega^2_{E_2/E_1} r_{E_1E_2}\right)\left(1-\frac{1}{2}\left(16\omega^4_{E_2/E_1} r^2_{E_1E_2}\right)\right)\right\}$$

$$F_c = m_b\left(2\omega^2_{E_2/E_1} r_{E_1E_2} - 16\omega^6_{E_2/E_1} r^3_{E_1E_2}\right) \tag{60}$$

For simulation purposes, eqn (60) can be used to study the behaviour of the cutting force in relation to the angular velocity and link length.

In a similar vein, we can determine the expression for simulating the behaviour of the cutting force in relation to the other angular velocity and link lengths.

For the other link lengths,

$$F_c = m_b\left\{\left(2\omega^2_{E_2/D} r_{DE_2}\right)\left(1-\frac{1}{2}\left(16\omega^4_{E_2/D} r^2_{DE_2}\right)\right)\right\} \tag{61}$$

$$F_c = m_b\left\{\left(2\omega^2_{C/D} r_{DC}\right)\left(1-\frac{1}{2}\left(16\omega^4_{C/D} r^2_{DC}\right)\right)\right\} \tag{62}$$

$$F_c = m_b\left\{\left(2\omega^2_{B_1/C} r_{CB_1}\right)\left(1-\frac{1}{2}\left(16\omega^4_{B_1/C} r^2_{CB_1}\right)\right)\right\} \tag{63}$$

$$F_c = m_b \left\{ \left(2\omega_{E_1/B_2}^2 r_{B_2E_1} \right) \left(1 - \frac{1}{2} \left(16\omega_{E_1/B_2}^4 r_{B_2E_1}^2 \right) \right) \right\} \tag{64}$$

Similarly, we can represent the model in terms of the cutting angle η

$$\frac{\Delta\theta}{\Delta t} = \frac{\theta_1 - \theta_0}{t - t_0}$$

$$\Delta\theta \approx \frac{\partial\theta}{\partial t}\Delta t$$

$$\frac{\Delta\theta}{\Delta t} \approx \frac{\partial\theta}{\partial t} = \omega$$

Hence $\dfrac{\theta_1 - \theta_0}{t - t_0} = \omega$

$$\theta = \theta_0 + \omega(t - t_0) \qquad , \ t_0 = 0$$

$$\theta = \theta_0 + \omega t$$

Hence

$$\omega = \frac{\theta - \theta_0}{t} = \frac{\Delta\theta}{t} \tag{65}$$

We can simulate the behaviour of the cutting angle with a particular length.

From eqn (59), substituting $\omega = \dfrac{\theta - \theta_0}{t} = \dfrac{\chi}{t}$ $\ for\ all\ \chi = \Delta\theta$, we obtain

$$F_c = m_b \left\{ 2\left(\frac{\chi^2}{t^2} \right) r_{E_1E_2} - 4\left(\frac{\chi^6}{t^6} \right) r_{E_1E_2}^3 \right\} \tag{66}$$

This equation can be used to study the behaviour of the cutting force, cutting angle and any link length of choice.

However, Singh assumed in his problem that the failure surface is a plane; the wedge can be represented as shown in Figure 11 where the forces acting on the wedge consist of:

(i) The shear force of the material away from itself which is a function of the cohesiveness of the material.

(ii) The reaction force of the soil against the sliding wedge.

(iii) The weight of the material in the wedge, and the weight of previously dug material known as the surcharge.

(iv) The adhesion of the soil to the tool.

(v) The force of the tool against the wedge.

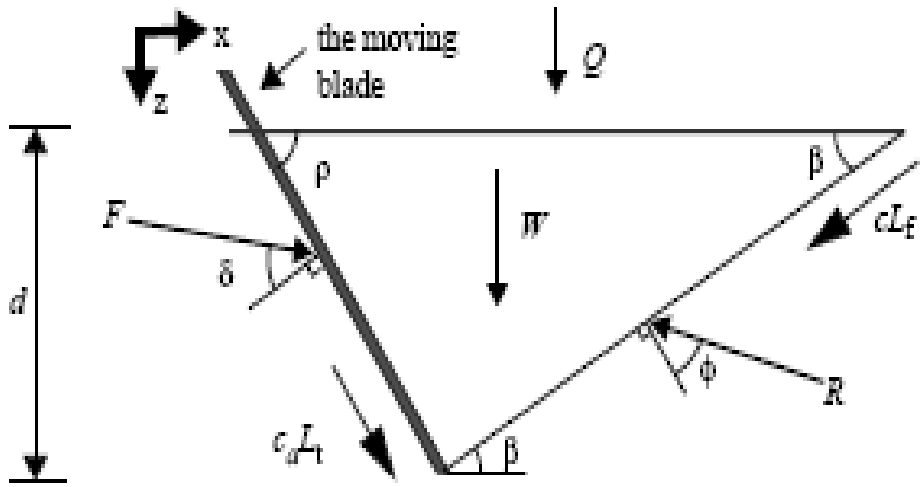

Fig 11: Static equilibrium analysis using an approximation of the failure surface.

W = weight of the moving soil wedge,

Lt = length of the tool and

Lf = length of the failure surface,

ϕ = angle of soil-soil friction

c = cohesion of soil

c_a = adhesion between the soil and blade

∂ = friction between the metal and the blade/ the soil-tool friction angle

ρ = the rake angle

γ = soil density

d = the depth of the tool in the soil

β = the failure surface

Q = the surcharge pressure,

R = the force resisting movement of the wedge

F = the resistive force experienced at a blade

Singh developed the force equilibrium equations for a blade of unit width as follows viz

$$F_x = F\,Sin(\rho+\delta) + c_a\,L_t\,Cos\rho - R\,Sin(\beta+\phi) - cL_f\,Cos\beta \;=\; 0$$
$$F_z = -F\,Cos(\rho+\delta) + c_a\,L_t\,Sin\rho + c\,L_f\,Sin\beta - R\,Cos(\beta+\phi) + W + Q = 0$$

From where he derived an expression for F in the eqn below

$$F = \frac{W + Q + cd\,[1 + Cot\beta\;Cot\,(\beta+\phi)] + c_a\,d[1 - Cot\rho\,Cot(\beta+\phi)]}{[Cos(\rho+\delta) + Sin(\rho+\delta)\;Cot(\beta+\phi)\,]}$$

In our own case, which is the dynamic equillibrium, introducing the cutting force, F_c, we can re-write Singhs' equation as

$$\sum Fx = F\,Sin(\rho+\delta) + (C_aL_t + F_c)Cos\rho - RSin(\phi+\beta) - cL_fCos\beta = 0 \qquad (67)$$

$$\sum Fz = -F\,Cos(\rho+\delta) + (C_aL_t + F_c)\,Sin\rho - RCos(\phi+\beta) + cL_fCos\beta + W + QCos(90^0 - \psi) \qquad (68)$$

Solving, we obtain

$$F = \frac{W + QCos(90^0 - \psi) + cd\,[1 + Cot\beta\;Cot\,(\beta+\phi)] + c_a\,d[1 - Cot\rho\,Cot(\beta+\phi)] + FcSin\rho + FcCos\rho\,Cot(\beta+\phi)}{[Cos(\rho+\delta) + Sin(\rho+\delta)\;Cot(\beta+\phi)\,]} \qquad (69)$$

Where eqn (69) is the generalized form of solution of the equation.

However, within the limit, we can recover Singh's problem by setting $\psi = 90^0, F_c = 0$

Hence Eqn (69) becomes

$$F = \frac{W + Q + cd\,[1 + Cot\beta\;Cot\,(\beta+\phi)] + c_a\,d[1 - Cot\rho\,Cot(\beta+\phi)] + 0\times Sin\rho + 0\times Cos\rho\,Cot(\beta+\phi)}{[Cos(\rho+\delta) + Sin(\rho+\delta)\;Cot(\beta+\phi)\,]} \qquad (70)$$

Hence

$$F = \frac{W + Q + cd\left[1 + Cot\beta\ Cot\left(\beta + \phi\right)\right] + c_a\, d\left[1 - Cot\rho\, Cot\left(\beta + \phi\right)\right]}{\left[Cos\left(\rho + \partial\right) + Sin\left(\rho + \partial\right)\ Cot(\beta + \phi)\right]} \tag{71}$$

This chapter has presented the excavation model and a generalised model of dynamic equations governing the motion of the various links of the excavator, the transmitted and cutting forces of the excavator bucket. The specific problems addressed in this chapter include the effect of the geometrical parameters such as link length on the cutting force by considering various scenarios. Here, the work is designed for the motion of the excavator bucket in a free swing.

CHAPTER FOUR

ANALYTICAL PREDICTION OF SCOOPED VOLUME DURING HYDRAULIC EXCAVATION

4.1 PREAMBLE

Methodology and basic formulations of forces between the tool and the material to be moved as well as the internal forces in the pile to be dug from are areas of utmost concern. The force formulation is based on simple physical parameters such as internal cohesion, density, angle of friction of the material and finally the adhesion between the tool and the granulated material. In this work, an approach which involves the use of rigid body dynamics with analytical geometry and circular functions is being proposed for predicting scooped volume during excavation. This concept adequately captures the relative motion of the links of the excavator as well as geometrical dimensions during excavation

This chapter presents analytical prediction of scooped volume in hydraulic excavation with respect to our previously derived dynamic equations governing the motion of the various links of the excavator, transmitted force, cutting force. Here, the bucket of the hydraulic excavator scoops through the cutting medium such as soil. Hence the medium/soil parameters are adequately captured in the analytical expressions. The work provides an insight into the effect of angle of inclination on the scooped volume.

4.1. Analysis of Scooped Volume

The scooped force is given as

$$F_s = F_c - R_s \tag{72}$$

where

$$R_s = \tau_s A_b \tag{73}$$

Hence

$$F_s = F_c - \tau_s A_b \tag{74}$$

$F_s = scooping\ force$
$R_s = resistance\ due\ to\ shear$
$F_c = cutting\ force$
$\tau_s = shear\ strength$
$A_b = area\ of\ bucket$
$d = depth\ of\ cut$
$m_b = mass\ of\ bucket$
$v_s = scooped\ volume$
$v_b = volume\ of\ bucket$
$\rho_s = density\ of\ soil$

Next we find an expression for the depth of cut as

$$d = \frac{1}{2}\left(\frac{F_c - \tau_s A_b}{m_b}\right)t^2 \tag{75}$$

which now allows us to compute an expression for the scooped volume as

$$v_s = \frac{1}{2}\left(\frac{F_c - \tau_s A_b}{\rho_s v_b}\right)t^2 A_b$$

$$v_s = \frac{1}{2}\left(\frac{F_c A_b - \tau_s A_b^2}{\rho_s v_b}\right)t^2 \tag{76}$$

Coulomb modeled the shear strength of a soil (Singh,1995) as

$$\tau_s = c + \sigma \tan\phi \tag{77}$$

where
c = cohesive force,
σ = normal pressure acting on the internal shear surface,
tan ϕ = coefficient of sliding friction.
ϕ is also called the angle of internal friction and is directly visible as the angle of repose of a pile of dry, uncompacted granular material like sand or sugar.

When soil shears, it does so along a surface called a failure surface. The shear strength of a soil can be understood to be the resistance per unit area to deformation along a surface of failure. Shear stress, on the other hand, is the pressure that pushes soil to move along a failure surface (Singh, 1995b).

Hence $v_s = \frac{1}{2}\left(\frac{F_c A_b - \tau_s A_b^2}{\rho_s v_b}\right)t^2$

$$v_s = \frac{1}{2}\left(\frac{F_c A_b - (c + \sigma \tan\phi) A_b^2}{\rho_s v_b}\right)t^2$$

$$v_s = \frac{1}{2}\left(\frac{F_c A_b - \left(c + \frac{F_c}{A_b}\tan\phi\right) A_b^2}{\rho_s v_b}\right)t^2 \qquad (78)$$

Substituting the cutting force F_c in eqn (78) yields

$$v_s = \frac{\frac{1}{2}\left(F_c A_b - \left(c + \frac{F_c}{A_b}\tan\phi\right) A_b^2\right)t^2}{\rho_s v_b}$$

$$v_s = \frac{\frac{1}{2}\left(F_c A_b - \left(c\, A_b^2 + F_c\, A_b \tan\phi\right)\right)t^2}{\rho_s v_b}$$

$$v_s = \frac{\frac{1}{2}t^2\left(F_c A_b - \left(c\, A_b^2 + F_c\, A_b \tan\phi\right)\right)}{\rho_s A_b d}$$

$$v_s = \frac{\frac{1}{2}t^2\left(F_c - \left(c\, A_b + F_c \tan\phi\right)\right)}{\rho_s d} = \frac{1}{2}t^2\,\frac{\left[F_c(1-\tan\phi) - c\, A_b\right]}{\rho_s d} \qquad (79)$$

Earlier, we derived an expression for the cutting force F_c which is given as

$$F_c = m_b \begin{Bmatrix} -2a_{O/\zeta}\sin\eta - 4\omega_{A/O}^2 r_{OA}(-\sin\eta) + 4\omega_{B_1/A}^2 r_{AB_1}[\sin(\theta_1+\eta)] \\ +2\omega_{B_2/B_1}^2 r_{B_1B_2}[\sin(\eta-\theta_B)] + 2\omega_{E_1/B_2}^2 r_{B_2E_1}[\sin(\eta-\theta_C)] \\ +2\omega_{E_2/E_1}^2 r_{E_1E_2}[\sin(\alpha_6+\eta)] + 2\omega_{C/B_1}^2 r_{B_1C}[\sin(\eta-\theta_A)] \\ -2\omega_{D/C}^2 r_{CD}[\sin(\theta_D-\eta)] - 2\omega_{E_2/D}^2 r_{DE_2}[\sin(\alpha_6+\eta)] \end{Bmatrix} \tag{80}$$

Substituting eqn (80) in eqn (79), we obtain

$$v_s = \frac{\frac{1}{2}t^2 \left(m_b \begin{Bmatrix} -2a_{O/\zeta}\sin\eta - 4\omega_{A/O}^2 r_{OA}(-\sin\eta) + 4\omega_{B_1/A}^2 r_{AB_1}[\sin(\theta_1+\eta)] + 2\omega_{B_2/B_1}^2 r_{B_1B_2}[\sin(\eta-\theta_B)] \\ +2\omega_{E_1/B_2}^2 r_{B_2E_1}[\sin(\eta-\theta_C)] + 2\omega_{E_2/E_1}^2 r_{E_1E_2}[\sin(\alpha_6+\eta)] \\ +2\omega_{C/B_1}^2 r_{B_1C}[\sin(\eta-\theta_A)] - 2\omega_{D/C}^2 r_{CD}[\sin(\theta_D-\eta)] - 2\omega_{E_2/D}^2 r_{DE_2}[\sin(\alpha_6+\eta)] \end{Bmatrix} - \left(c\,A_b + m_b \begin{Bmatrix} -2a_{O/\zeta}\sin\eta - 4\omega_{A/O}^2 r_{OA}(-\sin\eta) + 4\omega_{B_1/A}^2 r_{AB_1}[\sin(\theta_1+\eta)] + 2\omega_{B_2/B_1}^2 r_{B_1B_2}[\sin(\eta-\theta_B)] \\ +2\omega_{E_1/B_2}^2 r_{B_2E_1}[\sin(\eta-\theta_C)] + 2\omega_{E_2/E_1}^2 r_{E_1E_2}[\sin(\alpha_6+\eta)] \\ +2\omega_{C/B_1}^2 r_{B_1C}[\sin(\eta-\theta_A)] - 2\omega_{D/C}^2 r_{CD}[\sin(\theta_D-\eta)] - 2\omega_{E_2/D}^2 r_{DE_2}[\sin(\alpha_6+\eta)] \end{Bmatrix} \tan\phi \right) \right)}{\rho_s\, d} \tag{81}$$

which can be written as

$$v_s = \frac{\frac{1}{2}t^2\left(m_b\left\{\begin{array}{l} -2a_{O/\zeta}\sin\eta - 4\omega_{A/O}^2 r_{OA}(-\sin\eta) + 4\omega_{B_1/A}^2\left(\frac{r_{B_1B_2}\sin[180-(\alpha_1+\alpha_2)]}{\sin\alpha_1}\right)[\sin(\theta_1+\eta)] \\ +2\omega_{B_2/B_1}^2 r_{B_1B_2}[\sin(\eta-\theta_B)] + 2\omega_{E_1/B_2}^2 r_{B_2E_1}[\sin(\eta-\theta_C)] + 2\omega_{E_2/E_1}^2 r_{E_1E_2}[\sin(\alpha_6+\eta)] \\ +2\omega_{C/B_1}^2\left(\frac{r_{CE_1}\sin[180-(\alpha_3+\alpha_5)]}{\sin\alpha_3}\right)[\sin(\eta-\theta_A)] - 2\omega_{D/C}^2 r_{CD}[\sin(\theta_D-\eta)] \\ -2\omega_{E_2/D}^2 r_{DE_2}[\sin(\alpha_6+\eta)] \end{array}\right\} - \left(c\,A_b + m_b\left\{\begin{array}{l} -2a_{O/\zeta}\sin\eta - 4\omega_{A/O}^2 r_{OA}(-\sin\eta) + 4\omega_{B_1/A}^2\left(\frac{r_{B_1B_2}\sin[180-(\alpha_1+\alpha_2)]}{\sin\alpha_1}\right)[\sin(\theta_1+\eta)] \\ +2\omega_{B_2/B_1}^2 r_{B_1B_2}[\sin(\eta-\theta_B)] + 2\omega_{E_1/B_2}^2 r_{B_2E_1}[\sin(\eta-\theta_C)] + 2\omega_{E_2/E_1}^2 r_{E_1E_2}[\sin(\alpha_6+\eta)] \\ +2\omega_{C/B_1}^2\left(\frac{r_{CE_1}\sin[180-(\alpha_3+\alpha_5)]}{\sin\alpha_3}\right)[\sin(\eta-\theta_A)] - 2\omega_{D/C}^2 r_{CD}[\sin(\theta_D-\eta)] \\ -2\omega_{E_2/D}^2 r_{DE_2}[\sin(\alpha_6+\eta)] \end{array}\right\}\tan\phi\right)\right)}{\rho_s\, d} \quad (82)$$

For simulation purposes, we further simplify eqn (81) by finding $\frac{\partial v_s}{\partial \eta}$

$$\frac{\partial v_s}{\partial \eta} = \frac{\frac{1}{2}t^2\left(m_b\left\{\begin{array}{l} -2a_{O/\zeta}\cos\eta - 4\omega_{A/O}^2 r_{OA}\cos\eta + 4\omega_{B_1/A}^2 r_{AB_1}[\cos(\theta_1+\eta)] + 2\omega_{B_2/B_1}^2 r_{B_1B_2}\cos(\eta-\theta_B) \\ +2\omega_{E_1/B_2}^2 r_{B_2E_1}\cos(\eta-\theta_C) + 2\omega_{E_2/E_1}^2 r_{E_1E_2}\cos(\alpha_6+\eta) \\ +2\omega_{C/B_1}^2 r_{B_1C}\cos(\eta-\theta_A) - 2\omega_{D/C}^2 r_{CD}\cos(\theta_D-\eta) - 2\omega_{E_2/D}^2 r_{DE_2}\cos(\alpha_6+\eta) \end{array}\right\} - c\,A_b - m_b\tan\phi\left\{\begin{array}{l} -2a_{O/\zeta}\cos\eta - 4\omega_{A/O}^2 r_{OA}\cos\eta + 4\omega_{B_1/A}^2 r_{AB_1}[\cos(\theta_1+\eta)] + 2\omega_{B_2/B_1}^2 r_{B_1B_2}\cos(\eta-\theta_B) \\ +2\omega_{E_1/B_2}^2 r_{B_2E_1}\cos(\eta-\theta_C) + 2\omega_{E_2/E_1}^2 r_{E_1E_2}\cos(\alpha_6+\eta) \\ +2\omega_{C/B_1}^2 r_{B_1C}\cos(\eta-\theta_A) - 2\omega_{D/C}^2 r_{CD}\cos(\theta_D-\eta) - 2\omega_{E_2/D}^2 r_{DE_2}\cos(\alpha_6+\eta) \end{array}\right\}\right)}{\rho_s\, d} \quad (83)$$

In excavation process, $\omega < 1$ in the limiting case as $\theta_i \to 0$

$$\frac{\partial v_s}{\partial \eta} = \frac{\frac{1}{2}t^2 \cos\eta \left(\begin{array}{l} m_b \left\{ \begin{array}{l} -2a_{O/\zeta} - 4\omega_{A/O}^2 r_{OA} + 4\omega_{B_1/A}^2 r_{AB_1} + 2\omega_{B_2/B_1}^2 r_{B_1B_2} + 2\omega_{E_1/B_2}^2 r_{B_2E_1} \\ + 2\omega_{E_2/E_1}^2 r_{E_1E_2} + 2\omega_{C/B_1}^2 r_{B_1C} - 2\omega_{D/C}^2 r_{CD} - 2\omega_{E_2/D}^2 r_{DE_2} \end{array} \right\} - c\ A_b - \\ m_b \tan\phi \left\{ \begin{array}{l} -2a_{O/\zeta} - 4\omega_{A/O}^2 r_{OA} + 4\omega_{B_1/A}^2 r_{AB_1} + 2\omega_{B_2/B_1}^2 r_{B_1B_2} + 2\omega_{E_1/B_2}^2 r_{B_2E_1} \\ + 2\omega_{E_2/E_1}^2 r_{E_1E_2} + 2\omega_{C/B_1}^2 r_{B_1C} - 2\omega_{D/C}^2 r_{CD} - 2\omega_{E_2/D}^2 r_{DE_2} \end{array} \right\} \end{array} \right)}{\rho_s\ d} = 0 \qquad (84)$$

$\cos\eta = 0, \Rightarrow \eta = 90^0, \forall \theta_i \to 0$

Next we derive expression for $\frac{\partial^2 v_s}{\partial \eta^2}$

$$\frac{\partial^2 v_s}{\partial \eta^2} = \frac{\frac{1}{2}t^2 \left(\begin{array}{l} m_b \left\{ \begin{array}{l} -2a_{O/\zeta} \sin\eta - 4\omega_{A/O}^2 r_{OA} \sin\eta - 4\omega_{B_1/A}^2 r_{AB_1} \sin\eta \\ -2\omega_{B_2/B_1}^2 r_{B_1B_2} \sin\eta - 2\omega_{E_1/B_2}^2 r_{B_2E_1} \sin\eta - 2\omega_{E_2/E_1}^2 r_{E_1E_2} \sin\eta \\ -2\omega_{C/B_1}^2 r_{B_1C} \sin\eta + 2\omega_{D/C}^2 r_{CD} \sin\eta + 2\omega_{E_2/D}^2 r_{DE_2} \sin\eta \end{array} \right\} - c\ A_b - \\ m_b \tan\phi \left\{ \begin{array}{l} -2a_{O/\zeta} \sin\eta - 4\omega_{A/O}^2 r_{OA} \sin\eta - 4\omega_{B_1/A}^2 r_{AB_1} \sin\eta \\ -2\omega_{B_2/B_1}^2 r_{B_1B_2} \sin\eta - 2\omega_{E_1/B_2}^2 r_{B_2E_1} \sin\eta - 2\omega_{E_2/E_1}^2 r_{E_1E_2} \sin\eta \\ -2\omega_{C/B_1}^2 r_{B_1C} \sin\eta + 2\omega_{D/C}^2 r_{CD} \sin\eta + 2\omega_{E_2/D}^2 r_{DE_2} \sin\eta \end{array} \right\} \end{array} \right)}{\rho_s\ d} \qquad (85)$$

Setting $\eta = 90^0, \omega < 1$

$$\frac{\partial^2 v_s}{\partial \eta^2} < 0$$

Generally, for any η, the maximum scooped volume, v_s, can be computed.

Since $\frac{\partial^2 F_c}{\partial \eta^2} < 0$, it shows that the maximum scooped volume, v_s, can be obtained when $\eta = 90^0$

This now allows us to further simplify eqn (83) into the form

$$\frac{\partial v_s}{\partial \eta} = \frac{\frac{1}{2}t^2\left(\begin{array}{l} m_b\left\{\begin{array}{l} -2a_{O/\zeta}\cos\eta - 4\omega^2_{A/O}r_{OA}\cos\eta + 4\omega^2_{B_1/A}r_{AB_1}\cos\eta \\ +2\omega^2_{B_2/B_1}r_{B_1B_2}\cos\eta + 2\omega^2_{E_1/B_2}r_{B_2E_1}\cos\eta + 2\omega^2_{E_2/E_1}r_{E_1E_2}\cos\eta \\ +2\omega^2_{C/B_1}r_{B_1C}\cos\eta - 2\omega^2_{D/C}r_{CD}\cos\eta - 2\omega^2_{E_2/D}r_{DE_2}\cos\eta \end{array}\right\} - c\,A_b - \\ m_b\tan\phi\left\{\begin{array}{l} -2a_{O/\zeta}\cos\eta - 4\omega^2_{A/O}r_{OA}\cos\eta + 4\omega^2_{B_1/A}r_{AB_1}\cos\eta \\ +2\omega^2_{B_2/B_1}r_{B_1B_2}\cos\eta + 2\omega^2_{E_1/B_2}r_{B_2E_1}\cos\eta + 2\omega^2_{E_2/E_1}r_{E_1E_2}\cos\eta \\ +2\omega^2_{C/B_1}r_{B_1C}\cos\eta - 2\omega^2_{D/C}r_{CD}\cos\eta - 2\omega^2_{E_2/D}r_{DE_2}\cos\eta \end{array}\right\} \end{array}\right)}{\rho_s\, d} = 0 \tag{86}$$

Hence we find an expression for $\cos\eta$

$$\cos\eta\left\{\begin{array}{l} 2a_{O/\zeta} - 4\omega^2_{A/O}r_{OA} - 4\omega^2_{B_1/A}r_{AB_1} - 2\omega^2_{B_2/B_1}r_{B_1B_2} - 2\omega^2_{E_1/B_2}r_{B_2E_1} \\ -2\omega^2_{E_2/E_1}r_{E_1E_2} - 2\omega^2_{C/B_1}r_{B_1C} + 2\omega^2_{D/C}r_{CD} + 2\omega^2_{E_2/D}r_{DE_2} \end{array}\right\} = 0 \tag{87}$$

We now take any of the kernels representing the link of interest in eqn (87)

Expression for $\sin\eta$ is as given in eqn (59). The derivation is shown in Appendix I. It can be shown for any link length $r_{E_1E_2}$ that angle η can be expressed in terms of link $r_{E_1E_2}$ via the following relation

$$\sin\eta = \sqrt{1-(16\omega^4_{E_2/E_1}r^2_{E_1E_2})}$$

$$\sin\eta \approx 1 - \frac{1}{2}(16\omega^4_{E_2/E_1}r^2_{E_1E_2}) \tag{88}$$

In view of equation (88), the scooped volume can be determined as

$$v_s = \frac{\frac{1}{2}t^2\left(\begin{array}{l} m_b\left\{\left(2\omega^2_{E_2/E_1}r_{E_1E_2}\right)\left(1-\frac{1}{2}\left(16\omega^4_{E_2/E_1}r^2_{E_1E_2}\right)\right)\right\} - c\,A_b \\ -m_b\tan\phi\left\{\left(2\omega^2_{E_2/E_1}r_{E_1E_2}\right)\left(1-\frac{1}{2}\left(16\omega^4_{E_2/E_1}r^2_{E_1E_2}\right)\right)\right\} \end{array}\right)}{\rho_s\, d} \tag{89}$$

We can re-write eqn (89) as

$$v_s = \frac{\frac{1}{2}t^2\begin{pmatrix} m_b\left(2\omega_{E_2/E_1}^2 r_{E_1E_2} - 16\omega_{E_2/E_1}^6 r_{E_1E_2}^3\right) - c\,A_b \\ -m_b \tan\phi\left(2\omega_{E_2/E_1}^2 r_{E_1E_2} - 16\omega_{E_2/E_1}^6 r_{E_1E_2}^3\right) \end{pmatrix}}{\rho_s\, d} \tag{90}$$

For simulation purposes, eqn (90) can be used to study the behaviour of the scooped volume in relation to the angular velocity and link length.

In a similar vein, we can determine the expression for simulating the behaviour of the scooped volume in relation to the other angular velocity and link lengths.

For the other link lengths,

$$v_s = \frac{\frac{1}{2}t^2\begin{pmatrix} m_b\left(2\omega_{E_2/E_1}^2 r_{E_1E_2} - 16\omega_{E_2/E_1}^6 r_{E_1E_2}^3\right) - c\,A_b \\ -m_b \tan\phi\left(2\omega_{E_2/E_1}^2 r_{E_1E_2} - 16\omega_{E_2/E_1}^6 r_{E_1E_2}^3\right) \end{pmatrix}}{\rho_s\, d} \tag{91}$$

$$v_s = \frac{\frac{1}{2}t^2\begin{pmatrix} m_b\left(2\omega_{C/D}^2 r_{DC} - 16\omega_{C/D}^6 r_{DC}^3\right) - c\,A_b \\ -m_b \tan\phi\left(2\omega_{C/D}^2 r_{DC} - 16\omega_{C/D}^6 r_{DC}^3\right) \end{pmatrix}}{\rho_s\, d} \tag{92}$$

$$v_s = \frac{\frac{1}{2}t^2\begin{pmatrix} m_b\left(2\omega_{B_1/C}^2 r_{CB_1} - 16\omega_{B_1/C}^6 r_{CB_1}^3\right) - c\,A_b \\ -m_b \tan\phi\left(2\omega_{B_1/C}^2 r_{CB_1} - 16\omega_{B_1/C}^6 r_{CB_1}^3\right) \end{pmatrix}}{\rho_s\, d} \tag{93}$$

In this chapter, we have presented a scheme for analytical prediction of scooped volume in hydraulic excavation with respect to our previously derived dynamic equations governing the motion of the various links of the excavator, transmitted force and cutting force. With the excavator bucket cutting through a medium such as soil, medium/soil parameters were adequately captured in the analytical expressions. The work provides an insight into the effect of angle of inclination on scooped volume.

CHAPTER FIVE

ANALYTICAL MODELLING OF BUCKET TRAJECTORY DURING HYDRAULIC EXCAVATION

5.1 PREAMBLE

In this chapter, an analytical approach to model the bucket trajectory during hydraulic excavation through a medium is presented.

5.2 Derivation of Analytical Expression

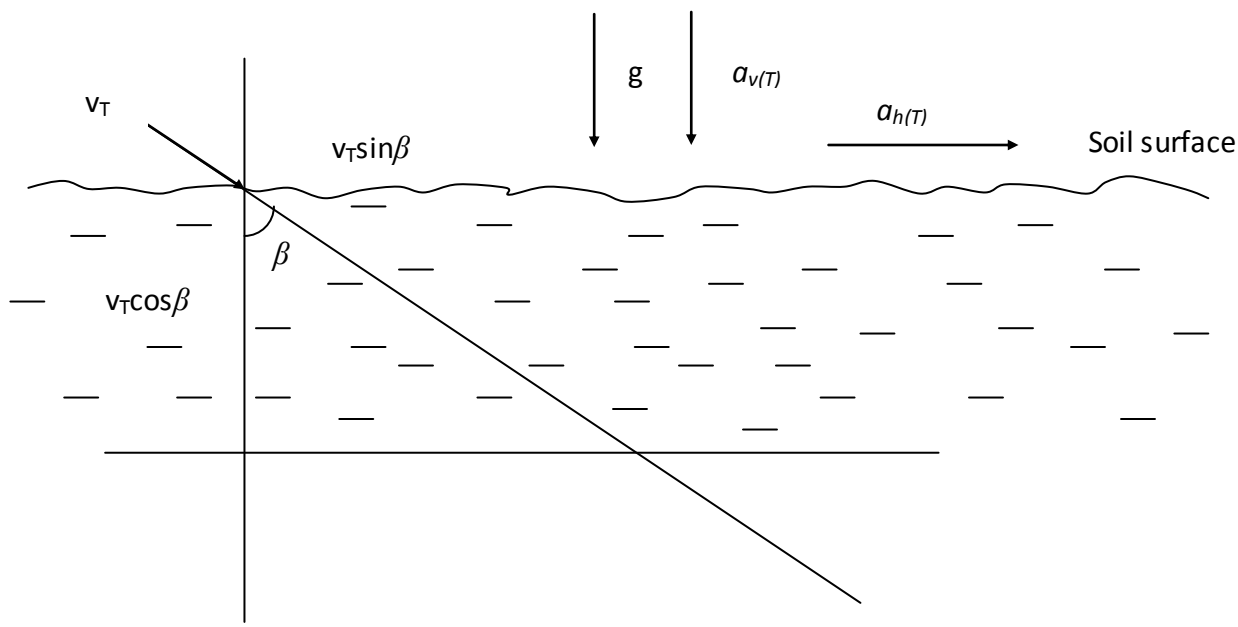

Fig. 12: Profile of the excavator blade cutting through a medium

For motion along y-axis,

$$\frac{d\vec{v}_y}{dt} = \vec{g} + \vec{a}_{v(T)} \tag{94}$$

Where

$$\vec{a} = \vec{\alpha} = \frac{d\vec{\omega}}{dt} \; and \; \vec{v} = \vec{\omega} = \frac{d\vec{x}}{dt} \tag{95}$$

$$\vec{v}_y = (\vec{g} + \vec{a}_{v(T)})t + constant \;\;)$$

At $t = 0, \quad \vec{v}_y = v_T \; \cos\beta$

Hence

$$\vec{v}_y = v_T \; \cos\beta + (\vec{g} + \vec{a}_{v(T)})t \tag{96}$$

However $\vec{v}_y = \dfrac{d\vec{y}}{dt}$

$$\frac{d\vec{y}}{dt} = v_T \; \cos\beta + (\vec{g} + \vec{a}_{v(T)})t + constant \tag{97}$$

$$y = v_T \; \cos\beta \, t + \frac{(g + a_{v(T)})t^2}{2} \tag{98}$$

Next we examine the motion in the x-axis

$$\frac{d\vec{v}_x}{dt} = \vec{a}_{h(T)} \tag{99}$$

where

$$\frac{d\vec{\omega}}{dt} = \vec{a}$$

$$\vec{v}_x = \vec{a}_{h(T)} \; + constant$$

At $t = 0, \quad \vec{v}_x = v_T \; \sin\beta \, \hat{i}$

$$\vec{v}_x = \vec{a}_{h(T)} \, \hat{i} + v_T \; \sin\beta \, \hat{i}$$

$$\vec{v}_x = \left(\vec{a}_{h(T)} \; + v_T \; \sin\beta\right)\hat{i} \tag{100}$$

Hence

$$x = v_T \sin\beta\, t \tag{101}$$

Next we determine the equation describing the cutting trajectory when the bucket is cutting through a medium.

$$a_{v(T)} = \frac{F_T - \tau}{(m_b + m_s)} \tag{102}$$

Where acceleration equation is as shown in chapter three

$$a_{v(T)} = \frac{F_{T(v)} - \tau}{(\rho_b v_b + \rho_s v_{sl})} \tag{103}$$

$$a_{h(T)} = \frac{F_{T(h)} - \tau}{(\rho_b v_b + \rho_s v_{sl})} \tag{104}$$

Hence Eqn (98) becomes

$$y = v_T \cos\beta\, t + \frac{(g + a_{v(T)})t^2}{2} - d \tag{105}$$

Substituting Eqn (103) in Eqn (105), we obtain

$$y = v_T \cos\beta\, t + \frac{1}{2}\left(g + \frac{F_{T(v)} - \tau}{(\rho_b v_b + \rho_s v_{sl})}\right)t^2 - d = \tag{106}$$

From Eqn (101), t can be expressed as

$$t = \frac{x}{v_T \sin\beta} \tag{107}$$

Substituting Eqn (107) in (106) gives

$$y = v_T \cos\beta \left(\frac{x}{v_T \sin\beta} \right) t + \frac{x^2}{2v_T^2 \sin^2\beta} \left(g + \frac{F_{T(v)} - \tau}{\left(\rho_b v_b + \rho_s v_{sl}\right)} \right) - d \tag{108}$$

But

$$\tau = c + \sigma \tan\phi \tag{109}$$

Hence Eqn (108) becomes

$$y = x \cot\beta + x^2 \frac{\operatorname{cosec}^2\beta}{2v_T^2} \left(g + \frac{F_{T(v)} - \left(c + \sigma \tan\phi\right)}{\left(\rho_b v_b + \rho_s v_{sl}\right)} \right) - d \tag{110}$$

Hence

$$y = x \cot\beta + x^2 \frac{\operatorname{cosec}^2\beta}{2v_T^2} \left(g + \frac{F_{T(v)} - \left(c + \frac{F_c}{A_b} \tan\phi \right)}{\left(\rho_b v_b + \rho_s v_{sl}\right)} \right) - d \tag{111}$$

Where

$$F_c = m_b \left\{ \begin{array}{l} -2a_{O/\zeta} \sin\eta - 4\omega_{A/O}^2 r_{OA}(-\sin\eta) + 4\omega_{B_1/A}^2 \left(\frac{r_{B_1B_2} \sin[180 - (\alpha_1 + \alpha_2)]}{\sin\alpha_1} \right) [\sin(\theta_1 + \eta)] \\ + 2\omega_{B_2/B_1}^2 r_{B_1B_2} [\sin(\eta - \theta_B)] + 2\omega_{E_1/B_2}^2 r_{B_2E_1} [\sin(\eta - \theta_C)] + 2\omega_{E_2/E_1}^2 r_{E_1E_2} [\sin(\alpha_6 + \eta)] + \\ 2\omega_{C/B_1}^2 \left(\frac{r_{CE_1} \sin[180 - (\alpha_3 + \alpha_5)]}{\sin\alpha_3} \right) [\sin(\eta - \theta_A)] - 2\omega_{D/C}^2 r_{CD} [\sin(\theta_D - \eta)] - 2\omega_{E_2/D}^2 r_{DE_2} [\sin(\alpha_6 + \eta)] \end{array} \right\} \tag{112}$$

Eqn (112) is the derived model which can now be used for simulation purposes.

In this chapter, we have presented an analytical approach for modeling the bucket trajectory during hydraulic excavation through a medium.

CHAPTER SIX

RESULTS AND DISCUSSIONS

6.1 Simulation Results

Using MATLAB software, a program was written based on the generalized dynamic model obtained. From this derived model in eqn (54), several simulation results were obtained. This describes the characteristics of the various parameters as encapsulated in the general equation governing the scooping operation. The essential parameters considered include the cutting force, mass of the bucket, angular velocity of the various links and the link geometrical variables in our model during the entire scooping exercise.

6.2 Simulation results of the General Profile of Cutting Force

In the case of hydraulic excavation in free swing, two cases were considered. In the first one, the adjustable link r_{A/B_1} is fixed when link $r_{B_1/C}$ is moving. Simulation was carried out based on this. In the second case, adjustable link r_{A/B_1} is moving when link $r_{B_1/C}$ is fixed.

Table 3: Simulation Parameters for General Profile of Cutting Force

S/N	Symbol	Meaning	Value
1	m_b	Mass of excavator bucket	150kg
2	$a_{O/\xi}$	Acceleration of point O relative to ξ	0m/s^2
3	$\vec{\omega}_{A/O}$	Angular velocity of point A relative to O	0rad/s
4	$\vec{\omega}_{B_1/A}$	Angular velocity of point B_1 relative to A	0.5rad/s
5	$\vec{\omega}_{B_2/B_1}$	Angular velocity of point B_2 relative to B_1	0.6rad/s
6	$\vec{\omega}_{E_1/B_2}$	Angular velocity of point E_1 relative to B_2	0rad/s
7	$\vec{\omega}_{E_2/E_1}$	Angular velocity of point E_2 relative to E_1	0.7rad/s
8	$\vec{\omega}_{D/C}$	Angular velocity of point D relative to C	0.6rad/s
9	ω_{D/E_2}	Angular velocity of point D relative to E_2	0.65rad/s
10	$\vec{r}_{O/A}$	Displacement of point O relative to A	1.5m
11	$\vec{r}_{A/B_1}$	Displacement of point A relative to B_1	2.7m
12	$\vec{r}_{B_1/B_2}$	Displacement of point B_1 relative to B_2	0.6m
13	$\vec{r}_{B_2/E_1}$	Displacement of point B_2 relative to E_1	3.6m

S/N	Symbol	Meaning	Value
14	$\vec{r}_{E_1/E_2}$	Displacement of point E_1 relative to E_2	0.5m
15	$\vec{r}_{C/D}$	Displacement of point C relative to D	0.6m
16	$\vec{r}_{D/E_2}$	Displacement of point D relative to E_2	0.6m
17	η	Cutting angle	$\pi/3$
18	θ_A	Angle of unit vector $\hat{e}_{B_1/C}$	$2\pi/1.4$
19	θ_B	Angle of unit vector $\hat{e}_{B_1/B_2}$	$\pi/1.05$
20	θ_C	Angle of unit vector $\hat{e}_{B_2/E_1}$	$2\pi/1.5$
21	θ_D	Angle of unit vector $\hat{e}_{C/D}$	$\pi/2.2$
22	θ_1	$O\hat{A}B_2$	$2\pi/3$
23	θ_2	$A\hat{B}_2E_1$	$2\pi/1.4$
24	α_1	$B_2\hat{A}B_1$	$\pi/20$
25	α_2	$B_2\hat{B}_1A$	$\pi/1.1$
26	α_3	$E_1\hat{B}_1C$	$\pi/20$
27	α_4	$E_1\hat{C}D$	$\pi/1.9$
28	α_5	$D\hat{E}_2E_1$	$\pi/18$
29	α_6	$E_2\hat{E}_1D$	$\pi/5$

The results obtained for the first case are presented in the curves shown below in Fig. 13-18.

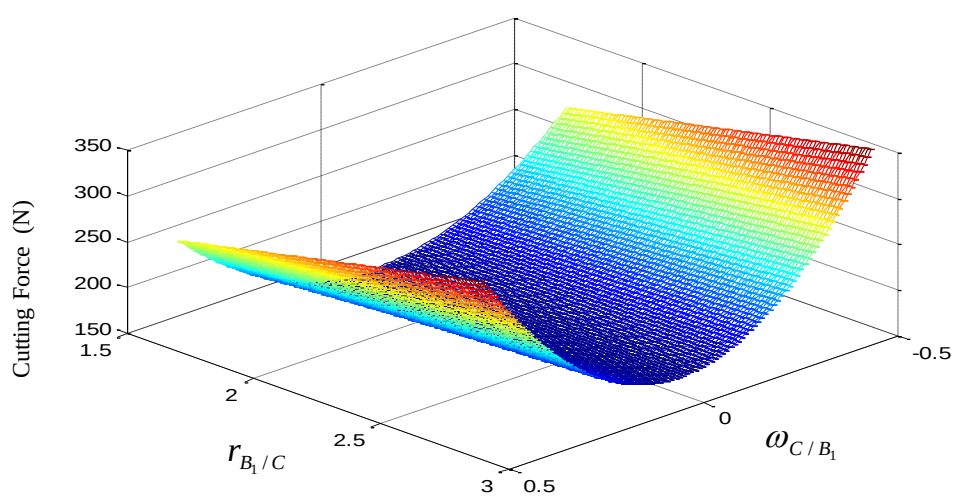

Fig. 13: Typical profile of cutting force, link length and angular velocity for the case r_{A/B_1} fixed at *1.0m* and $r_{B_1/C}$ moving from 1.7 - 2.9m

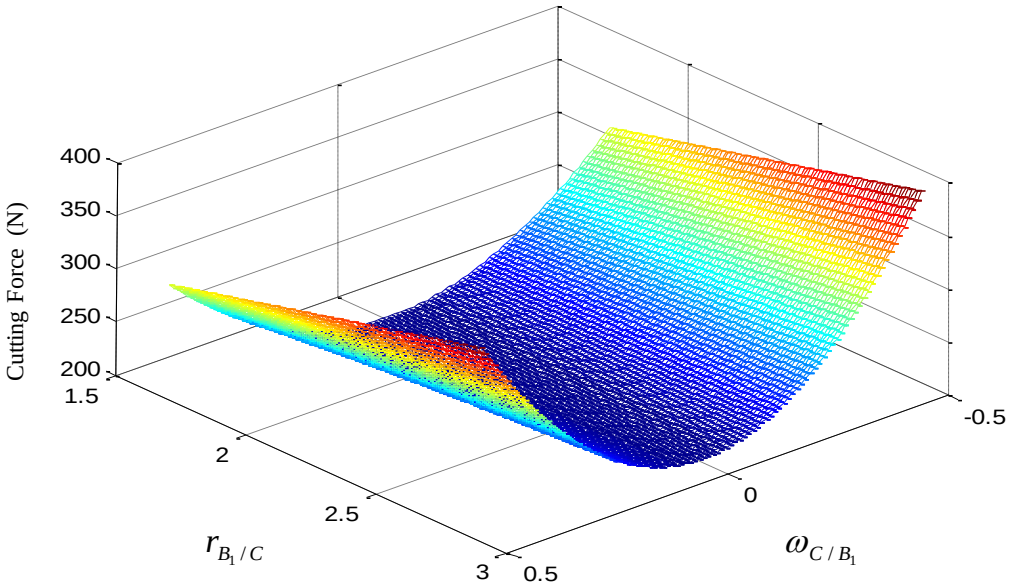

Fig. 14: Typical profile of cutting force, link length and angular velocity for the case r_{A/B_1} fixed at *1.4m* and $r_{B_1/C}$ moving from 1.7 - 2.9m

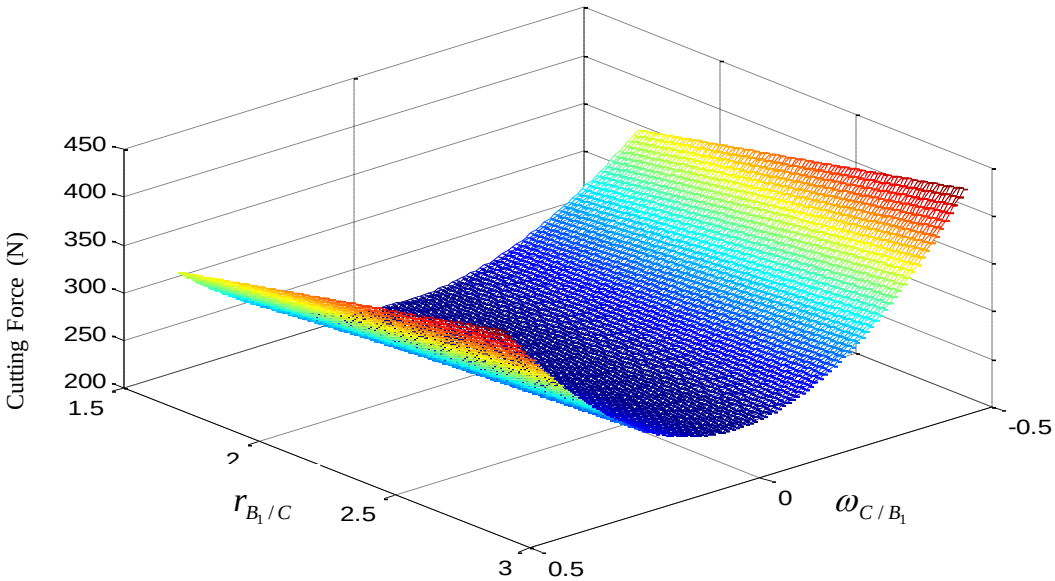

Fig. 15: Typical profile of cutting force, link length and angular velocity for the case r_{A/B_1} fixed at *1.8m* and $r_{B_1/C}$ moving from 1.7 - 2.9m

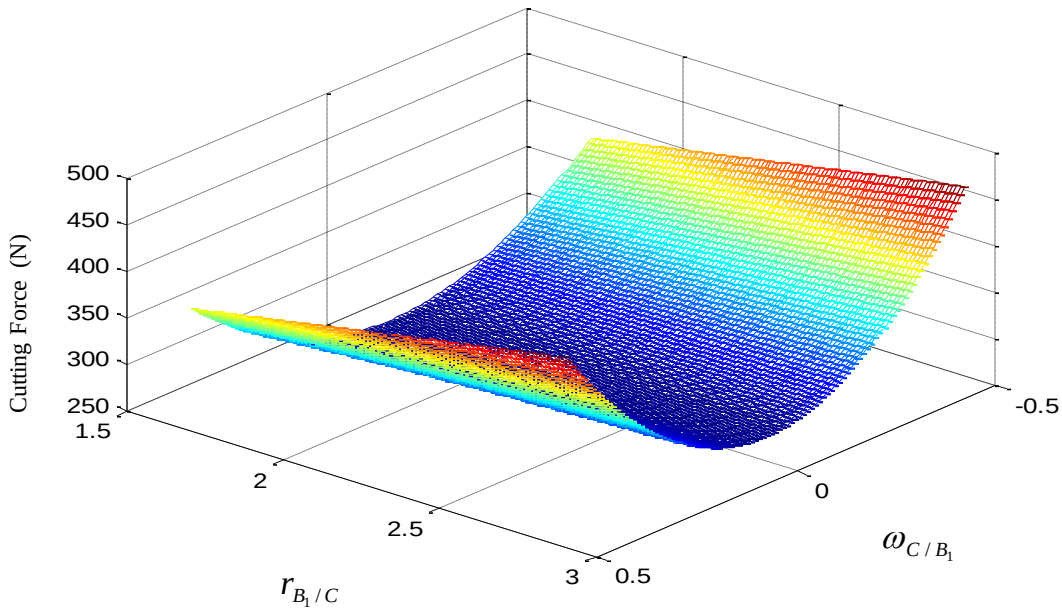

Fig. 16: Typical profile of cutting force, link length and angular velocity for the case r_{A/B_1} fixed at *2.2m* and $r_{B_1/C}$ moving from 1.7 - 2.9m

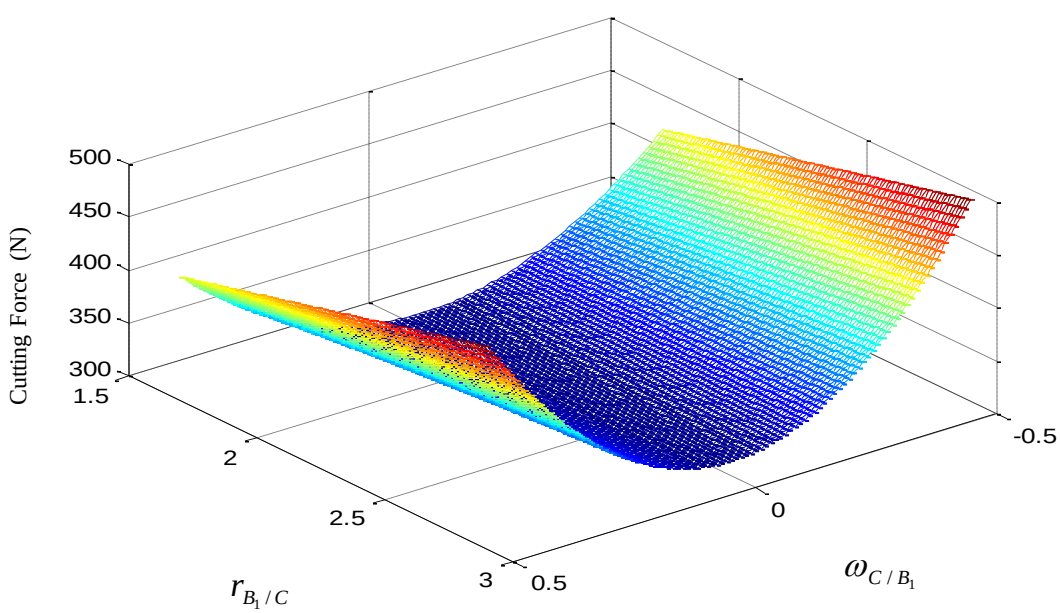

Fig. 17: Typical profile of cutting force, link length and angular velocity for the case r_{A/B_1} fixed at *2.6m* and $r_{B_1/C}$ moving from 1.7 - 2.9m

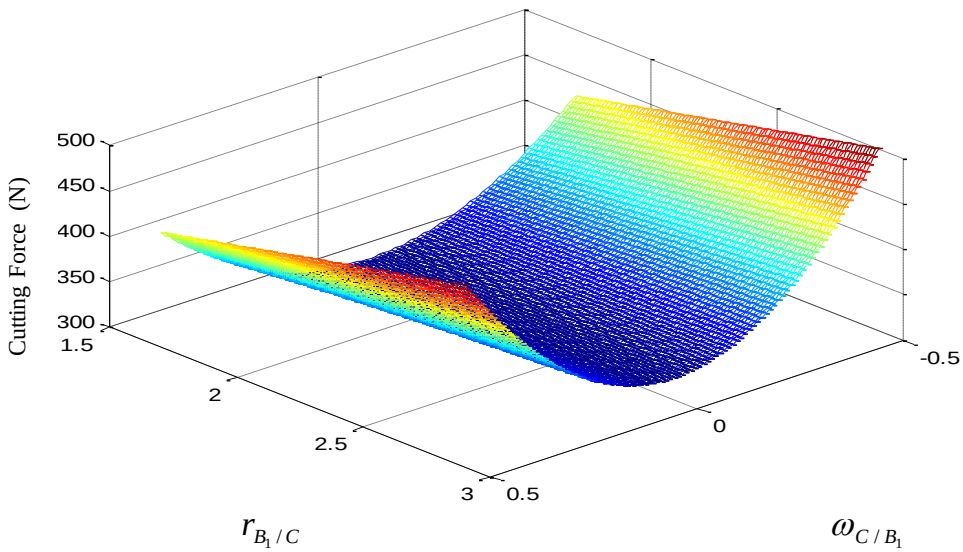

Fig. 18: Typical profile of cutting force, link length and angular velocity for the case r_{A/B_1} fixed at *2.6m* and $r_{B_1/C}$ moving from 1.7 - 2.9m

6.3 Optimum Results of the Maximum Cutting force and adjustable link length $r_{B_1/C}$ (link $r_{B_1/C}$ is moving when link r_{A/B_1} is fixed)

The result of the general profile of the maximum cutting force is shown below in figure 19.

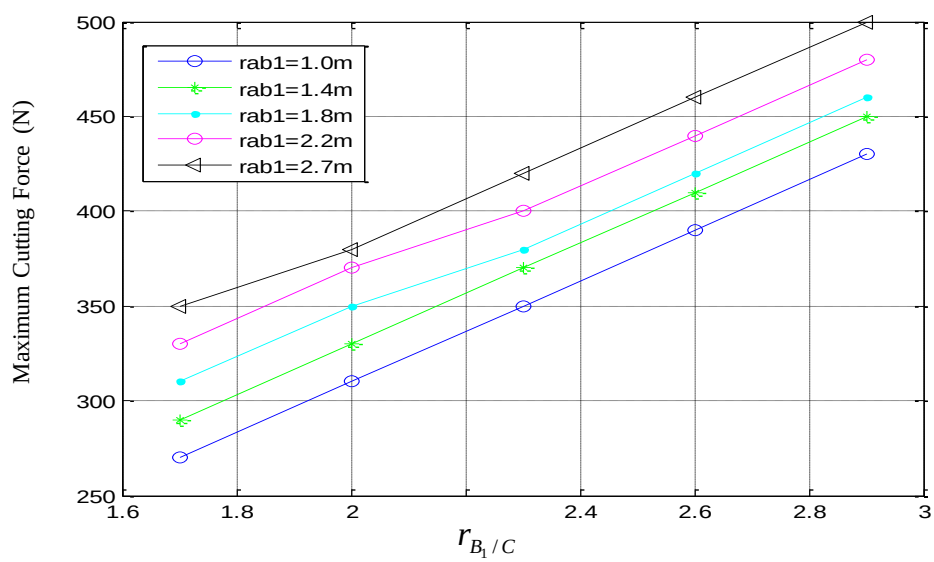

Fig. 19: General profile of maximum cutting force and link length $r_{B_1/C}$ when r_{A/B_1} is fixed and $r_{B_1/C}$ is moving from 1.7 - 2.9m

6.4 Simulation results of the profile of the cutting force and adjustable link length r_{A/B_1} (link r_{A/B_1} is moving when link $r_{B_1/C}$ is fixed)

The results obtained for the second case are presented in the curves shown below in Fig. 20-25.

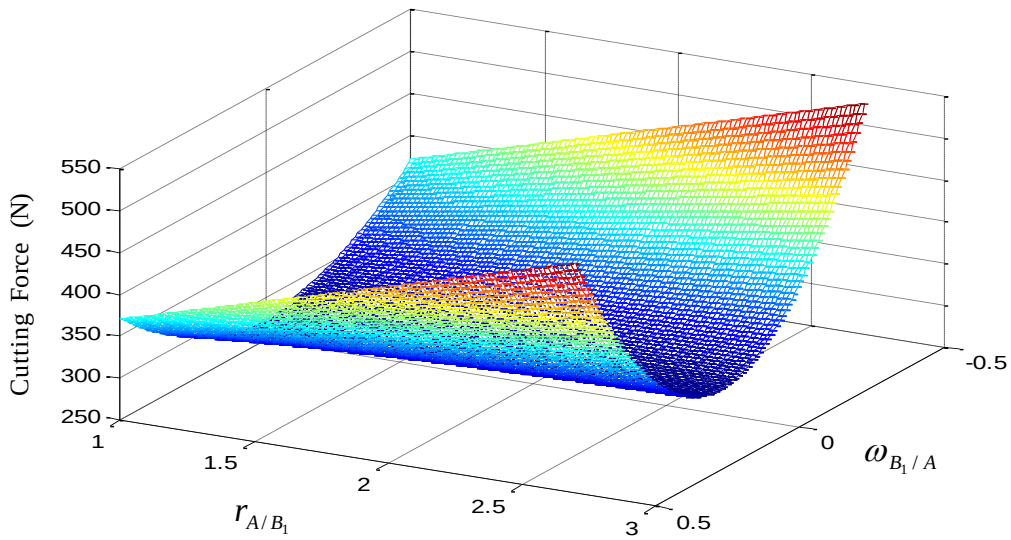

Fig. 20: Typical profile of cutting force, link length and angular velocity for the case $r_{B_1/C}$ fixed at 1.7m and r_{A/B_1} moving from 1.0 - 2.7m

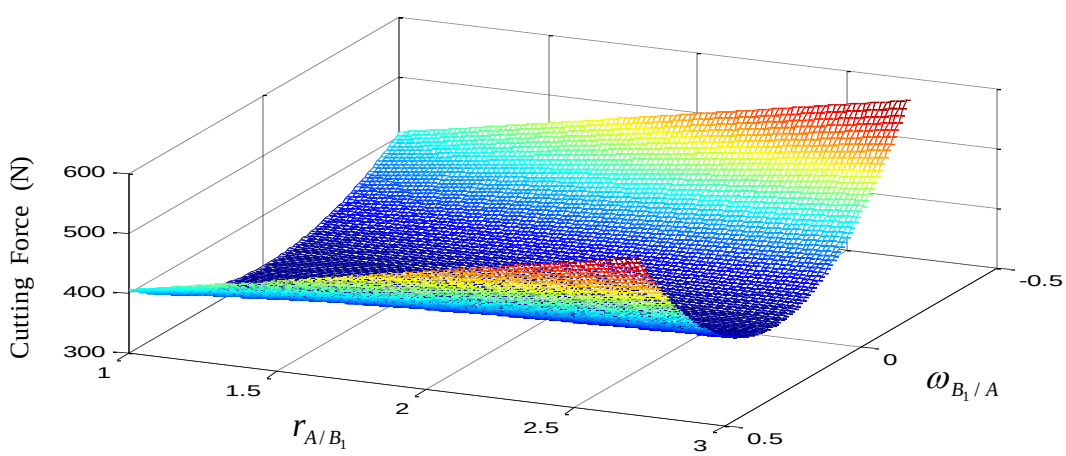

Fig. 21: Typical profile of cutting force, link length and angular velocity for the case $r_{B_1/C}$ fixed at 2.0m and r_{A/B_1} moving from 1.0 - 2.7m

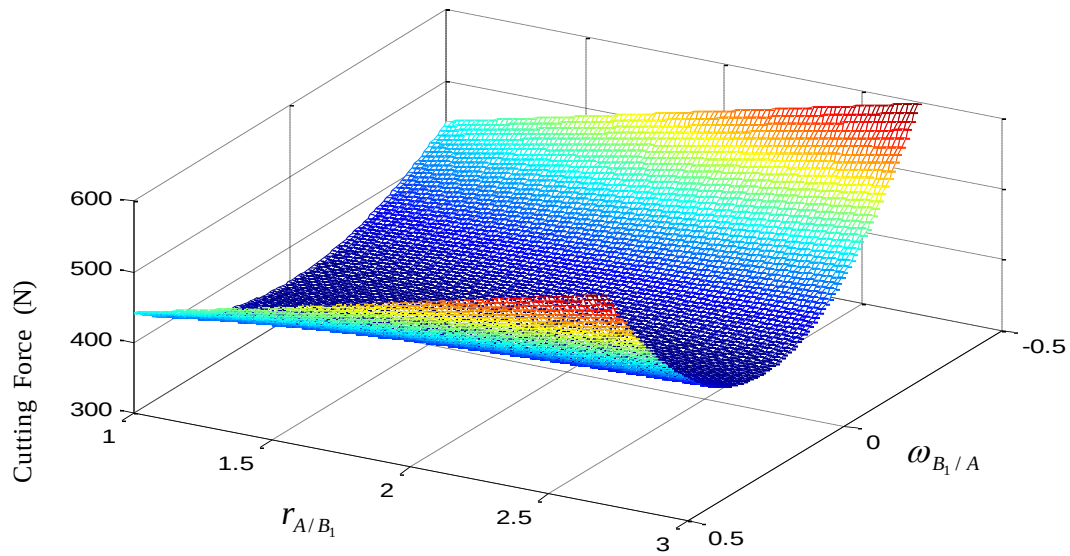

Fig. 22: Typical profile of cutting force, link length and angular velocity for the case $r_{B_1/C}$ fixed at 2.3m and r_{A/B_1} moving from 1.0 - 2.7m

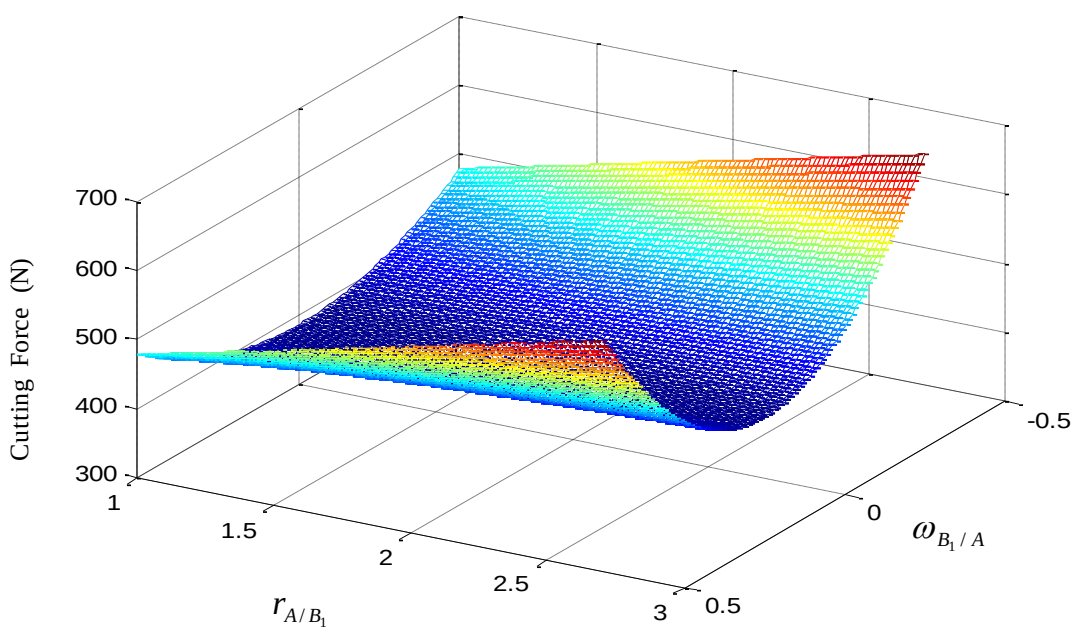

Fig. 23: Typical profile of cutting force, link length and angular velocity for the case $r_{B_1/C}$ fixed at 2.6m and r_{A/B_1} moving from 1.0 - 2.7m

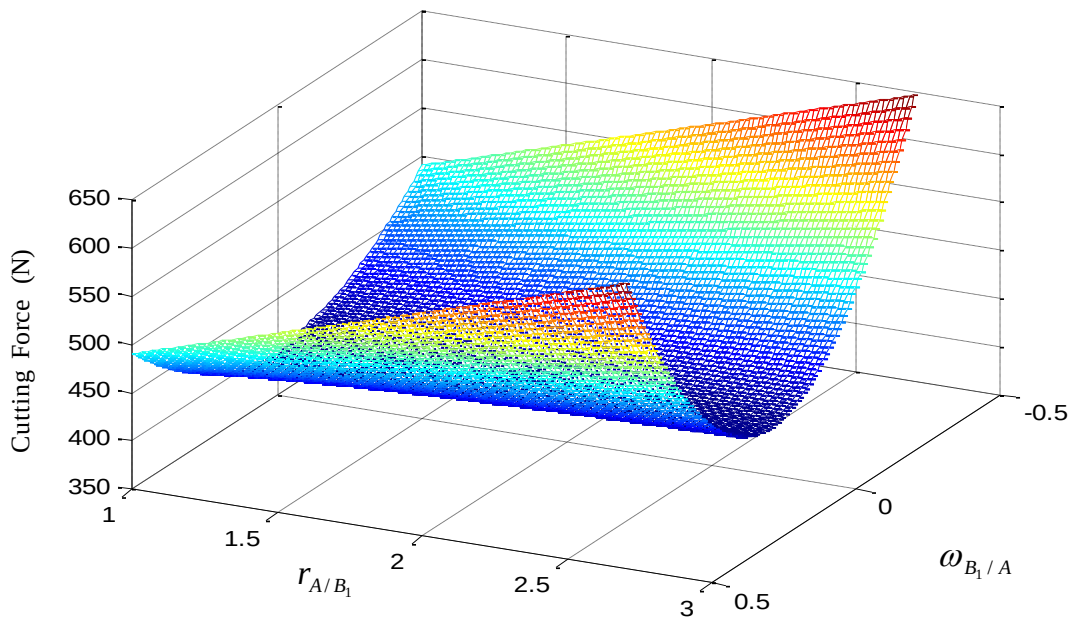

Fig. 24: Typical profile of cutting force, link length and angular velocity for the case $r_{B_1/C}$ fixed at 2.7m and r_{A/B_1} moving from 1.0 - 2.7m

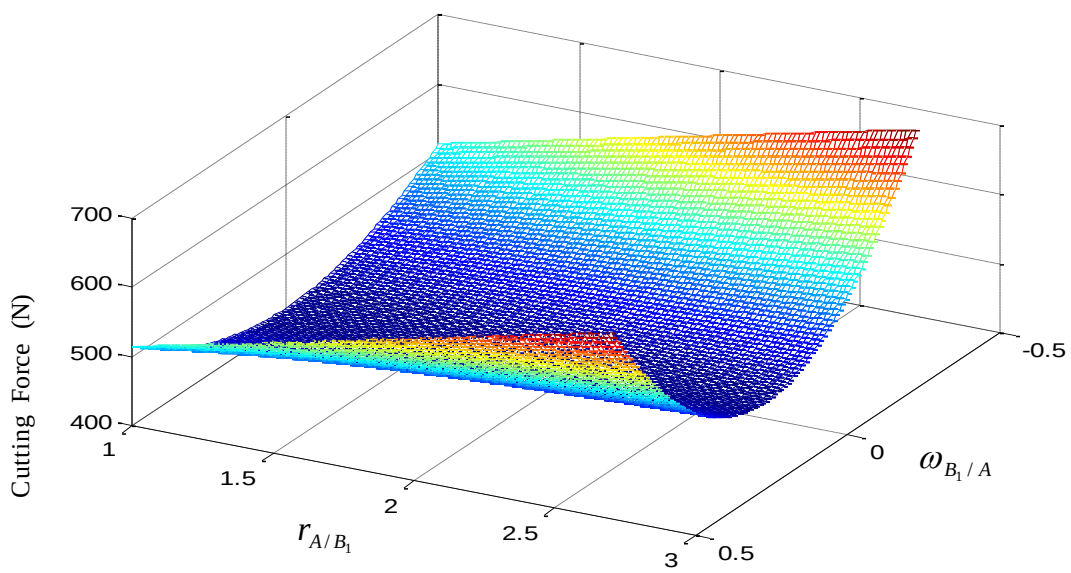

Fig. 25: Typical profile of cutting force, link length and angular velocity for the case $r_{B_1/C}$ fixed at 2.9m and r_{A/B_1} moving from 1.0 - 2.7m

6.5 Optimum Results of the Maximum Cutting force and adjustable link length r_{A/B_1} (link r_{A/B_1} is moving when link $r_{B_1/C}$ is fixed)

The simulation result is shown in figure 26 below.

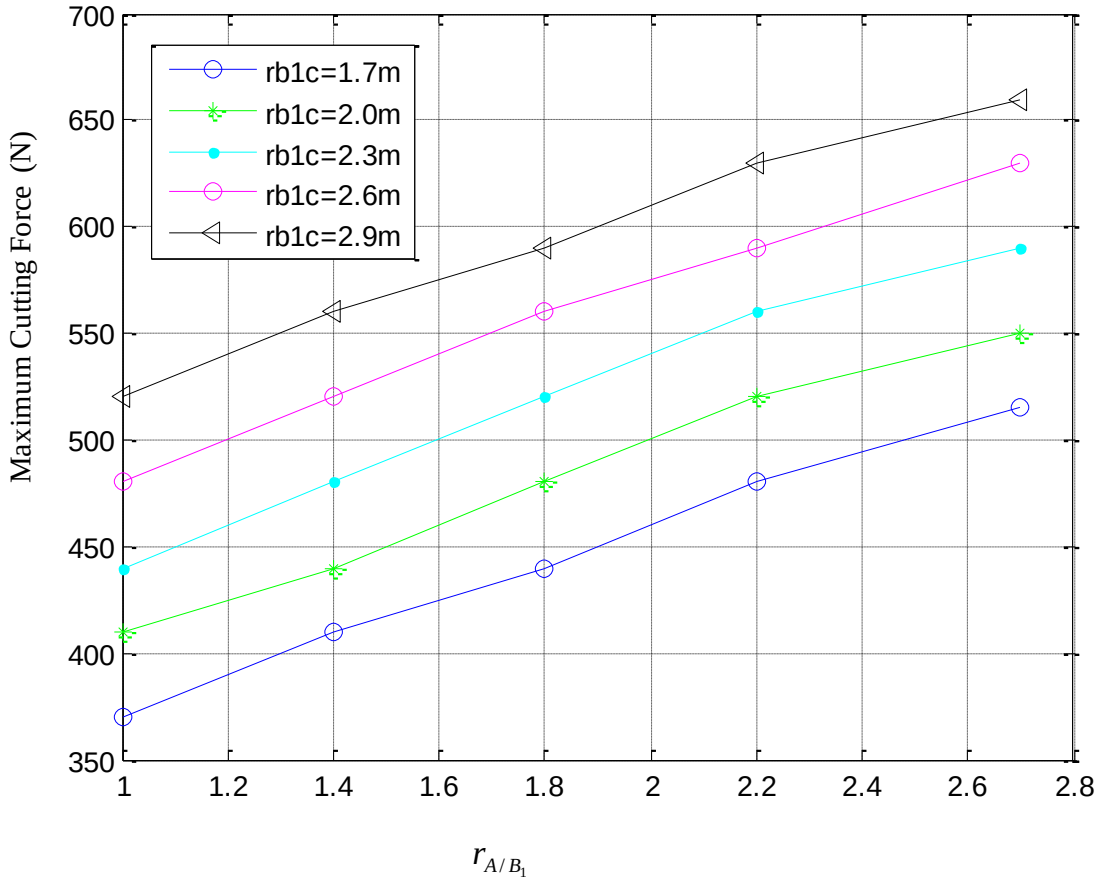

Fig. 26: General profile of maximum cutting force and link length r_{A/B_1} when $r_{B_1/C}$ is fixed and r_{A/B_1} is moving from 1.0 - 2.7m

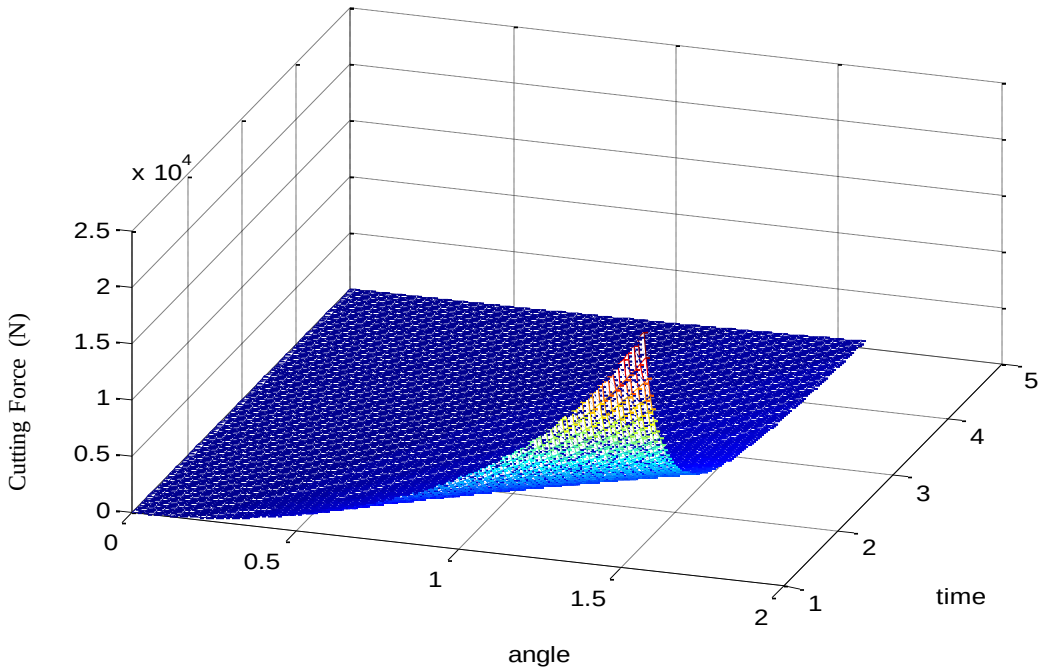

Fig. 27: Profile of Cutting force, cutting angle and time *(r = 3.0m)*

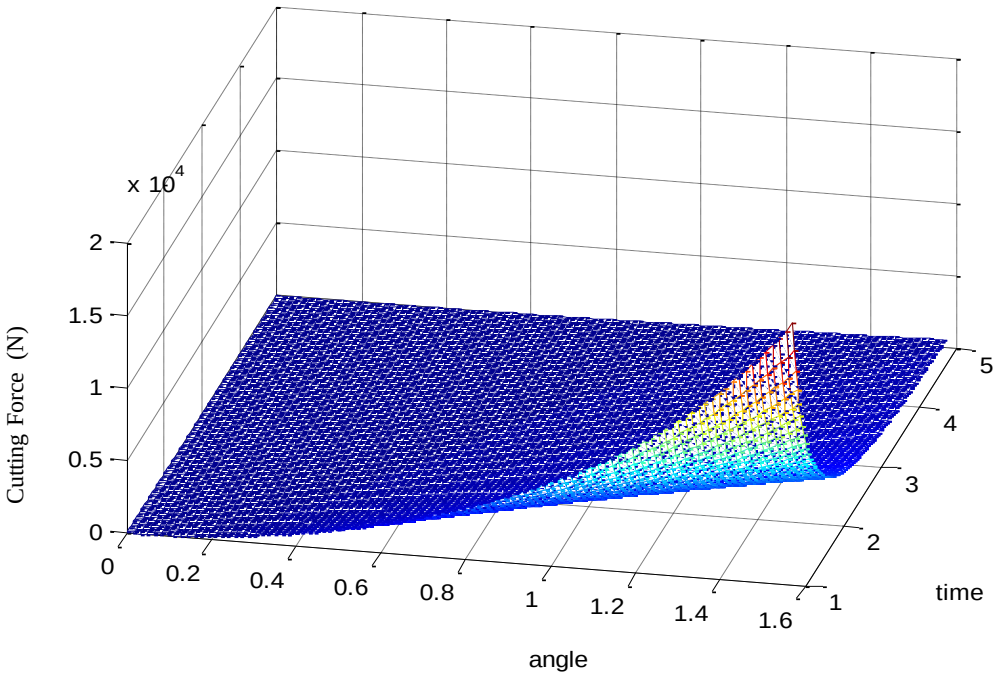

Fig. 28**:** Profile of Cutting force, cutting angle and time *(r =2.7m)*

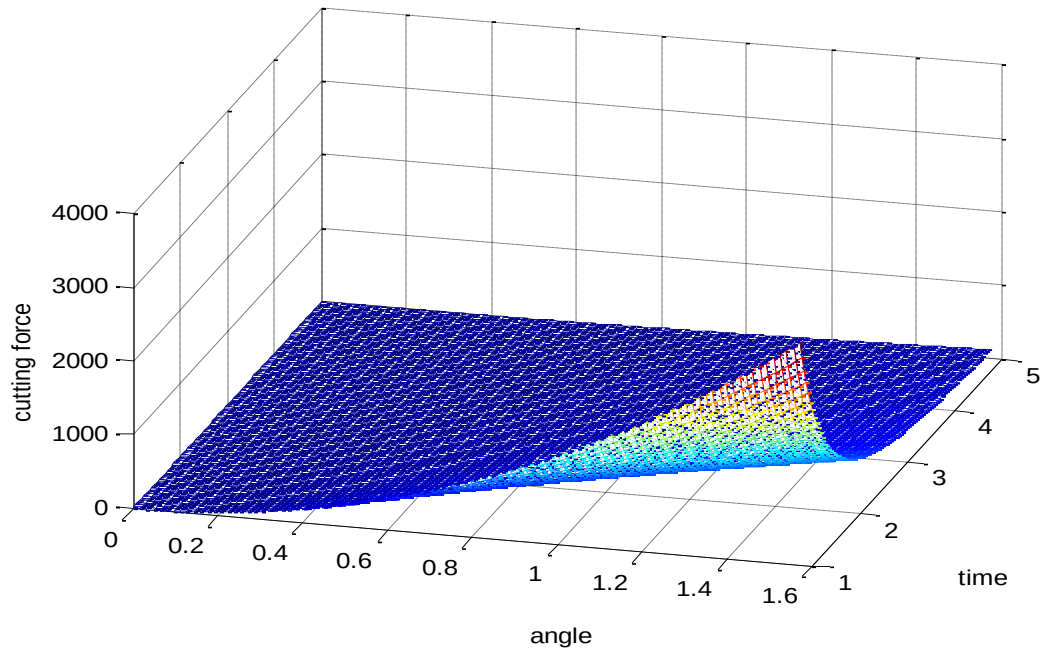

Fig. 29: Profile of Cutting force, cutting angle and time *(r =0.6m)*

6.6 Optimum Results of Analytical Prediction of Scooped Volume

Table 4: Table of Parameters used for Predicting Scooped Volume.

S/N	Symbol	Meaning	Value
1	m_b	Mass of excavator bucket	150kg
2	d	Depth of cut	1.2m
3	t	Time	5s
4	c	Cohesive force	0.5N
5	A_b	Area of bucket	$0.9m^2$
6	ρ_s	Density of soil	$1442kg/m^3$
7	ϕ	Coefficient of sliding friction	20
8	$a_{O/\xi}$	Acceleration of point O relative to ξ	$0m/s^2$
9	$\vec{\omega}_{A/O}$	Angular velocity of point A relative to O	0rad/s
10	$\vec{\omega}_{B_1/A}$	Angular velocity of point B_1 relative to A	0.5rad/s
11	$\vec{\omega}_{B_2/B_1}$	Angular velocity of point B_2 relative to B_1	0.6rad/s

S/N	Symbol	Meaning	Value
12	$\vec{\omega}_{E_1/B_2}$	Angular velocity of point E_1 relative to B_2	0rad/s
13	$\vec{\omega}_{E_2/E_1}$	Angular velocity of point E_2 relative to E_1	0.7rad/s
14	$\vec{\omega}_{D/C}$	Angular velocity of point D relative to C	0.6rad/s
15	ω_{D/E_2}	Angular velocity of point D relative to E_2	0.65rad/s
16	$\vec{r}_{O/A}$	Displacement of point O relative to A	1.5m
17	$\vec{r}_{A/B_1}$	Displacement of point A relative to B_1	2.7m
18	$\vec{r}_{B_1/B_2}$	Displacement of point B_1 relative to B_2	0.6m
19	$\vec{r}_{B_2/E_1}$	Displacement of point B_2 relative to E_1	3.6m
20	$\vec{r}_{E_1/E_2}$	Displacement of point E_1 relative to E_2	0.5m
21	$\vec{r}_{C/D}$	Displacement of point C relative to D	0.6m
22	$\vec{r}_{D/E_2}$	Displacement of point D relative to E_2	0.6m
23	η	Cutting angle	$\pi/3$
24	θ_A	Angle of unit vector $\hat{e}_{B_1/C}$	$2\pi/1.4$
25	θ_B	Angle of unit vector $\hat{e}_{B_1/B_2}$	$\pi/1.05$
26	θ_C	Angle of unit vector $\hat{e}_{B_2/E_1}$	$2\pi/1.5$
27	θ_D	Angle of unit vector $\hat{e}_{C/D}$	$\pi/2.2$
28	θ_1	$O\widehat{A}B_2$	$2\pi/3$
29	θ_2	$A\widehat{B}_2E_1$	$2\pi/1.4$
30	α_1	$B_2\widehat{A}B_1$	$\pi/20$
31	α_2	$B_2\widehat{B}_1A$	$\pi/1.1$
32	α_3	$E_1\widehat{B}_1C$	$\pi/20$
33	α_4	$E_1\widehat{C}D$	$\pi/1.9$
34	α_5	$D\widehat{E}_2E_1$	$\pi/18$
35	α_6	$E_2\widehat{E}_1D$	$\pi/5$

The results of analytical prediction of scooped volume are presented in fig.30-36.

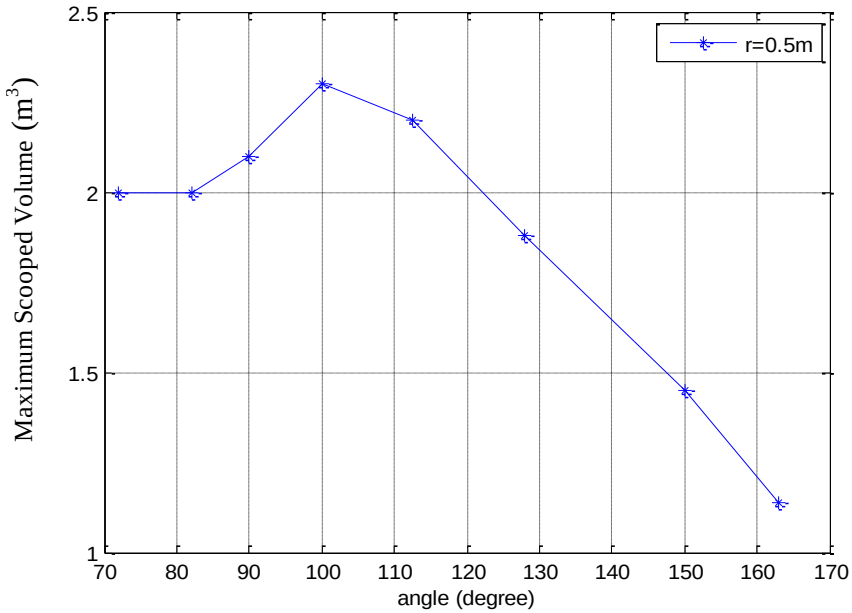

Fig.30: Profile of maximum scooped volume and angle of inclination, α_2 (length=0.5m)

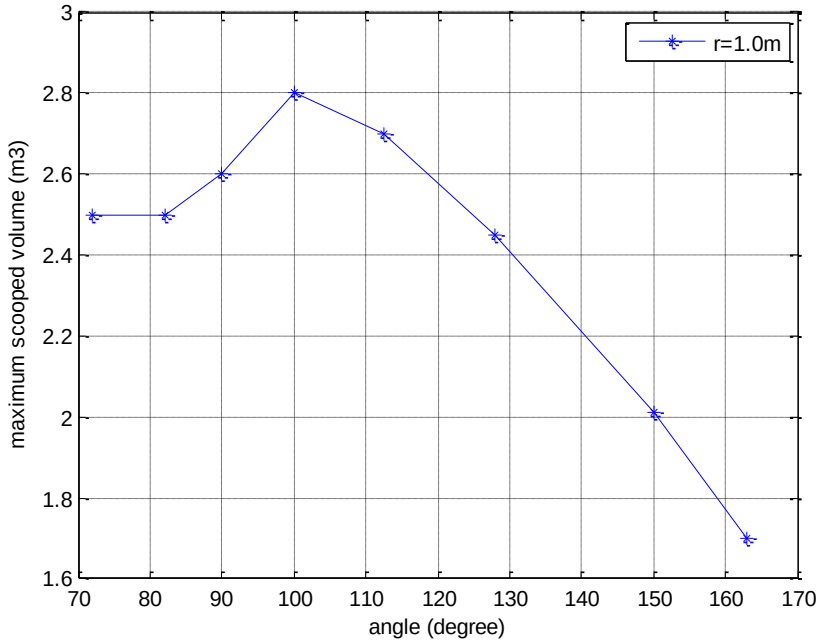

Fig.31: Profile of maximum scooped volume and angle of inclination, α_2 (length = 1.0m)

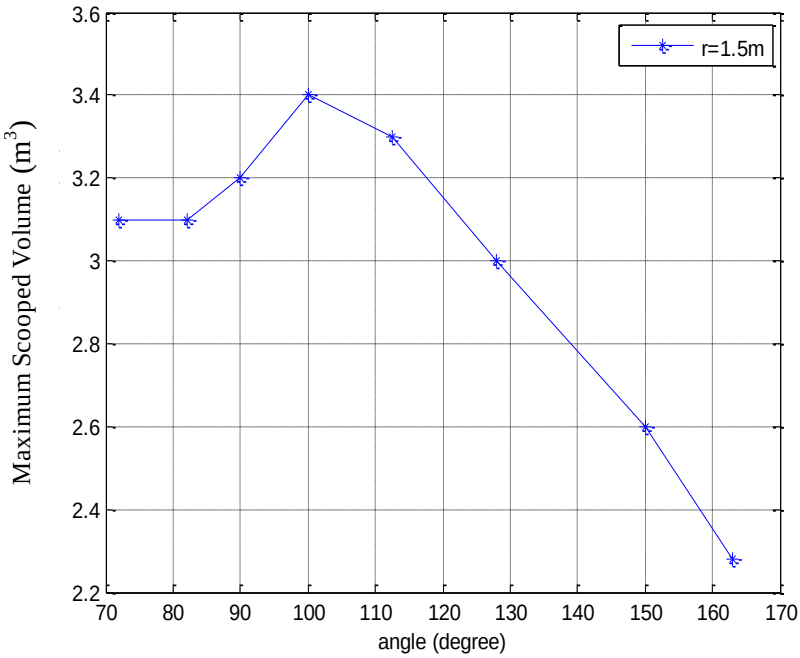

Fig.32: Profile of maximum scooped volume and angle of inclination, α_2 (length=1.5m)

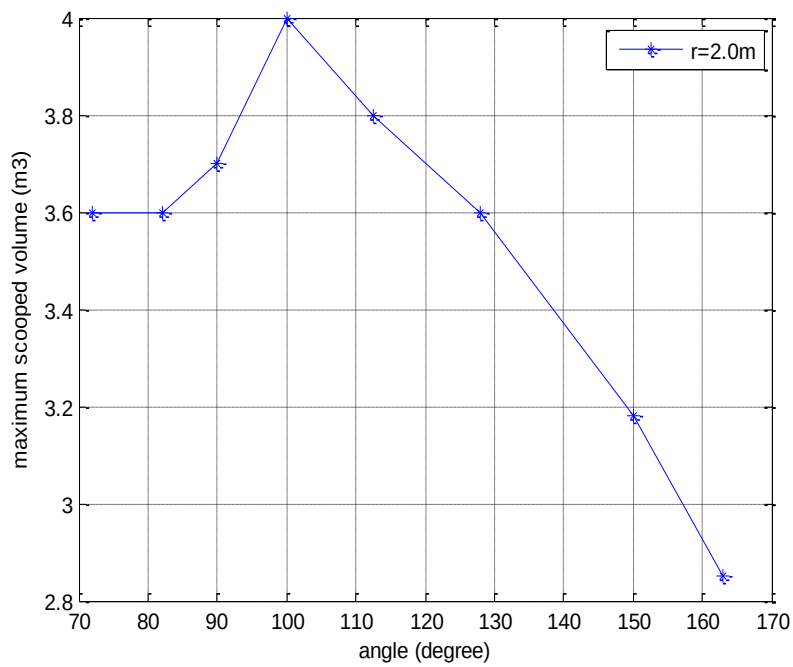

Fig.33: Profile of maximum scooped volume and angle of inclination, α_2 (length=2.0m)

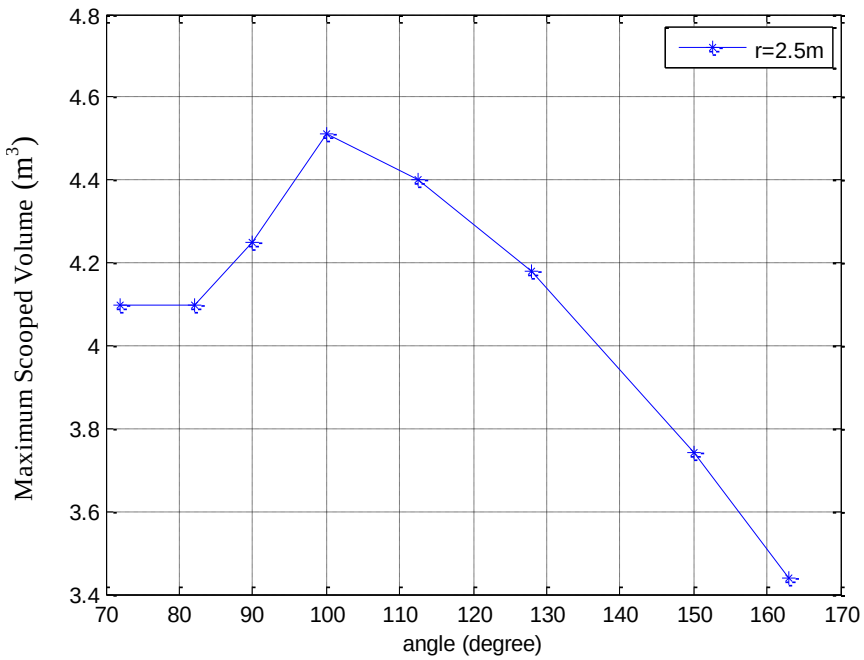

Fig.34: Profile of maximum scooped volume and angle of inclination, α_2 (length=2.5m)

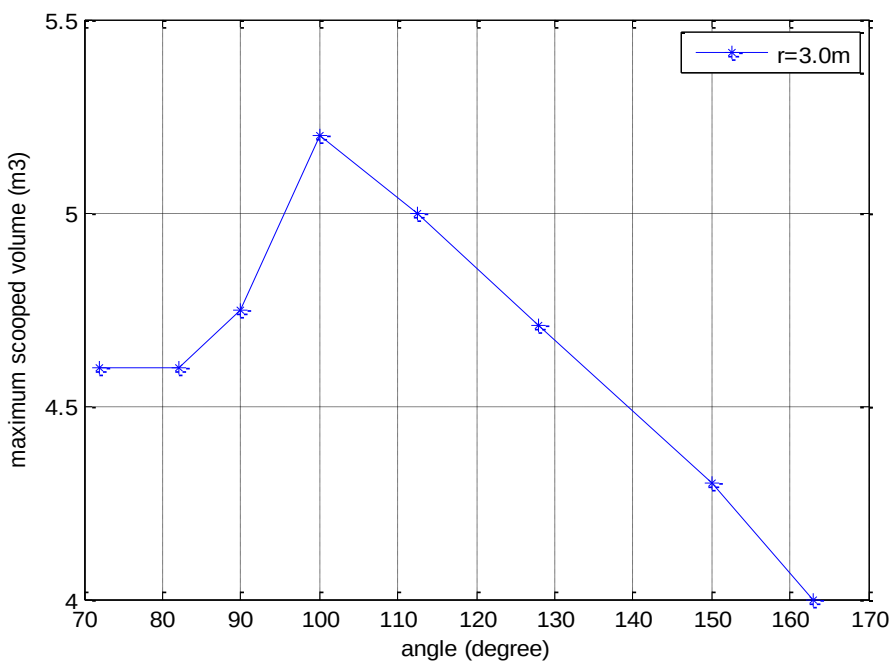

Fig.35: Profile of maximum scooped volume and angle of inclination, α_2 (length=3.0m)

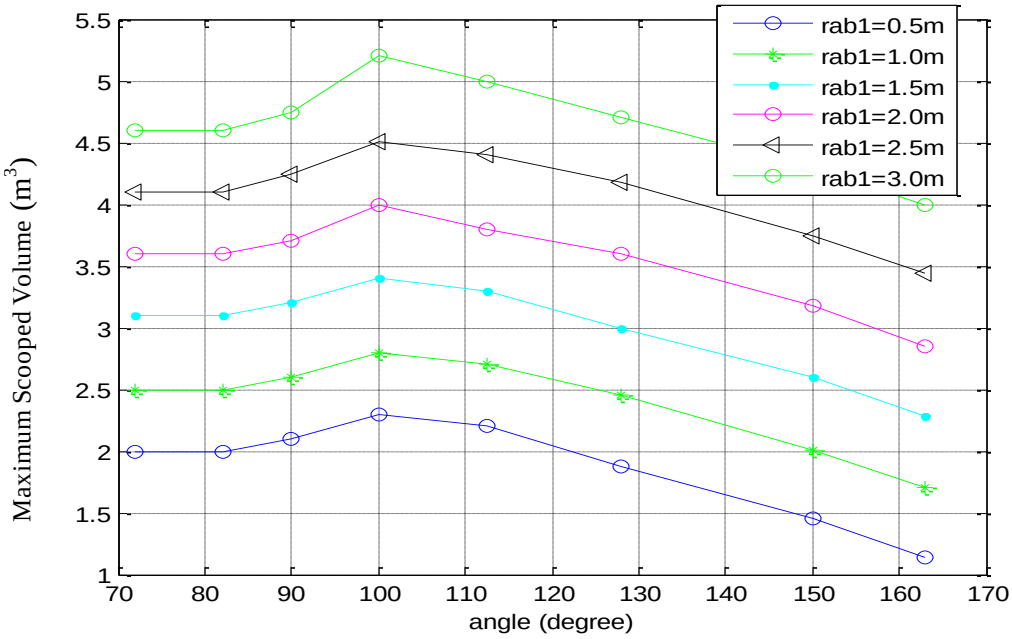

Fig.36: Maximum scooped volume and angle of inclination, α_2 with varying length r_{A/B_1}

6.7 Simulation Results: Analytical Modeling of Bucket Trajectory during Hydraulic Excavation

Table 5: Parameters of Simulation for Bucket Trajectory

S/N	Symbol	Meaning	Value
1	m_b	Mass of excavator bucket	150kg
2	d	Depth of cut	0-1.2m
3	t	Time	5s
4	c	Cohesive force	0.5N
5	A_b	Area of bucket	$0.9m^2$
6	g	Acceleration due to gravity	$9.8m/s^2$
7	ρ_s	Density of soil	$1442kg/m^3$
8	ρ_b	Density of bucket	$7450\ kg/m^3$
9	v_b	Volume of bucket	$1m^3$
10	ϕ	Coefficient of sliding friction	20
11	$a_{O/\xi}$	Acceleration of point O relative to ξ	$0m/s^2$
12	$\vec{\omega}_{A/O}$	Angular velocity of point A relative to O	0rad/s

13	$\vec{\omega}_{B_1/A}$	Angular velocity of point B_1 relative to A	0.5rad/s
14	$\vec{\omega}_{B_2/B_1}$	Angular velocity of point B_2 relative to B_1	0.6rad/s
15	$\vec{\omega}_{E_1/B_2}$	Angular velocity of point E_1 relative to B_2	0rad/s
16	$\vec{\omega}_{E_2/E_1}$	Angular velocity of point E_2 relative to E_1	0.7rad/s
17	$\vec{\omega}_{D/C}$	Angular velocity of point D relative to C	0.6rad/s
18	ω_{D/E_2}	Angular velocity of point D relative to E_2	0.65rad/s
19	$\vec{r}_{O/A}$	Displacement of point O relative to A	1.5m
20	$\vec{r}_{A/B_1}$	Displacement of point A relative to B_1	2.7m
21	$\vec{r}_{B_1/B_2}$	Displacement of point B_1 relative to B_2	0.6m
22	$\vec{r}_{B_2/E_1}$	Displacement of point B_2 relative to E_1	3.6m
23	$\vec{r}_{E_1/E_2}$	Displacement of point E_1 relative to E_2	0.5m
24	$\vec{r}_{C/D}$	Displacement of point C relative to D	0.6m
25	$\vec{r}_{D/E_2}$	Displacement of point D relative to E_2	0.6m
26	η	Cutting angle	$\pi/3$
27	θ_A	Angle of unit vector $\hat{e}_{B_1/C}$	$2\pi/1.4$
28	θ_B	Angle of unit vector $\hat{e}_{B_1/B_2}$	$\pi/1.05$
29	θ_C	Angle of unit vector $\hat{e}_{B_2/E_1}$	$2\pi/1.5$
30	θ_D	Angle of unit vector $\hat{e}_{C/D}$	$\pi/2.2$
31	θ_1	$O\hat{A}B_2$	$2\pi/3$
32	θ_2	$A\hat{B}_2E_1$	$2\pi/1.4$
33	α_1	$B_2\hat{A}B_1$	$\pi/20$
34	α_2	$B_2\hat{B}_1A$	$\pi/1.1$
35	α_3	$E_1\hat{B}_1C$	$\pi/20$
36	α_4	$E_1\hat{C}D$	$\pi/1.9$
37	α_5	$D\hat{E}_2E_1$	$\pi/18$
38	α_6	$E_2\hat{E}_1D$	$\pi/5$

The results are presented in fig.37-44 below.

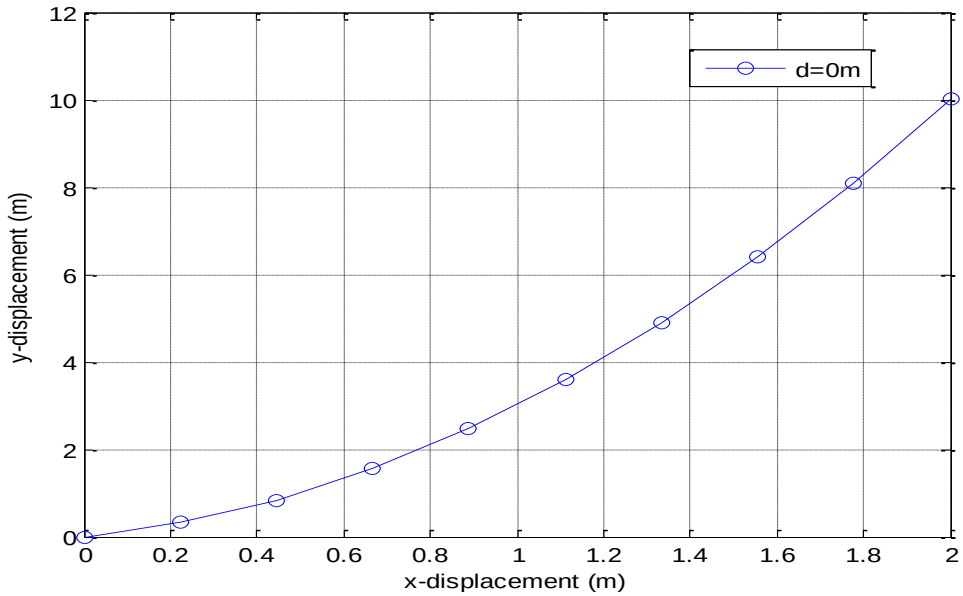

Fig.37: Profile of bucket trajectory for a free swing *(d=0)*

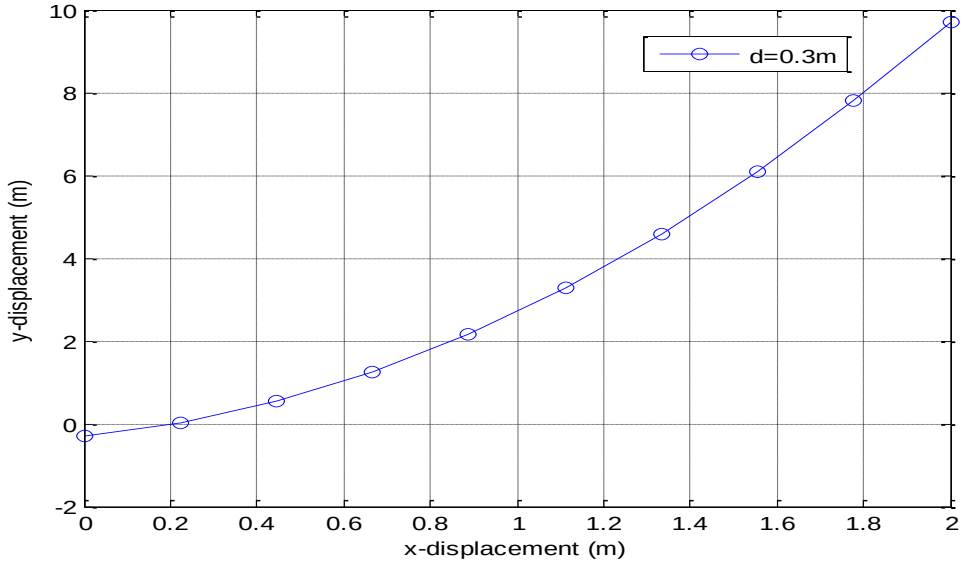

Fig.38: Profile of bucket trajectory through a medium *(d=0.3m)*

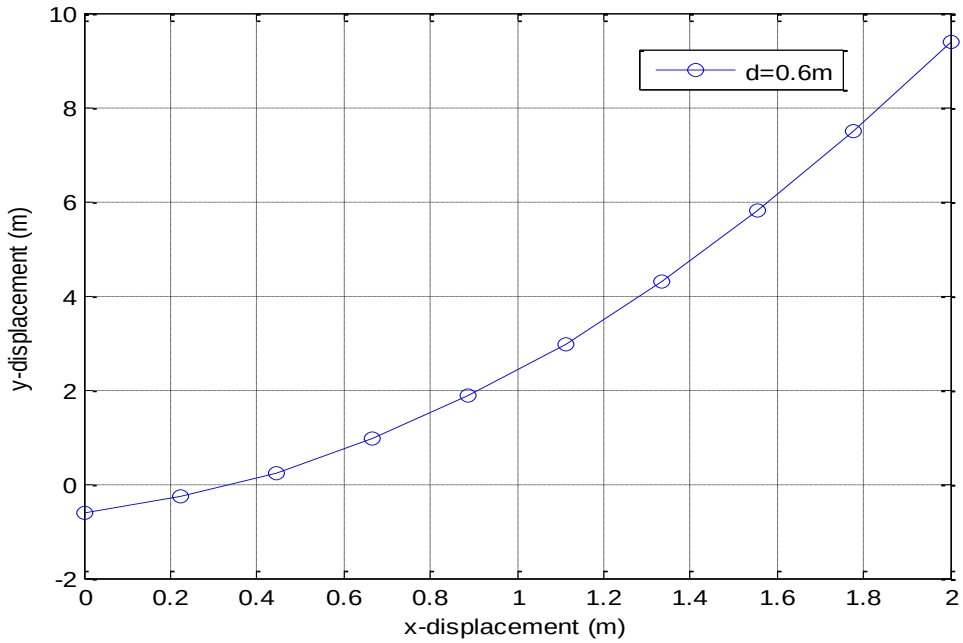

Fig.39: Profile of bucket trajectory through a medium (*d=0.6m*)

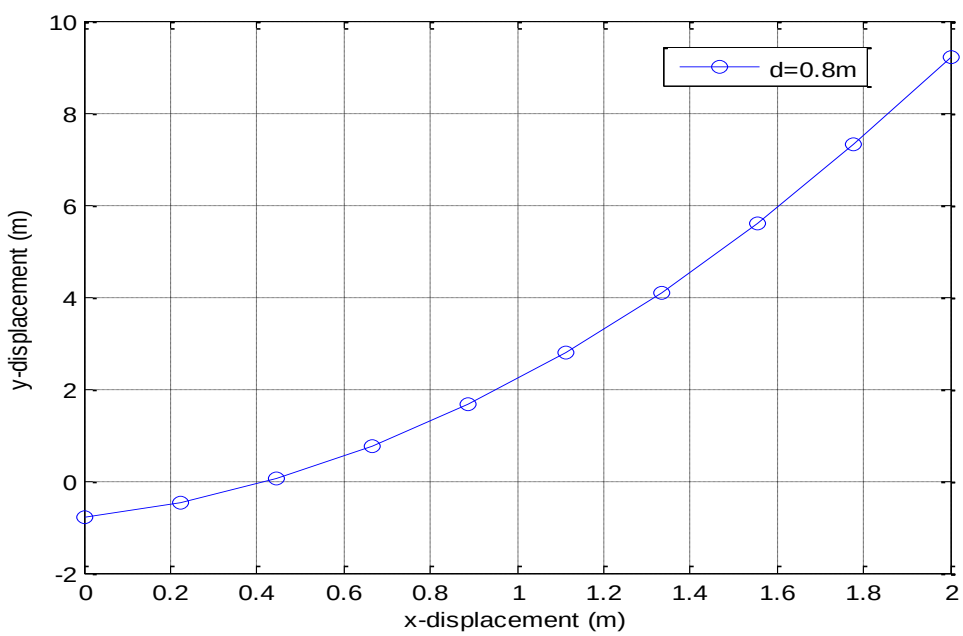

Fig.40: Profile of bucket trajectory through a medium (*d=0.8m*)

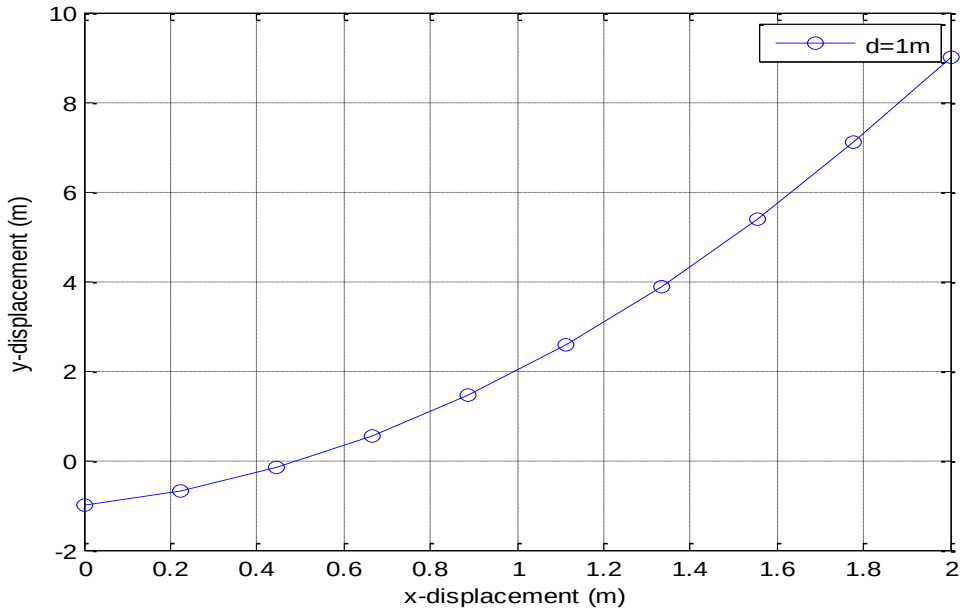

Fig.41: Profile of bucket trajectory through a medium (*1.0m*)

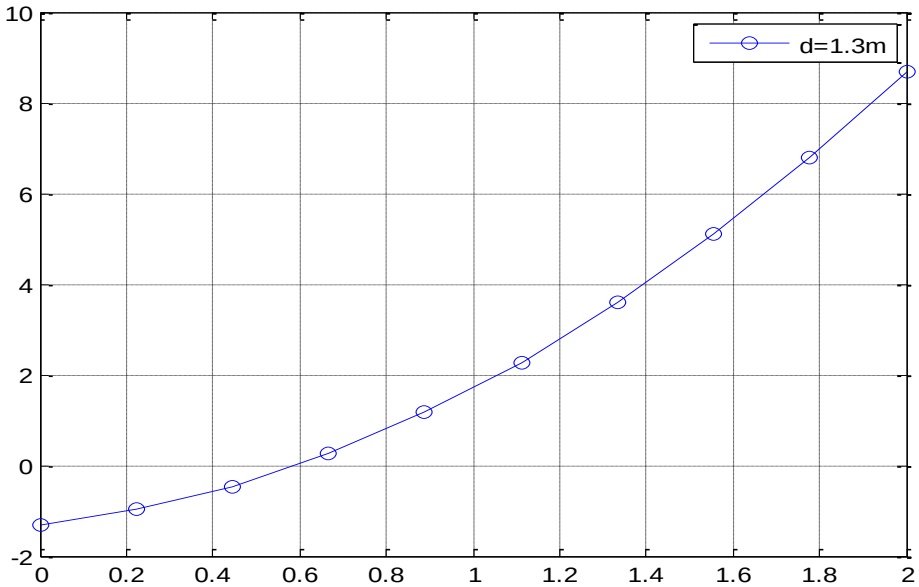

Fig.42: Profile of bucket trajectory through a medium (*d=1.3m*)

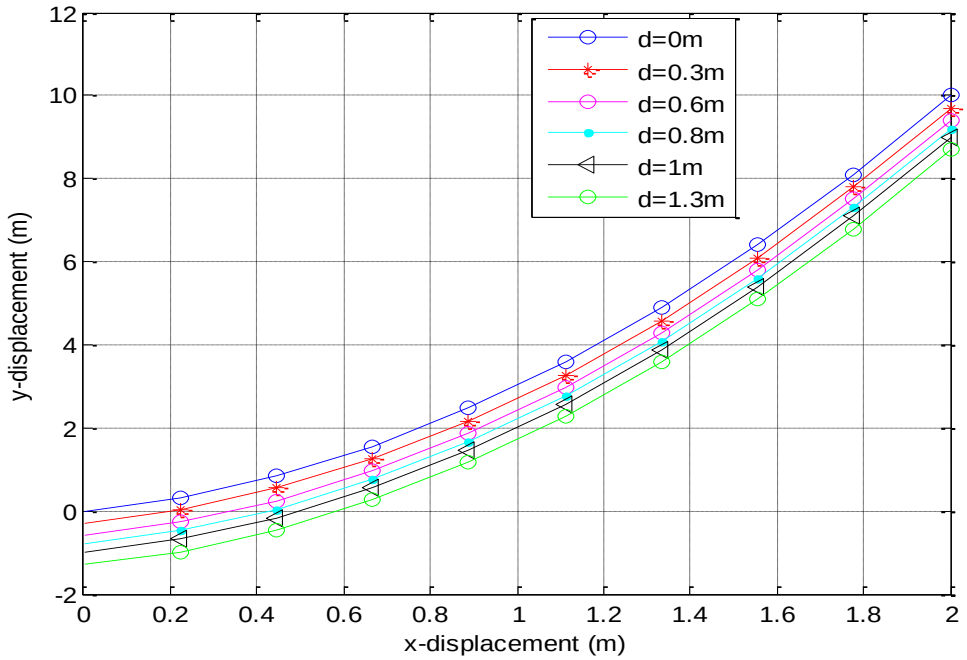

Fig.43: General profile of bucket trajectory *(d=0 -1.3)*

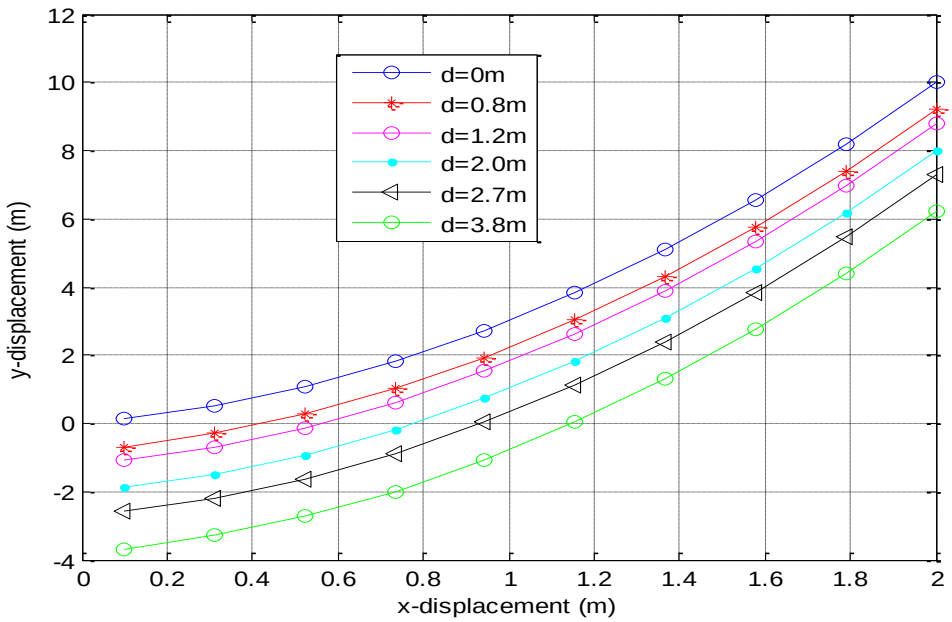

Fig.44: General profile of bucket trajectory

6.8 Discussion of Results

6.8.1. In Fig. 13-18, the profile of the cutting force F_c, angular velocity $\omega_{B_1/C}$ and adjustable link length $r_{B_1/C}$ is displayed in 3D. In this case, the adjustable link length r_{A/B_1} is fixed while link $r_{B_1/C}$ is moving. In the first place, the adjustable link length r_{A/B_1} is fixed at 1.0m while link $r_{B_1/C}$ is moving at different values of 1.7m, 2.0m, 2.3m, 2.6m and 2.9m respectively. Subsequently, the adjustable link length r_{A/B_1} is also fixed at 1.4m while link $r_{B_1/C}$ is moving at intervals from 1.7m-2.9m and so on until r_{A/B_1} is fixed at 2.7m. The result shows that the cutting force increases monotonically with the angular velocity as well as link length. Also, higher magnitude of the cutting force was achieved for greater values of the adjustable link length. Here, it can be observed that the link $r_{B_1/C}$ cannot extend beyond 2.9m while the length can also not reduce below 1.7m. From this result, it can be deduced that the hydraulic excavator can only be optimally operated within the range $1.7m < r_{B_1/C} < 2.9m$. In other words, any operation of the machine outside this range is not efficient. This forms a basis to advise the operator on the optimal range in carrying out the excavation exercise. Hence, it can be concluded that the cutting force magnitude is ordered in consonance with a range of combination of the angular velocity of the linkages and also with the link geometrical dimension.

The implication of this in actual practice is that, the maximum cutting force can be attained within a range of specified link geometrical dimensions. If the objective of the design engineer is to enhance the ability of the blade to penetrate more during the scooping operation, a mechanism that will allow a process to increase the geometry of the link via hydraulic strut system beyond what is presently obtained should be given serious consideration in modern design.

6.8.2. The simulation result displayed in Fig. 19 is a profile of the optimum results of maximum cutting force and adjustable link length $r_{B_1/C}$, when r_{A/B_1} is fixed. The legend on the curve reveal the simulation results obtained for fixed values of r_{A/B_1} at 1.0m, 1.4m, 1.8m, 2.2m and 2.7m respectively. Also, the result shows that for every fixed value of r_{A/B_1} , the link length $r_{B_1/C}$ is moving at different values of 1.7m, 2.0m, 2.3m, 2.6m and 2.9m respectively. Here, it is

generally observed that the longer the adjustable link length, the more the magnitude of the maximum cutting force in all the cases displayed in the curve. For example, when r_{A/B_1} is fixed at 1.8m, the magnitude of the cutting force is 350N for link length $r_{B_1/C}$ = 2m, while this increases to 460N when $r_{B_1/C}$ = 2.9m. From the result in fig. 19, the following inferences can be drawn: (1). Increasing the fixed value of r_{A/B_1} from 1.0m to 2.7m yields higher values of the magnitude of the maximum cutting force in all cases. This shows that operating r_{A/B_1} at a fixed value of 1.0m yields lower output of the maximum cutting force than greater lengths of the fixed link. In other words, higher values of the fixed length results in a better output of the maximum cutting force. Considering this result, it is imperative to adequately inform the operator of the implications as well as advantages of this first hand information on the geometrical parameters to be involved during the operation. (2). Also, at a lower values of the fixed length r_{A/B_1}, a higher magnitude of the cutting force can be obtained when link length $r_{B_1/C}$ is varied beyond 2.6m. This shows that the machine can also be operated to obtain a greater output of the maximum cutting force when link length $r_{B_1/C}$ is varied at 2.6m and beyond especially when r_{A/B_1} is fixed at 1.0m, 1.4m and 1.8m. In the same vein, a good performance can also be achieved when r_{A/B_1} is fixed at 2.2m and 2.7m while varying $r_{B_1/C}$ from any value between 2.3m and 2.9m. Similarly, for an improved output of the maximum cutting force, the fixed length r_{A/B_1} = 2.7m yields better results especially when moving $r_{B_1/C}$ from 2.6m to 2.9m. Equally, a similar assertion can be established for fixed lengths of r_{A/B_1} =1.8m and 2.2m especially when $r_{B_1/C}$ =2.9m. (3). When r_{A/B_1} is fixed at 2.7m, the gradient between $r_{B_1/C}$ = 1.7m-2m is 10; between 2.0m-2.3m is 13.3; between 2.3m to 2.6m is 13.3 and between 2.6m and 2.9m is 13.3. In other words, the gradient is lower at the beginning. Subsequently, there is a constant increase in the gradient at the other stages. This reveals an initial rise in the gradient, subsequently followed by a constant increase in the other stages as the link length is further varied upward. The operator can therefore be advised to operate at a higher region of gradient in order to ensure effective utilization of the excavator. (4). For fixed lengths r_{A/B_1} = 1.0m and 1.4m, the gradient is constant throughout the region of the

curve. As a result of this, operating the excavator at values of $r_{B_1/C}$ below 2.6m will amount to inefficient operation or under utilization of the machine. Hence, $r_{B_1/C}$ of 2.6m-2.9m is found to be more desirable. (5). It can also be seen that for the lowest link length r_{A/B_1} = 1.0m, the highest magnitude of the maximum cutting force is 430N, for r_{A/B_1} = 1.4m, the highest magnitude of the maximum cutting force is 450N, for r_{A/B_1} = 1.8m, the highest magnitude of the maximum cutting force is 460N, for r_{A/B_1} = 2.2m, the highest magnitude of the maximum cutting force is 480N while for r_{A/B_1} = 2.7m, the highest magnitude of the maximum cutting force is 500N. This is largely accounted for by the upward variation of the link length. Hence, it can be generally established that higher values of the link length yields greater output of the maximum cutting force. For optimality, the operator is expected to work within the identified regions of higher output of the link length in order to reduce the number of passes to fill the dump truck, thereby minimizing cycle time and increasing profit. Advantages of carrying out the excavation exercise within this range includes enhanced efficiency, reduced cycle time which will in turn reduce production cost, hence maximization of profit. This is also useful for the purpose of enhanced design.

6.8.3. In Fig. 20-25, the profile of the maximum cutting force, link length r_{A/B_1} and angular velocity is displayed in 3D. Here, the adjustable link length $r_{B_1/C}$ is fixed for each case at 1.7m, 2.0m, 2.3m, 2.6m and 2.9m respectively while r_{A/B_1} is varying from 1.0m, 1.4m,1.8m, 2.2m, to 2.7m in each of the fixed cases of $r_{B_1/C}$. The result shows that the cutting force increases monotonically with the angular velocity as well as link length. A similar pattern is observed as earlier discussed in section 6.8.1 above. Here, it can be established that the link r_{A/B_1} cannot extend beyond 2.7m while the length can also not reduce below 1.0m. In other words, any operation of the machine outside this range is inefficient. The hydraulic excavator can be judiciously operated within the range $1.m < r_{B_1/C} < 2.7m$. However, higher values of the adjustable link length yields a better output of the cutting force in all the cases observed in the simulation result. In particular, a better performance of the maximum cutting force was achieved when

$r_{B_1/C}$ is fixed at 2.9m and r_{A/B_1} is varied from1.8m to 2.7m. Hence, this can be a basis of advising the operator in order to achieve a better result in the course of operating the machine.

6.8.4. Fig. 26 shows the profile of the optimum results of maximum cutting force and adjustable link length r_{A/B_1} keeping $r_{B_1/C}$ fixed. In this case, the curves reveal the simulation results obtained when $r_{B_1/C}$ is fixed at 1.7m, 2.0m, 2.3m, 2.6m and 2.9m respectively. Also, the result shows that for every fixed value of $r_{B_1/C}$, the link length r_{A/B_1} is varying at different values of 1.0m, 1.4m, 1.8m, 2.2m and 2.7m respectively. The results show that higher magnitude of the cutting force is achieved when the adjustable link length r_{A/B_1} is increasing. Hence, the longer the link length, the higher the output of the maximum cutting force achieved in all the situations considered in the curve. For example, in the case where $r_{B_1/C}$ is fixed at 1.7m, the output of the maximum cutting force is 440N when r_{A/B_1} = 1.8m. At the same fixed length $r_{B_1/C}$ =1.7m, the output of the maximum cutting force increases to 520N when r_{A/B_1} = 2.7m. The trend of increased output of the maximum cutting force as a result of increase in the adjustable link length is the same in all cases. Considering the output of 500N for the maximum cutting force, for instance, it is possible to compare a similar output in relation to other fixed lengths of $r_{B_1/C}$. Relating this output to other fixed lengths of $r_{B_1/C}$, a similar result can be achieved when r_{A/B_1} = 2.2m and $r_{B_1/C}$ is fixed at 2.0m; when r_{A/B_1} = 1.8m and $r_{B_1/C}$ is fixed at 2.3m; when r_{A/B_1} = 1.4m and $r_{B_1/C}$ is fixed at 2.6m and when r_{A/B_1} = 1.0m and $r_{B_1/C}$ is fixed at 2.9m. Therefore, it can be deduced that for the same output of maximum cutting force considering all the links, the fixed length $r_{B_1/C}$ is operated in an increasing order of 2.0m, 2.3m, 2.6m and 2.9m while the adjustable link length r_{A/B_1} is considered in a decreasing order of 2.2m, 1.8m, 1.4m and 1.0m respectively. This result can serve as a basis of adequate information for the operator to work with in order to achieve a better performance during operation. It can also be observed that a generally better output of maximum cutting force is achievable when $r_{B_1/C}$ is fixed at 2.9m. In this case, as r_{A/B_1} increases, maximum cutting force of 520N, 560N, 580N, 630N and 660N respectively is achieved. To achieve an output of 630N, the operator can work with r_{A/B_1} = 2.2m and 2.6m

when $r_{B_1/C}$ is fixed at 2.9m and 2.6m respectively. Generally, a similar trend can observed as discussed in section 6.8.2 except for an observed variation in the values obtained which can easily be seen in the curves. It can also be observed that for the lowest link length 1.0m, the maximum cutting force is 520N while for the longest link length of 2.7m; the maximum cutting force is 660N. From the results obtained and for optimality, the operator should work within an appreciable range of the link length in order to reduce the number of passes to fill the dump truck, thereby minimizing cycle time and increasing profit.

6.8.5. Fig. 27-29 presents the profile of the cutting force F_c, cutting angle and time. The nature of this result reveals that the magnitude of the cutting force increases monotonically with that of the cutting angle until the maximum cutting angle is attained. However, it can also be observed from simulation result that cutting force reduces monotonically as time increases until a point where the cutting force plateaus. In actual practice, this shows that when the highest magnitude of the cutting angle is attained, the excavator bucket will no longer cut the pile, rather, it will just swing as no cutting is done.

6.8.6. In fig. 30-35, the profile of the optimum results of maximum scooped volume and angle is displayed in 2D. Considering a particular length of the hydraulic strut, the results generally show that the maximum cutting force increases as angle α_2 increases until a maximum point is reached after which it decreases as angle α_2 further increases. The maximum scooped volume of the lowest link length is 2.4m^3 while that of the highest link length is 5.2 m^3. Hence, the longer the link length, the more the scooped volume achieved.

In figure 36, a general profile of maximum scooped volume versus angle α_2 is presented. The result captures the profile for various length scenarios with the highest value of maximum scooped volume occurring at $\alpha_2 = 100^0$. A generally acceptable magnitude the optimum scooped volume is achieved within the range $90^0 < \alpha_2 < 120^0$. However, when $\alpha_2 > 130^0$, a downward trend in the magnitude of the maximum scooped volume is observed, likewise a similar trend when $\alpha_2 < 100^0$. This shows that within this range, the magnitude of the scooped volume is very appreciable and comparable to that which obtains in practice. This is very essential for the design engineer for the purpose of improved/enhanced design of earthmoving machines. This will

ultimately reduce the number of passes to fill the truck in a mining terrain, thereby reducing the cycle time, reducing production cost and eventually increasing the profit.

6.8.7. In Fig. 37-44, the profile of the bucket trajectory is displayed in 2D. The general trajectory of the bucket is parabolic irrespective of whether it is in free swing or cutting through a medium. A similar parabolic nature of the profile of the bucket is seen in literature (Yu et al, 2010 and Alaydi, 2009).

The nature of the profiles indicates the following:

1. The harder the medium, the less the penetration and vise versa, although with similar bucket trajectory profile.

2. The interpretation in engineering application is that different materials should have been ideally used to construct the bucket such that each has almost a direct relation with the density of the medium. If not, when the same bucket material is used to penetrate a different medium, the temperature of the material itself has to be varying in different cutting media. This will result in having the effect of material modulation of the drag when the bucket is moving through the cutting medium. A robotic design can be introduced such that whenever the density of the medium is identified, the appropriate blade material will automatically swing in to form the bucket geometry so that the effect of temperature variation as it is cutting through the medium will not have a significant effect on the geometry of the bucket and operational efficiency.

CHAPTER SEVEN

CONCLUSION

[SUMMARY AND FINDINGS, CONTRIBUTION TO KNOWLEDGE AND FUTURE WORK]

7.1 SUMMARY AND FINDINGS

In this research, we have presented a generalised model of dynamic equations governing the motion of the various links of the excavator, the transmitted and cutting forces of the excavator bucket. We have also demonstrated the robustness of the proposed model by simulating the behaviour of these forces via various scenarios for the purpose of optimized excavation and enhanced design.

From this result, it can be deduced that the hydraulic excavator can only be optimally operated within the range $1.7m < r_{B_1/C} < 2.9m$. The machine can also be effectively used within the range $1.0m < r_{B_1/C} < 2.7m$. An optimal force of 660N is achieved when link length $r_{B_1/C}$ is fixed at 2.9m and r_{A/B_1} is varied from 2.2m to 2.7m while 500N is achieved when link length r_{A/B_1} is fixed at 2.7m and $r_{B_1/C}$ is varied from 2.6m to 2.9m. Hence, a better output of the maximum cutting force is achieved when link length $r_{B_1/C}$ is fixed.

Furthermore, we have successfully provided a scheme for the analytical prediction of scooped volume during hydraulic excavation. The results compare favourably with what obtains in practice. This is also a basis for design engineers to improve and enhance the design and manufacture of hydraulic excavators. Our results show that within the range $90^0 < \alpha_2 < 120^0$, scooped volume can be optimized during excavation exercise, thereby reducing cycle time and cost of production.

Also, we have presented an analytical model for the bucket trajectory during hydraulic excavation. The results compare favourably with what obtains in practice. With this scheme, design engineers can improve and enhance the design and manufacture of hydraulic excavators. Our results show that the bucket trajectory has a general parabolic profile. Hence energy

consumed by the excavator during a scooping operation can be optimized as a function of the depth of cut.

7.2 CONTRIBUTION TO KNOWLEDGE

Contributions to the field of hydraulic excavation include:

1. A generalized mathematical model for hydraulic excavation was developed.

2. The model was solved by analytical methods and numerical simulations were performed.

3. The forces involved for various geometric configurations were quantified for optimality studies.

4. The work provided the necessary operating range for the inclination angles to achieve the optimal scooped volume.

REFERENCES

Alaydi, J.Y. (2009), "Modeling and Simulation of a Hydraulic Excavator", IUG (Islamic University of Gaza) Journal, ISSN 1726-6807, Vol.17. No. 2 pp 75-96.

Alekseeva, T. V., Artem'ev, K. A. , Bromberg, A. A., Voitsekhovskii, R. I. and Ul'yanov, N.A. (1992), "Machines for Earthmoving Work, Theory and Calculations", A. A. Balkema, Rotterdam.

Aluko, O.B. and Seig, D.A. (2000), "An Experimental Investigation of the Characteristics of and Conditions for Brittle Fracture in Two-Dimensional Soil Cutting", Elsevier, Soil and Tillage Research, Vol. 57, pp. 143-157.

Ayomoh, M.K.O. (2008), "A Hybrid Virtual Force Field Model for Autonomous Mobile Robot Navigation", Unpublished Ph.D Thesis, Department of Systems Engineering, University of Lagos, Nigeria.

Asaolu, O.S. (2002), "An Intelligent Path Planner for Autonomous Mobile Robots", Unpublished Ph.D Thesis, Department of Systems Engineering, University of Lagos, Nigeria.

Bares, J, Leger, P. C., Rowe, P., Singh, S., Stenz A., and Lay, N. K. (2000), "System for Autonomous Excavation and Truck Loading". United Kingdom Patent No.GB2342640, Carnegie Mellon University, April 2000.

Bhaveshkumar P. P., Prajapati, J.M., and Bhargav J.G, (2011), "An Excavation Force Calculations and Applications: an Analytical Approach", International Journal of Engineering Science and Technology (IJEST), ISSN: 0975-5462, Vol. 3 No. 5, pp 3831-3837.

Bhaveshkumar P. P.and Prajapati, J.M., (2011), **"**Soil-Tool Interaction as a Review for Digging Operation of mini Hydraulic Excavator" International Journal of Engineering Science and Technology (IJEST), ISSN : 0975-5462, Vol. 3 No., pp. 894-901.

Blouin, S., Hemami, A., and Lipsett, M. (2001), "Review of Resistive Force Models for Earthmoving Processes*",* Journal of Aerospace Engineering, Vol. 14, No.3, pp 102-111.

Bodur, M., Zontul, H., Ersak, A., Kiovo, A.J., Yurtseven, H.O., Kocaoglan, E. and Pasamehmetoglu, G. (1994),” Dynamic cognitive force control for an automatic land excavation robot”, Proceedings of IEEE Transaction, pp703-706.

Bradley, D.A., Seward, D.W, Mann, J.E., and Goodwin, M.R. (1993), “Artificial intelligence in the Control and Operation of Construction Plant-the Autonomous Robot Excavator”. Automation in Construction. 2(3), pp. 217-228.

Bradely, D.A. and Seward, D.W. (2004),”The Development, Control and Operation of an Autonomous Robotic Excavator”, Journal of Intelligent and Robotic Systems, Vol.21, No. 1, pp.73-97.

Bullock, D.M., and Oppenheim, I.J. (1989), “A Laboratory Study of Force-Cognitive Excavation”. In Proc. Sixth International Symposium on Automation and Robotics in Construction. June.

Burks, B.L., Killough, S.M., and Thompson, D.H.(1992), “Remote Excavation using the Telerobotic Small Emplacement Excavator”, Winter Meeting, International Conference on Fifty Years of Controlled Nuclear Chain Reaction: Past, Present and Future, American Nuclear Society, November. pp. 559- 560.

Carter, D. and Alleyne, A. (2003), “Load Modeling and Emulation for an Earthmoving Vehicle Powertrain”, Proceedings of American Control Conference, pp 4963-4968.

Chen, J. and Lu, Z. (1985),”The Further Study of High Performance Adaptive Controller for Hydraulic Servo-systems”, In Proceedings of International Conference of Fluid Power Transmission and Control, pp 163-175.

DiMaio, S.P., Salcudean S.E., Reboulet C, (2001),” A Virtual Environment for the Simulation and Programming of Excavation Trajectories”, MIT Press Journal, Vol. 10, No. 5, pp 465-476.

Ericsson, A. and Slättengren, J. (2000), “A Model for Predicting Digging Forces when Working in Gravel or other Granulated Material”, 15th ADAMS European Users Conference, Rome, pp. 1-9.

Fabrichnyi, Y. F. and Kolokolov, S. B. (1975), "Calculating the Resistance of Blasted Rock to Scooping by a Bucket", Soviet Mining Science, 11(4): pp 438-441.

Feng, P. Y., Qi Yang. Z. and Sun, S. (1992), "Research on Control Method of Planning Level for Excavation Robot". In Proc. 9th International Symposium on Automation and Robotics in Construction. Tokyo.

Fiorenzo Malaguti, (2009), "Classic Soil Cutting Models for Geomechatronics Applications", 16th International Society for Terrain-Vehicle Systems (ISTVS) Conference, Turin, Italy ,2009, No. IV. pp. 361-371.

FitzSimons, P. and Palazzolo, J. (1997), "Modeling of a One Degree of Freedom Active Hydraulic Mount", Journal of Dynamic Systems, Measurement and Control, 118(6), pp 439-448.

Forsman, B. and Pan, C. L. (1989), "Shear Properties of Fragmented Rock Masses: Model Tests and Theories", International Journal of Rock Mechanics and Mining Science & Geomechanical Abstracts, 26(1): pp 25-36.

Fox, B., Jennings, L.S. and Zomaya, A.Y. (2002), "On the Modeling of Actuator Dynamics and the Computation of Prescribed Trajectories", www.sciencedirect.com/science/ journal/00457949, Vol. 80, Issues 7-8, pp 605-614.

Friedland, B., and Park, Y., (1992), "On Adaptive Friction Compensation", IEEE Transactions on Automatic Control, 40:1609-1612.

Frimpong, S., Hu, Y. and Szymanski, J. (2002) "Dynamic Shovel Excavation Simulator in Surface Mining Operations", Summer Computer Simulation Conference SCSC 2002 Proc. San Diego, CA, July, pp 14-19 (CDROM).

Frimpong, S., Hu, Y. and Chang, Z. (2003) "Hydraulic Shovel Simulator in Surface Mining Excavation Engineering", 12th International Symposium on Mine Planning and Equipment Selection, MPES, Kalgoorlie, West Australia, April, pp 23-25 (CDROM).

Gregory, C.E. (1981), A Concise History of Mining, Pergamon Press, Elmsford, NY, pp 259.

Ha, Q.P., Nguyen, Q.H., Rye, D.C., Durrant-Whyte, H.F. (2000), "Impedance Control of a Hydraulically Actuated Robotic Excavator" Elsevier, Automation in Construction 9, (2000), pp 421-435.

Hartman, H. L. (1987), Introductory Mining Engineering, pp 2-7.

Heintze, J. (1997), "Design and Control of a Hydraulically Actuated Industrial Brick Laying Robot", Ph.D Thesis, Delft University.

Hemami, A. and Daneshmend, L. K. (1992), "Force Analysis for Automation of the Loading Operation in an LHD-Loader", In Proceedings of the 1992 IEEE International Conference on Robotics and Automation, pages 645-650.

Hemami, A. (1992), "A Conceptual Approach to Automation of LHD-loaders". In Proceedings of the Canadian Symposium on Mining Automation, pp 178-183.

Hemami, A. (1993a), "Force Analysis in the Scooping/Loading Operation of an LHD Loader". In Proceedings of the 2nd International Symposium on Mine Mechanization and Automation, pp 415-424.

Hemami, A. (1993b), "Study of Bucket Trajectory in Automatic Scooping with Load-Haul-Dump Loaders". In Transactions of the Institution of Mining and Metallurgy, Series A: Mining Industry, volume 102, pages A37-A42.

Hemami, A. (1994a), "Modelling, Analysis and Preliminary Studies for Automatic Scooping". Advanced Robotics, vol 8(5):511-529, 1994.

Hemami, A. (1994b), Motion Trajectory Study in the Scooping Operation of an LHD-Loader, IEEE Transactions on Industry Applications, vol. 30, No. *5*, September (1994), pp1333-1338.

Hemami, A. (1994c), "An Approximation of the Weight of the Loaded Material during the Scooping Operation of a Mechanical Loader". Transactions of the Canadian Society for Mechanical Engineering, 18(3):191-205.

Hemami, A. (1995), "Fundamental Analysis of Automatic Excavation", Journal of Aerospace Engineering, 8(4): pp175-179.

Ibidapo-Obe, O., Olowookere, D. and Ayomoh, M.K.O. (2011), "A Simulation Model for Mobile Manipulator Navigation System for Lunar Oxygen Production", International Journal of Agile Manufacturing (IJAM), Vol. 11(2), pp 37-51.

Ibidapo-Obe, O. and Asaolu, O.S. (2006), "Optimization Problems in Applied Sciences: From Classical Through Stochastic To Intelligent MetaHeuristic Approaches" 22:1-18; Contributed Chapter in Handbook of Industrial and Systems Engineering, Edited by Badiru, A.B., CRC press, Taylor and francis Group, New York.

Ibidapo-Obe, O., Asaolu, O.S. and Badiru, A.B. (1999), "Generalized Solutions of the Pursuit Problem in Three Dimensional Euclidean Space", Applied Mathematics and Computation, Elsevier Science Inc.6580, pp1-11.

Ibidapo-Obe, O., Asaolu, O.S. and Badiru, A.B. (2002), "A New Method for the Numerical Solution of Simultaneous Non-Linear Equations", Applied Mathematics and Computation, Elsevier Science Inc. 125(1), pp133-140.

Ji, Q. and Sanford, R. L. (1993), "Autonomous excavation of fragmented rock using machine vision". In Emerging Computer Techniques for the Minerals Industry, chapter 24, pp 221-228. Society for Mining, Metallurgy & Exploration Inc., Littleton CO, U.S.A.

Karmakar, S. and Kushwaha, R.L. (2006), "Dynamic Modeling of Soil-Tool Interaction: An Overview from a Fluid Flow Perspective, Journal of Terramechanics, 43: pp. 411-425.

Kiovo, A.J. (1994), "Kinematics of Excavator (backhoes) for Transferring Surface Material", Journal of Aerospace Engineering, 7(1), pp7-31.

Kiovo, A.J., Thoma, M., Kocaoglan, E., Andrade-Cetto, J. (1996), "Modeling and Control of Excavator Dynamics During Digging Operation", Journal of Aerospace Engineering, Vol. 9, No.1, pp 10-18.

Kojima, Y., Fukuda, J., Kuramoto, S., Sano, Y. and Akiba, N. (1990), "Remote Control Type Excavation Robot for Deep Foundation", Fujikira Technical Review, pp. 35-42.

Kulkarni, M., Trivedi, D., and Chandrasekhar, J. (1984), "An Adaptive Control of an Electro-Hydraulic Position Control System", In Proceedings of the American Control Conference, pp 443-448.

Kumar, D and Vagenas, N. (1993), "Performance Evaluation of an Automatic Load-Haul-Dump Vehicle". CIM Bulletin, 86(974):39-42.

Kusmierczyk, J. and Szlagowski, J. (2008), "Automated Excavation Process analysis for a given trajectory and soil parameters" Proceedings of the 25th International Symposium on Automation and Robotics in Construction, June 26-29, pp. 95-99.

Lawrence, P. (1995), "Coordinated and Force Feedback Control of Hydraulic Excavators", In Proceedings of the International Symposium on Experimental Robotics, pp 551-557.

Lee, S. and Chang, P.H. (2001), "Trajectory control of an electro-hydraulic excavator using a robust controller", Proceedings of the 32nd ISR (International Symposium on Robotics), April 19-21, 2001.

Lever, P., Wang, F. and Chen, D. (1994), "Intelligent Excavator Control for a Lunar Mining System". In Proc. ASCE Conference on Robotics for Challenging Environments, pp 97-105.

Lever, P.A. and Wang, F.Y. (1995), "Intelligent Excavator Control System for Lunar Mining System", Journal of Aerospace Engineering, 8(1): pp 16-24.

Lever, P. J. A., Wang, F.Y. and Shi, X. (1996), "Using Bucket Force/Torque Feedback for Control of an Automated Excavator", In Transactions, Vol. 300, pp 135-139, Society for Mining, Metallurgy & Exploration.

Lewis, R.S. and Clark, G.B. (1964), "Elements of Mining", 3rd Ed, Wiley, New York, pp768.

Marshall, J. A. (2001), "Towards Autonomous Excavation of Fragmented Rock: Experiments, Modelling, Identification and Control", M.Sc. Thesis, Queen's University, Kingston, Ontario, Canada.

Marshall, J. A., Murphy, P.F. and Daneshmend, L.K. (2008), "Toward Autonomous Excavation of Fragmented Rock: Full-Scale Experiments", IEEE Transactions On Automation Science And Engineering, Vol. 5, No. 3, pp562-566.

Matsuura, T., Shigematsu, N., Nakashima, K, and Moribe, K., (1994),"Hydraulic Screwdown Control System for Mandrel Mill", IEEE Transactions on Industrial Applications, 30:568-572.

Merritt, E. (1976), "Hydraulic Control Systems", Jonh Wiley, New York.

Mikhirev, P. A. (1983), "Theory of the Working Cycle of Automated Rock-Loading Machines of Periodic Action", Soviet Mining Science, 19(6):515-522.

Mikhirev, P. A. (1986), "Design of Automated Loading Buckets", Soviet Mining Science, 22(4): pp 292-298.

Nakano, E., (1989), "Development of Adavanced Way of Improvement of the Manueverability of a backhoe machine", Proceeding of International Symposium on Automation and Robotics in Construction, pp 351-357.

Nease, A.D. and Alexander, E.F. (1993), "Air Force Construction Automation/Robotics". In *Proc*. 10th International Symposium on Automation and Robotics in Construction (ISARC). Houston.

Olunloyo, V.O.S. and Ayomoh, M.K.O. (2009), "Autonomous Mobile Robot Navigation Using Hybrid Virtual Force Field Concept", European Journal of Scientific Research, Vol.31 No. 2, pp 204-228.

Olunloyo, V.O.S. and Ayomoh, M.K.O. (2010), "A Hybrid Path Planning Model For Autonomous Mobile Vehicle Navigation, 25th International Conference of CAD/CAM, Robotics and Factories of the Future, 13-16 July, CSIR International Convention Centre, Pretoria, South Africa, pp. 1-11.

Olunloyo, V.O.S. and Ayomoh, M.K.O. (2011), "An Efficient Path Planning Model in an Unstructured Obstacle Domain", IASTED Conference on Robotics and Applications (RA), Vancouver, Canada, June 1st-3rd, pp. 38-45.

Olunloyo, V.O.S., Ayomoh, M.K.O. and Ibidapo-Obe, O. (2009), "A Path Planning Model For Autonomous Vehicle In An Unstructed Obstacle Domain, IASTED Conference on Robotics and Applications (RA), Cambridge, Massachusetts, USA, pp 180-187.

Osumi, H., Sarata, S., Hirai, Y., and Kanai, O. (2004) "Analysis of Reaction Force with a Scooping Soil", Proceedings of Symposium on Construction Robot, pp 201-208.

Ozsoy, C., Kural, A. and Kuzucu, A. (1994), "Pole-Placement Position Control of a Hydraulic Arm", Journal of System and Control Engineering, pp149-156.

Parker, N., Salcudean, S., and Lawrence, P. (1993), "Application of Force Feedback to Heavy Duty Hudraulic Machines", In proceedings of IEEE International Conference on Robotics and Automation, Vol.1, pp 375-381.

Petty, M. K., Billingsley, J. and Tran-Cong, T., (1997), Autonomous LHD Loading. In Proceedings of the Annual IEEE Conference on Mechatronics and Machine Vision in Practice, pp 219-224.

Ridley, P. and Corke, P. (2001)," Dragline automation", Proceedings of the IEEE International Conference on Robotics and Automation, Seoul Korea, May 21-26, pp 3742-3747.

Rocke, D.J. (1994), "Control System for Automatically Controlling a Work Implement of an Earthmoving Machine to Capture Material", US Patent 5528843.

Romero-Lois, H., Hendrickson, C. and Oppenheim, I. (1989). "A Strategic Planner for Robot Excavation". In Proceeding of Sixth International Symposium on Automation and Robotics in Construction.

Rowe, P. and Stenz, A., (1997),"Parameterized Sripts for Motion Planning", In Proceedings of International Conference on Intelligent Robots and Systems, Vol 2, pp 1119-1124.

Rowe, P. S. (2000), "Learning System and Method for Optimizing Control Of Autonomous Earthmoving Machinery", United States Patent No. 6076030, Carnegie Mellon University.

Saeedi, P. , Lawrence, P.D., Lowe, D.G., Jacobson, P., Kusalovic, D., Ardon, K. and Sorensen, P.H. (2005), "An Autonomous Excavator with Vision-Based Track-Slippage Control", IEEE Transactions on Control Systems Technology, January, Vol. 13, No. 1, pp 67-84.

Sakai, T., and Cho, K. (1988), "Operation System for Hydraulic Excavator for Deep Trench Works", In Proceeding of 5th International Symposium on Robotics in Construction. Tokyo.

Sakaida, Y., Chugo, D., Kawabata, K., Kaetsu, H. and Asama, H.,(2006), "The analysis of excavator operation by a skillful operator", In Proceecing of 23rd International Symposium on Automation and Robotics in Construction, pp 543-547.

Salcudean, S.E., Tafazoli, S., Lawrence, P.D., and Chau, I. (1997), "Impedance Control of a Teleoperated Mini Excavator", In Proceeding of the 8th IEEE International Conference on Advanced Robotics (ICAR), Monterey, California.

Sameshima, M., and Tozawa, S., (1992), "Development of Auto Digging Controller for Construction Machine by Fuzzy Logic Control", In Proceeding of Conference Japanese Society of Mechanical Engineers.

Sarata, S., Sato, K., and Yuta, S., (1995), "Motion Control System for Autonomous Wheel Loader Operation", Proceedings of the International Symposium of mine Mechanisation and Automation, pp 155-165.

Sarata, S., Sata, K., and Tsukuba, S., (1998), "Motion Control System for Autonomous Wheel Loader Operation", In Proceedings of the International Conference on Mine Mechanization and Automation, pages 13.1-13.12, 1998.

Sarata, S., Osumi, H., Hirai, Y., Matsushima, G., and Tsubouchi, T., (2001), "Motion Control for Bucket of Wheel Loader based on Shape of Pile and Resistance Force", Proceedings of 18th International Symposium on Automation and Robotics in Construction, pp 259-264.

Sarata, S., Osumi, H., Hirai, Y., and Matsushima, G. (2003), "Trajectory Arrangement of Bucket Motion of Wheel Loader", Proceedings of 20th International Symposium on Automation and Robotics in Construction, pp 135-140.

Sarata, S., Osumi, H., Kawai,Y., and Tomita, F., (2004)," Trajectory Arrangement Based on Resistance Force and Shape of Pile at Scooping Motion", Proceedings of IEEE International Conference of Robotics and Automation, Vol.4, pp 3488-3493, 26 April - May 1.

Serata, S., Weeramhaeng, Y., and Tsubouchi, T., (2005) "Planning of Scooping Position and Approach Path for Loading Operation by a Wheel Loader", 22nd International Symposium on Automation and Robotics in Construction, September 11-14, Ferrara (Italy)

Seward, D., Bradley, D., Mann, J., and Goodwin, M. (1992), "Controlling an Intelligent Excavator for Autonomous Digging in Difficult Ground", In Proceeding of 9th International Symposium on Automation and Construction, Tokyo (Japan) 743-750.

Shi, X., Lever, P. J. A., and Wang, F.Y. (1996), "Experimental Robotic Excavation with Fuzzy Logic and Neural Networks", In Proceedings of the IEEE International Conference on Robotics and Automation, vol. 1, pp 957-962.

Singh, S., and Simmons, R., (1992), "Task Planning for Robotic Excavation", Proc. IEEE/RSJ International Conference on Intelligent Robots.

Singh, S. (1995a), "Synthesis of Tactical Plans for Robotic Excavation", Ph.D Thesis, Robotics Institute, Carnegie Mellon University, Pittsburgh, PA.

Singh, S. (1995b), "Learning to Predict Resistive Forces During Robotic Excavation", In Proceedings of the IEEE International Conference on Robotics and Automation, Nagoya, Japan, Vol. 2, pp 2102-2107.

Singh, S. (1997), State of the Art in Automation of Earthmoving, ASCE Journal of Aerospace Engineering, Vol 10, (4), 179-188.

Singh, S. and Cannon H., (1998), "Multi-Resolution Planning for Earthmoving", Proceedings of International Conference on Robotics and Automation (ICRA), pp 121-126.

Stentz, A., Bares, J., Singh, S., and Rowe, P., (1998), "A Robotic Excavator for Autonomous Truck Loading", In Proceedings of the IEEE/RSJ International Conference on Intelligent Robotic Systems, Canada. 13-17 October, vol. 3, pp. 1885-1893.

Storces, B. (1954), Introduction to Mining, Vol 2, Lange, Maxwell and Springer, London, pp. 1068.

Subrata Karmakar, R. Lal Kushwaha,(2006), "Dynamic Modeling of Soil–Tool Interaction: An Overview from a Fluid Flow Perspective", Journal of Terramechanics, Vol. 43, pp. 411–425.

Tafazoli, S., de Silva, C., and Lawrence, P. (1998),"Tracking Controlof an Electrohydraulic Manipulator in the Presence of Friction", IEEE Transactions on Control Systems Technology, Vol6, No. 3, pp 401-411.

Takahashi, H., Kamata, H., Masuyama, T., and Sarata, S. (1995), "Autonomous Shoveling of Rocks by using Image Vision System on LHD", In Proceedings of International Symposium on Mine Mechanization and Automation, Golden, Colorado, pp. 1.33-1.44.

Takahashi, H., Kamata, H., Masuyama, T., and Sarata, S. (1998), "Autonomous Shoveling of Rocks by using Image Vision System on LHD''. In Proceedings of International Conference on Mine Mechanization and Automation, pp 1.33-1.44

Takahashi H., Hasegawa, M. and Nakano, E. (1999), "Analysis of Resistive Forces Acting on the Bucket of a Load-Haul-Dump Machine and a Wheel Loader in the Scooping Task", Advanced Robotics, Vol. 13, No. 2 , pp. 97-114.

Tan, C.P., Zweiri, Y.H., Althoefer, K., Seneviratne, L.D., (2005), "Online Soil Parameter Estimation Scheme Based on Newton-Raphson Method for Autonomouns Excavation" IEEE/ASME Transaction on Mechatronics, Vol.10, No.2, pp 221-229.

Tsubouchi, T., Sarata, S., Osumi, H., Kurisu, M., (2002), "Introduction of Yamaazumi Project-Trial for Autonomous Heavy Vehicles at Construction Sites", Proceedings of 2002 IEEE International Conference on Industrial Technology, pp 514-518.

Vaha, P.K., Skibniewski, M.J., and Kiovo, A.J., (1991), "Kinematics and Trajectory Planning of Exacavation", In Proceedings of ASCE construction Congress, pp 787-793.

Vaha, P.K., and Skibniewski, M.J. (1993), "Dynamic Model of Exacavator", Journal of Aerospace Engineering, ASCE, 6(2), pp 148-158.

Viersma, T. (1990), "Analysis, Synthesis and Design of Hydraulic Servosystems and Pipelines", University of Delft.

Welch, T. (1962), "The Use of Derivative Pressure Feedback in a High Performance Hydraulic Servomachanism" Journal of Engineering Industrial Transactions, ASME, 84: pp 8-14.

Wohlford, W.P., Bode, B.D., and Griswold, F.D. (1990), "New Capability for Remotely Controlled Excavation", In Proceeding of 1990 Winter Meeting of the American Nuclear Society, American Nuclear Society, pp. 628-629.

Xiaobo, S., Paul, J., and Fei-Yue, W. (1998),"Autonomous Rock Excavation", World Scientific.

Yao, B., Chiu, G., and Reedy, J., (1997), "Nonlinear Adaptive Robust Control of One Degree of Freedom Electro-hydraulic Servo Systems", In ASME International Mechanical Engineering Congress and Exposition, Vol. 4, pp. 191-197.

Yu, H., Liu, Y. and Hasan, M.S. (2010) 'Review of modelling and remote control for excavators', International Journal of Advanced Mechatronic Systems, Vol. 2, Nos. 1/2, pp.68–80.

Zelenin, A. N. and Balovnev, V. I. and Kerov, L. P.(1992), "Machines for Moving the Earth", Amerind Publishing Co., New Delhi

Zhang, H., Sato, K. and Itakura, K. (2001), "Strategy trajectory generation and control for scooping (2nd report)" Journal of the Mining and Materials Processing Institute of Japan, Vol. 117, pp 947-954.

(http://en.wikipedia.org/wiki/Dragline_excavator), Accessed on 13/07/2011

(http://en.wikipedia.org/wiki/backhoe), Accessed on 13/07/2011

(http://en.wikipedia.org/wiki/Wheel_tractor-scraper), Accessed on 13/07/2011

(http://en.wikipedia.org/wiki/Power_shovel), Accessed on 13/07/2011

APPENDIX I

Next we find expression for $\vec{r}_{OA}, \vec{r}_{AB_1}, \vec{r}_{B_1B_2}, \vec{r}_{B_2E_1}, \vec{r}_{B_1C}, \vec{r}_{CD}, \vec{r}_{DE_2}$, respectively.
From Fig. 1, we find expression for $\vec{r}_{OA}$

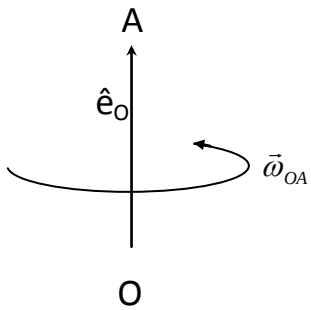

Fig 1: Vector notation for link OA

$$\vec{r}_{O/A} = |\vec{r}_{O/A}|\hat{e}_{OA} = OA\hat{j} \qquad (A1)$$

From Fig. 2, we find expression for $\vec{r}_{AB_1}$

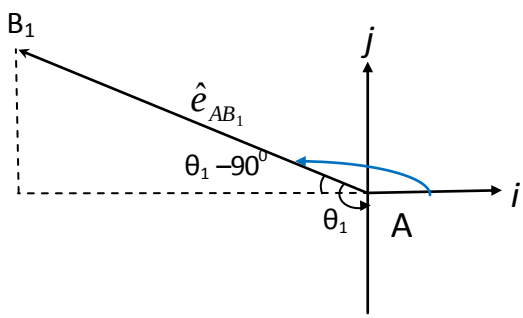

Fig 2: Vector notation for link AB_1

$$\vec{r}_{AB_1} = |\vec{r}_{AB_1}| \,.\, \hat{e}_{AB_1} = r_{AB_1}\hat{e}_{AB_1}$$

$$\hat{e}_{AB_1} = -\cos(\theta_1 - 90^0)\hat{i} + \sin(\theta_1 - 90^0)\hat{j}$$

$$-\cos(\theta_1 - 90^0)\hat{i} = -[\cos\theta_1 \cos 90^0 + \sin\theta_1 \sin 90^0]\hat{i}$$
$$= -\sin\theta_1\hat{i}$$
$$\sin(\theta_1 - 90^0)\hat{j} = [\sin\theta_1 \cos 90^0 - \cos\theta_1 \sin 90^0]\hat{j}$$
$$= -\cos\theta_1\hat{j}$$

$$\therefore \vec{r}_{AB_1} = r_{AB_1}\hat{e}_{AB_1} = r_{DE_2}[-\sin\theta_1\hat{i} - \cos\theta_1\hat{j}] = r_{DE_2}[-(\sin\theta_1\hat{i} + \cos\theta_1\hat{j})] \qquad (A2)$$

Next, we find expression for $\vec{r}_{B_1C}$ from fig 3

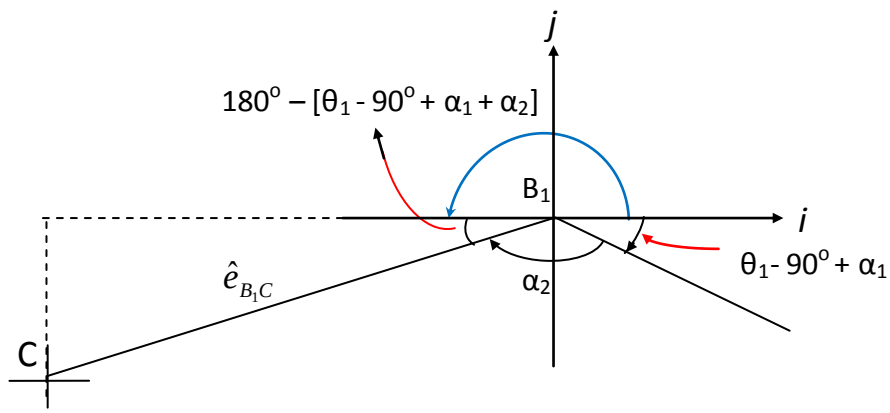

Fig 3: Vector notation for link B_1C

$$\hat{e}_{B_1C} = -\cos(270^0 - \theta_1 - \alpha_1 - \alpha_2 - \alpha_4)\hat{i} - \sin(270^0 - \theta_1 - \alpha_1 - \alpha_2 - \alpha_4)\hat{j}$$

$\hat{e}_{B_1C}$ *is* exp *ressed as*

$$-\cos(270^0 - \theta_1 - \alpha_1 - \alpha_2 - \alpha_4)\hat{i} - \sin(270^0 - \theta_1 - \alpha_1 - \alpha_2 - \alpha_4)\hat{j}$$

$$-\cos(270^0 - \theta_1 - \alpha_1 - \alpha_2 - \alpha_4) =$$

$$= -[\cos 270^0 \cos(\theta_1 + \alpha_1 + \alpha_2 + \alpha_4) + \sin 270^0 \sin(\theta_1 + \alpha_1 + \alpha_2 + \alpha_4)]$$

$$= \sin(\theta_1 + \alpha_1 + \alpha_2 + \alpha_4)$$

Also, $[-\sin(270^0 - \theta_1 - \alpha_1 - \alpha_2 - \alpha_4)] = -\sin[270^0 - (\theta_1 + \alpha_1 + \alpha_2 + \alpha_4)]$

$$= -[\sin 270^0 \cos(\theta_1 + \alpha_1 + \alpha_2 + \alpha_4) - \cos 270^0 \sin(\theta_1 + \alpha_1 + \alpha_2 + \alpha_4)]$$

$$= \cos(\theta_1 + \alpha_1 + \alpha_2 + \alpha_4)$$

Therefore,

$$\vec{r}_{B_1C} = \left|\vec{r}_{B_1C}\right| . \hat{e}_{B_1C} = r_{B_1C}\hat{e}_{B_1C}$$

$$r_{B_1C}\hat{e}_{B_1C} = r_{B_1C}[\sin(\theta_1 + \alpha_1 + \alpha_2 + \alpha_4)\hat{i} + \cos(\theta_1 + \alpha_1 + \alpha_2 + \alpha_4)\hat{j}]$$

$$r_{B_1C}\hat{e}_{B_1C} = r_{B_1C}[\sin(\theta_1+\alpha_1+\alpha_2+\alpha_4)\hat{i} + \cos(\theta_1+\alpha_1+\alpha_2+\alpha_4)\hat{j}]$$

$$r_{B_1C}\hat{e}_{B_1C} = r_{B_1C}[\sin\theta_A\hat{i} + \cos\theta_A\hat{j}] \qquad (A3)$$

$$where\ \ \theta_A = (\theta_1+\alpha_1+\alpha_2+\alpha_4)$$

Next, we find expression for $\vec{r}_{CD}$ from fig 4

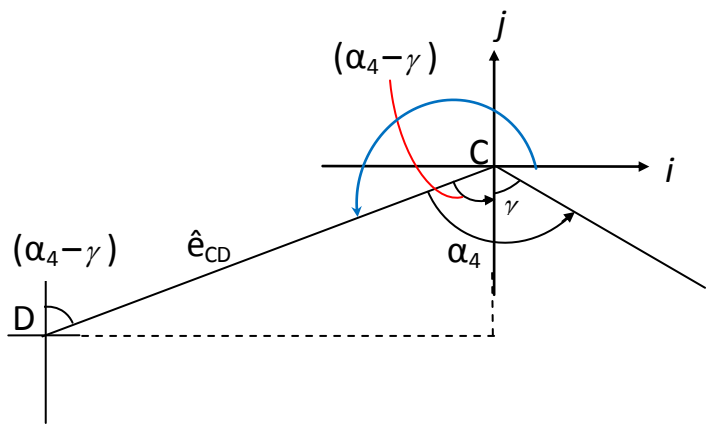

Fig 4: Vector notation for link CD

$$\vec{r}_{CD} = |\vec{r}_{CD}|.\hat{e}_{CD} = r_{CD}\hat{e}_{CD}$$

$$where\ \ \hat{e}_{CD} = [-\cos(90^0-\alpha_4-\gamma)\hat{i} - \sin(90^0-\alpha_4-\gamma)\hat{j}]$$

$$-\cos(90^0-\alpha_4-\gamma) = -\cos[90^0+(\gamma-\alpha_4)]$$

$$-\cos[90^0+(\gamma-\alpha_4)] = -[\cos 90^0\cos(\gamma-\alpha_4) - \sin 90^0\sin(\gamma-\alpha_4)]$$

$$= \sin(\gamma-\alpha_4)$$

Also,

$$-\sin(90^0-\alpha_4-\gamma) = -\sin[90^0+(\gamma-\alpha_4)]$$

$$-\sin[90^0+(\gamma-\alpha_4)] = -[\sin 90^0\cos(\gamma-\alpha_4) + \cos 90^0\sin(\gamma-\alpha_4)]$$

$$= -\cos(\gamma-\alpha_4)$$

$$\therefore \vec{r}_{CD} = r_{CD}[\sin(\gamma-\alpha_4)\hat{i} - \cos(\gamma-\alpha_4)\hat{j}] \qquad (A4)$$

Next, we find expression for $\vec{r}_{DE_2}$ from fig 5

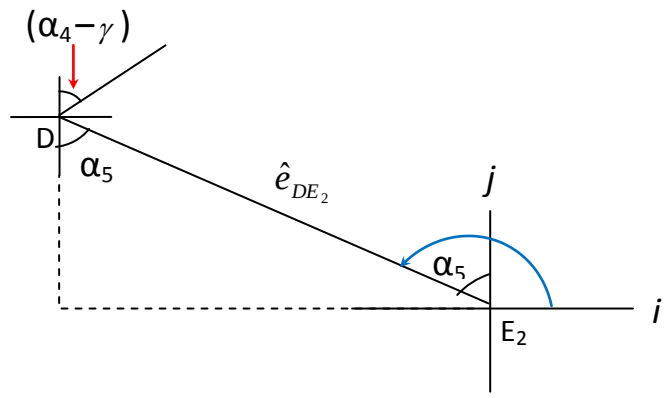

Fig 5: Vector notation for link DE_2

$$\vec{r}_{DE_2} = \left|\vec{r}_{DE_2}\right| . \hat{e}_{DE_2} = r_{DE_2}\hat{e}_{DE_2}$$

$$\hat{e}_{DE_2} = [\cos(90^0 - \alpha_5)\hat{i} - \sin(90^0 - \alpha_5)\hat{j}]$$

$$\cos(90^0 - \alpha_5) = \cos 90^0 \cos\alpha_5 + \sin 90^0 \sin\alpha_5$$

$$= \sin\alpha_5$$

Also,

$$-\sin(90^0 - \alpha_5) = -[\sin 90^0 \cos\alpha_5 - \cos 90^0 \sin\alpha_5]$$

$$= -\cos\alpha_5$$

$$\therefore \vec{r}_{DE_2} = r_{DE_2}\hat{e}_{DE_2} = r_{DE_2}[\sin\alpha_5\hat{i} - \cos\alpha_5\hat{j}] \qquad (A5)$$

Next, we find expression for $\vec{r}_{B_1B_2}$ from fig 6

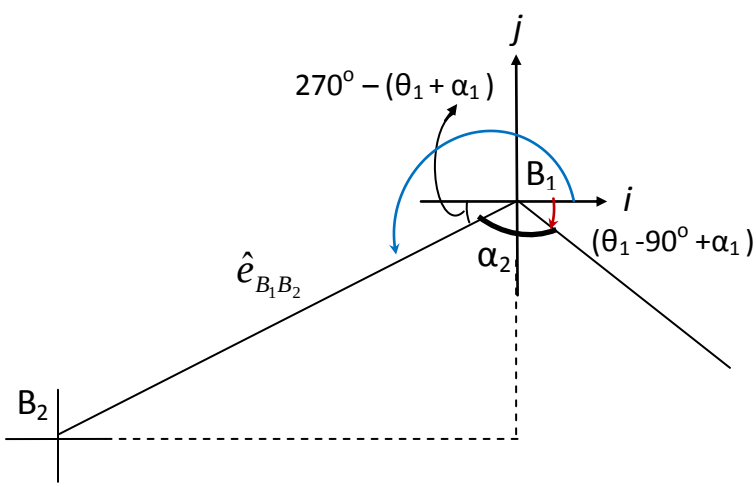

Fig 6: Vector notation for link B_1B_2

$$\vec{r}_{B_1B_2} = \left|\vec{r}_{B_1B_2}\right| . \hat{e}_{B_1B_2} = r_{B_1B_2}\hat{e}_{B_1B_2}$$

$$\hat{e}_{B_1B_2} = -\cos(270^0 - \theta_1 - \alpha_1 - \alpha - \alpha_3)\hat{i} - \sin(270^0 - \theta_1 - \alpha_1 - \alpha - \alpha_3)\hat{j}$$

$$= -[\cos 270^0 - (\theta_1 + \alpha_1 + \alpha + \alpha_3)]\hat{i} - [\sin 270^0 - (\theta_1 + \alpha_1 + \alpha + \alpha_3)]\hat{j}$$

$$-[\cos 270^0 - (\theta_1 + \alpha_1 + \alpha + \alpha_3)] = -[\cos 270^0 \cos(\theta_1 + \alpha_1 + \alpha + \alpha_3) + \sin 270^0 \sin(\theta_1 + \alpha_1 + \alpha + \alpha_3)]$$

$$= \sin(\theta_1 + \alpha_1 + \alpha + \alpha_3)$$

Also

$$-[\sin 270^0 - (\theta_1 + \alpha_1 + \alpha + \alpha_2)] = -[\sin 270^0 \cos(\theta_1 + \alpha_1 + \alpha + \alpha_2) - \cos 270^0 \sin(\theta_1 + \alpha_1 + \alpha + \alpha_2)$$

$$= \cos(\theta_1 + \alpha_1 + \alpha + \alpha_3)$$

$$\therefore \vec{r}_{B_1B_2} = r_{B_1B_2}[\sin(\theta_1 + \alpha_1 + \alpha + \alpha_3)\hat{i} + \cos(\theta_1 + \alpha_1 + \alpha + \alpha_3)\hat{j}]$$

$$\vec{r}_{B_1B_2} = r_{B_1B_2}[\sin\theta_B \hat{i} + \cos\theta_B \hat{j}] \qquad (A6)$$

$$where \;\; \theta_B = (\theta_1 + \alpha_1 + \alpha + \alpha_3)$$

Next, we find expression for $\vec{r}_{B_2E_1}$ from fig 7

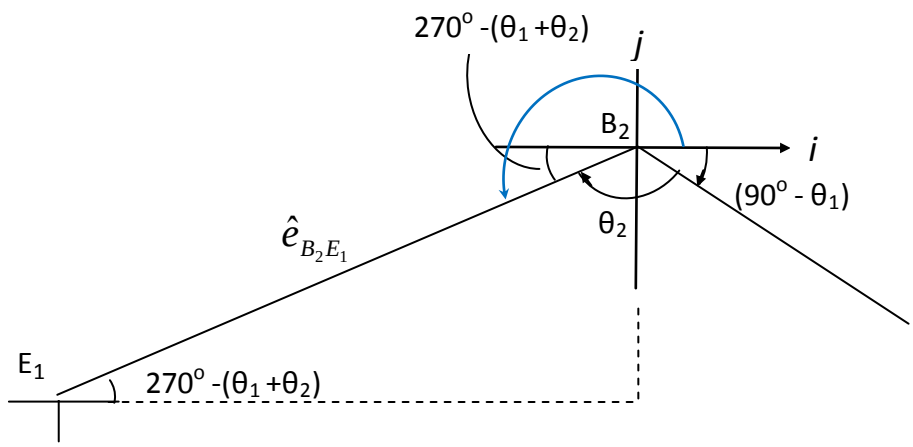

Fig 7: Vector notation for link B_2E_1

$$\vec{r}_{B_2E_1} = \left|\vec{r}_{B_2E_1}\right| . \hat{e}_{B_2E_1} = r_{B_2E_1}\hat{e}_{B_2E_1}$$

$$\hat{e}_{B_2E_1} = -\cos[270^0 - (\theta_1 + \theta_2)]\hat{i} - \sin[270^0 - (\theta_1 + \theta_2)]\hat{j}$$

$$-\cos[270^0 - (\theta_1 + \theta_2)] = -[\cos 270^0 \cos(\theta_1 + \theta_2) + \sin 270^0 \sin(\theta_1 + \theta_2)]$$

$$= \sin(\theta_1 + \theta_2)$$

Also

$$-\sin[270^0-(\theta_1+\theta_2)]=-[\sin 270^0\cos(\theta_1+\theta_2)+\cos 270^0\sin(\theta_1+\theta_2)]$$
$$=\cos(\theta_1+\theta_2)$$

$$\therefore \vec{r}_{B_2E_1}=r_{B_2E_1}[\sin(\theta_1+\theta_2)\hat{i}+\cos(\theta_1+\theta_2)\hat{j}] \qquad (A7)$$

Next, we find expression for $\vec{r}_{E_1E_2}$ from fig 8

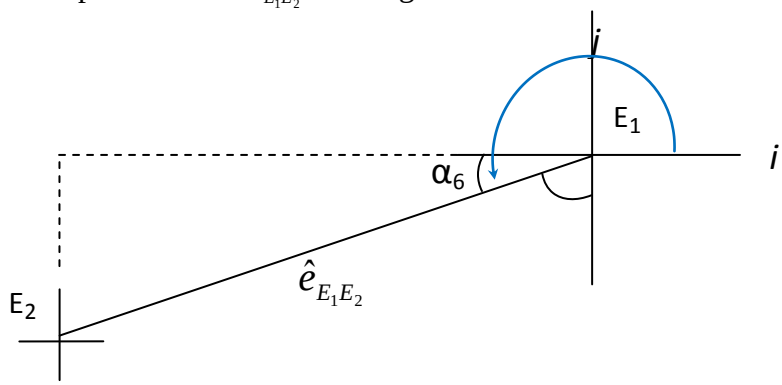

Fig 8: Vector notation for link E_1E_2

$$\vec{r}_{E_1E_2}=\left|\vec{r}_{E_1E_2}\right|.\hat{e}_{E_1E_2}=r_{E_1E_2}\hat{e}_{E_1E_2}$$

$$\hat{e}_{E_1E_2}=-\cos\alpha_6\hat{i}-\sin\alpha_6\hat{j}$$

$$\vec{r}_{E_1E_2}=r_{E_1E_2}\left[-\cos\alpha_6\hat{i}-\sin\alpha_6\hat{j}\right] \qquad (A8)$$

DERIVATION OF $\sin\eta=$

$$\sin^2\eta+\cos^2\eta=1, \quad \Rightarrow \sin^2\eta=1-\cos^2\eta$$
$$\sin^2\eta=\sqrt{1-\cos^2\eta}$$
$$\sin\eta=\left(1-\cos^2\eta\right)^{\frac{1}{2}}$$
$$\approx 1-\frac{1}{2}\cos^2\eta$$
$$\cos\eta=-4\omega^2_{E_2/E_1}r_{E_1/E_2}$$
$$\therefore \sin\eta=1-\frac{1}{2}\left(-4\omega^2_{E_2/E_1}r_{E_1/E_2}\right)^2$$
$$\therefore \sin\eta=1-\frac{1}{2}\left(16\omega^4_{E_2/E_1}r^2_{E_1/E}\right)$$

APPENDIX II

MATLAB CODE ((Maximum Cutting force and adjustable link length $r_{B_1/C}$ (link $r_{B_1/C}$ is moving when link r_{A/B_1} is fixed))

```
eta=pi/8;
theta1=2*pi/3;
thetaA=2*pi/1.4;
thetaB=pi/1.05;
thetaC=2*pi/1.5;
thetaD=-pi/2.2;
alpha1=pi/20;
alpha2=pi/1.1;
alpha3=pi/20;
alpha5=pi/18;
alpha6=pi/5;
a_o=0;
x1=0;
x2=0.5;
x3=0.6;
x4=0;
x5=0.8;
x7=0.6;
x8=0.65;
r1=1.5;
r2=2.7;
r3=0.8;
r4=3.6;
r5=0.5;
r7=0.6;
r8=0.6;
xi=linspace(-0.5,0.5,100);
yi=linspace(1.7,2.9,100);
[xxi,yyi]=meshgrid(xi,yi)
A1=(-2*a_o*sin(eta)+4*x1^2*r1*sin(eta));
A2=(4*x2^2*r2*sin(theta1+eta));
A3=(2*x3^2*r3*sin(eta+thetaB));
A4=(2*x4^2*r4*sin(eta+thetaC));
A5=(2*x5^2*r5*sin(alpha6+eta));
A6=(2*xxi.^2.*yyi.*sin(eta-thetaA));
A7=-(2*x7^2*r7*sin(thetaD+eta));
A8=-(2*x8^2*r8*sin(alpha5+eta));
```

```
M=150;
zi=abs(M*(A1+A2+A3+A4+A5+A6+A7+A8));
figure(1),mesh(xxi,yyi,zi)
x=[1.7 2.0 2.3 2.6 2.9];
y1=[270 310 350 390 430];
y2=[290 330 370 410 450];
y3=[310 350 380 420 460];
y4=[330 370 400 440 480];
y5=[350 380 420 460 500];
figure(2),plot(x,y1,'-ob',x,y2,'-*g',x,y3,'.-c',x,y4,'o-m',x,y5,'-<k')
grid on
legend('r=1.7m','r=2.0m','r=2.3m','r=2.6m','r=2.9m')
```

APPENDIX III

MATLAB CODE ((Maximum Cutting force and adjustable link length r_{A/B_1} (link r_{A/B_1} is moving when link $r_{B_1/C}$ is fixed))

```
alpha2=pi/1.1;
alpha3=pi/20;
alpha5=pi/18;
alpha6=pi/5;
eta=pi/8;
theta1=2*pi/3;
thetaA=2*pi/1.4;
thetaB=pi/1.05;
thetaC=2*pi/1.5;
thetaD=-pi/2.2;
alpha1=pi/20;
r1=1.5;
r2=3.3;
r3=0.8;
r4=3.6;
r5=0.5;
r6=2.9;
r7=0.6;
r8=0.6;
a_o=0;
x1=0;
x2=0.5;
x3=0.6;
x4=0;
x5=0.8;
x6=0.7;
```

```
x7=0.6;
x8=0.65;

xi=linspace(-0.5,0.5,100);
yi=linspace(1.0,2.7,100);
[xxi,yyi]=meshgrid(xi,yi)
a=sin(2*pi-(alpha1+alpha2));
b=sin(alpha1);
c=sin(2*pi-(alpha3+alpha5));
d=sin(alpha3);
A1=(-2*a_o*sin(eta)+4*x1^2*r1*sin(eta));
A2=(4*xxi.^2.*yyi.*sin(theta1+eta));
A3=(2*x3^2*r3*sin(eta+thetaB));
A4=(2*x4^2*r4*sin(eta+thetaC));
A5=(2*x5^2*r5*sin(alpha6+eta));
A6=(2*x6^2*r6*sin(eta-thetaA));
A7=-(2*x7^2*r7*sin(thetaD+eta));
A8=-(2*x8^2*r8*sin(alpha5+eta));
M=150;
zi=abs(M*(A1+A2+A3+A4+A5+A6+A7+A8));
figure(1),mesh(xxi,yyi,zi)


x=[1.0 1.4 1.8 2.2 2.7];
y1=[370 410 440 480 515];
y2=[410 440 480 520 550];
y3=[440 480 520 560 590];
y4=[480 520 560 590 630];
y5=[520 560 590 630 660];
figure(2),plot(x,y1,'-ob',x,y2,'-*g',x,y3,'.-c',x,y4,'o-m',x,y5,'-<k')
grid on
legend('r=1.0m','r=1.4m','r=1.8m','r=2.2m','r=2.7m')
x=[1.0 1.4 1.8 2.2 2.6 2.7];
F1=[370 410 440 480 490 515];
F2=[410 440 480 520 530 550];
F3=[440 480 520 560 570 590];
F4=[480 520 560 590 600 630];
F5=[520 560 590 630 640 660];
F6=[530 570 600 640 650 670];

figure(3),plot(x,F1,'-ob',x,F2,'-*g',x,F3,'.-c',x,F4,'o-m',x,F5,'-
<k',x,F6,'.-k')
grid on
legend('r=1.0m','r=1.4m','r=1.8m','r=2.2m','r=2.6m','r=2.7m')
```

APPENDIX IV

MATLAB CODE (SCOOPED VOLUME, ANGULAR VELOCITY AND LINK LENGTH)

```
M=150;
t=5;
Ab=0.9;
cho=0.5;
phi=pi/9;
rho=1442;
dph=1.2;
eta=pi/8;
theta1=2*pi/3;
thetaA=2*pi/1.4;
thetaB=pi/1.05;
thetaC=2*pi/1.5;
thetaD=-pi/2.2;
alpha1=pi/20;
alpha2=pi/2.5;
alpha3=pi/20;
alpha5=pi/18;
alpha6=pi/5;
a_o=1;
x1=0;
x2=0;
x3=0.4;
x4=0;
x5=0.8;
x6=0.7;
x7=0.6;
x8=1.0;
r1=3.0;
r2=3.3;
r3=0.8;
r4=3.6;
r5=0.5;
r6=2.6;
r7=0.6;
r8=0.6;
r61=3.0;

xi=linspace(-0.4,0.4,100);
yi=linspace(0.1,0.8,100);
[xxi,yyi]=meshgrid(xi,yi)
a=sin(2*pi-(alpha1+alpha2));
```

```
b=sin(alpha1);
c=sin(2*pi-(alpha3+alpha5));
d=sin(alpha3);

A1=(-2*a_o*sin(eta)+4*x1^2*r1*sin(eta));
A2=(4*xxi.^2.*yyi.*(a/b)*sin(theta1+eta));
A3=(2*x3^2*r3*sin(eta+thetaB));
A4=(2*x4^2*r4*sin(eta+thetaC));
A5=(2*x5^2*r5*sin(alpha6+eta));
A6=(2*x6^2*r61*(c/d)*sin(eta-thetaA));
A7=-(2*x7^2*r7*sin(thetaD+eta));
A8=-(2*x8^2*r8*sin(alpha5+eta));
C1=M*(A1+A2+A3+A4+A5+A6+A7+A8);
C2=cho*Ab;
C3=tan(phi)*(M*(A1+A2+A3+A4+A5+A6+A7+A8));
C4=rho*dph;
C5=t^2/2;
zi=abs(C5*((C1-C2-C3)/C4));
figure(1),mesh(xxi,yyi,zi);
xlabel('omega (rad/s)'),ylabel('link (m)'),zlabel('scooped volume
(m3)')
```

APPENDIX V

MATLAB CODE (MAXIMUM SCOOPED VOLUME AND ANGLE OF INCLINATION)

```
Y1=[1.14 1.45 1.88 2.20 2.30 2.10 2.00 2.00];
X1=[163 150 128 112.5 100 90 82 72];
Y2=[1.70 2.01 2.45 2.70 2.80 2.60 2.50 2.50];
X2=[163 150 128 112.5 100 90 82 72];
Y3=[2.28 2.60 3.00 3.30 3.40 3.20 3.10 3.10];
X3=[163 150 128 112.5 100 90 82 72];
Y4=[2.85 3.18 3.60 3.80 4.00 3.70 3.60 3.60];
X4=[163 150 128 112.5 100 90 82 72];
Y5=[3.44 3.74 4.18 4.40 4.51 4.25 4.10 4.10];
X5=[163 150 128 112.5 100 90 82 72];
Y6=[4.00 4.30 4.71 5.00 5.20 4.75 4.60 4.60];
X6=[163 150 128 112.5 100 90 82 72];
figure(1),plot(X1,Y1,'-*'),
xlabel('angle (degree)'),ylabel('maximum scooped volume (m3)')
legend('r=0.5m')
grid on
figure(2),plot(X2,Y2,'-*'),
xlabel('angle (degree)'),ylabel('maximum scooped volume (m3)')
legend('r=1.0m')
grid on
figure(3),plot(X3,Y3,'-*'),
xlabel('angle (degree)'),ylabel('maximum scooped volume (m3)')
legend('r=1.5m')
grid on
figure(4),plot(X4,Y4,'-*'),
xlabel('angle (degree)'),ylabel('maximum scooped volume (m3)')
legend('r=2.0m')
grid on
figure(5),plot(X5,Y5,'-*'),
xlabel('angle (degree)'),ylabel('maximum scooped volume (m3)')
legend('r=2.5m')
grid on
figure(6),plot(X6,Y6,'-*'),
xlabel('angle (degree)'),ylabel('maximum scooped volume (m3)')
legend('r=3.0m')
grid on
figure(7),plot(X1,Y1,'-ob',X2,Y2,'-*g',X3,Y3,'.-c',X4,Y4,'o-
m',X5,Y5,'-<k',X6,Y6,'-og')
xlabel('angle (degree)'),ylabel('maximum scooped volume (m3)')
legend('r=0.5m','r=1.0m','r=1.5m','r=2.0m','r=2.5m','r=3.0m')
grid on
```

APPENDIX VI

MATLAB CODE FOR BUCKET TRAJECTORY WHEN THERE IS Y-DISPLACEMENT

```
vt=1,
B=pi/2;
A=0;
g=9.8;
cho=7.8;
phi=pi/4;
Fc=1;
Ft=1;
d=0;
Ab=1;
rhob=0.5;
rhos=0.5;
vb=1;
vs=1;
x=linspace(0,2,10);
A6=x*cos(A)/sin(B);
A7=(x.^2/(vt^2))*(1/sin(B)^2);
A8=g;
A9=cho+((Fc*tan(phi))/(Ab)),
A10=Ft;
A11=(rhob*vb)+(rhos*vs);
y1=A6+A7*(A8+(A10-A9)/A11)-d;
figure(1),plot(x,y1,'-ob');
xlabel('x-displacement (m)'),ylabel('y-displacement (m)')
legend('d=0m')
grid on

d=0.3;
y2=A6+A7*(A8+(A10-A9)/A11)-d;
figure(2),plot(x,y2,'-ob');
xlabel('x-displacement (m)'),ylabel('y-displacement (m)')
legend('d=0.3m')
grid on

d=0.6;
y3=A6+A7*(A8+(A10-A9)/A11)-d;
figure(3),plot(x,y3,'-ob');
legend('d=0.6m')
xlabel('x-displacement (m)'),ylabel('y-displacement (m)')
grid on
```

```
d=0.8;
y4=A6+A7*(A8+(A10-A9)/A11)-d;
figure(4),plot(x,y4,'-ob');
legend('d=0.8m')
xlabel('x-displacement (m)'),ylabel('y-displacement (m)')
grid on

d=1;
y5=A6+A7*(A8+(A10-A9)/A11)-d;
figure(5),plot(x,y5,'-ob');
xlabel('x-displacement (m)'),ylabel('y-displacement (m)')
legend('d=1m')
grid on

d=1.3;
y6=A6+A7*(A8+(A10-A9)/A11)-d;
figure(6),plot(x,y6,'-ob');
legend('d=1.3m')
grid on

figure(7),plot(x,y1,'-ob',x,y2,'-*r',x,y3,'o-m',x,y4,'.-c',x,y5,'-
<k',x,y6,'o-g');
xlabel('x-displacement (m)'),ylabel('y-displacement (m)')
legend('d=0m','d=0.3m','d=0.6m','d=0.8m','d=1m','d=1.3m')
grid on
```

APPENDIX VII

MATLAB CODE FOR BUCKET TRAJECTORY WHEN THERE IS NO Y-DISPLACEMENT

```
rhob=0.5;
rhos=0.5;
vb=1;
vs=1;
vt=1,
B=pi/2;
A=0;
g=9.8;
cho=7.8;
phi=pi/4;
Fc=1;
Ft=1;
d=0;
Ab=1;
x=linspace(0.1,2,10);
A6=x*cos(A)/sin(B);
A7=(x.^2/(vt^2))*(1/sin(B)^2);
A8=g;
A9=cho+((Fc*tan(phi))/(Ab)),
A10=Ft;
A11=(rhob*vb)+(rhos*vs);

y1=A6+A7*(A8+(A10-A9)/A11)-d;
figure(1),plot(x,y1,'-ob');
xlabel('x-displacement (m)'),ylabel('y-displacement (m)')
legend('d=0m')
grid on

d=0.8;
y2=A6+A7*(A8+(A10-A9)/A11)-d;
figure(2),plot(x,y2,'-ob');
xlabel('x-displacement (m)'),ylabel('y-displacement (m)')
legend('d=0.8m')
grid on

d=1.2;
y3=A6+A7*(A8+(A10-A9)/A11)-d;
figure(3),plot(x,y3,'-ob');
legend('d=1.2m')
```

```
xlabel('x-displacement (m)'),ylabel('y-displacement (m)')
grid on

d=2.0;
y4=A6+A7*(A8+(A10-A9)/A11)-d;
figure(4),plot(x,y4,'-ob');
legend('d=2.0m')
xlabel('x-displacement (m)'),ylabel('y-displacement (m)')
grid on

d=2.7;
y5=A6+A7*(A8+(A10-A9)/A11)-d;
figure(5),plot(x,y5,'-ob');
xlabel('x-displacement (m)'),ylabel('y-displacement (m)')
legend('d=2.7m')
grid on

d=3.8;
y6=A6+A7*(A8+(A10-A9)/A11)-d;
figure(6),plot(x,y6,'-ob');
legend('d=3.8m')
grid on

figure(7),plot(x,y1,'-ob',x,y2,'-*r',x,y3,'o-m',x,y4,'.-c',x,y5,'-
<k',x,y6,'o-g');
xlabel('x-displacement (m)'),ylabel('y-displacement (m)')
legend('d=0m','d=0.8m','d=1.2m','d=2.0m','d=2.7m','d=3.8m')
grid on
```